Investigation of Heat Transfer in a Rectangular Packed Duct with Constant Heat Flux and Asymmetrical Wall Temperatures

by

Yassir T. Makkawi

A Thesis Presented to the

FACULTY OF THE COLLEGE OF GRADUATE STUDIES

KING FAHD UNIVERSITY OF PETROLEUM & MINERALS

DHAHRAN, SAUDI ARABIA

In Partial Fulfillment of the
Requirements for the Degree of

MASTER OF SCIENCE

In

CHEMICAL ENGINEERING

June, 1995

Investigation of Heat Transfer in a Rectangular Packed Duct with Constant Heat Flux and Asymmetrical Wall Temperatures

BY

YASSIR T. MAKKAWI

A Thesis Presented to the

FACULTY OF THE COLLEGE OF GRADUATE STUDIES

KING FAHD UNIVERSITY OF PETROLEUM & MINERALS

DHAHRAN, SAUDI ARABIA

In Partial Fulfillment of the
Requirements for the Degree of

MASTER OF SCIENCE

In

CHEMICAL ENGINEERING

June, 1995

KING FAHD UNIVERSITY OF PETROLEUM AND MINERALS
DHAHRAN 31261, SAUDI ARABIA

COLLEGE OF GRADUATE STUDIES

This thesis, written by

YASSIR T. MAKKAWI

Under the direction of his Thesis Advisor and approved by his Thesis Committee, has been presented to and accepted by the Dean of the College of Graduate studies, in partial fulfillment of the requirement of the degree of

MASTER OF SCIENCE IN CHEMICAL ENGINEERING

Thesis committee

Dr. Habib H. Al-Ali
(Thesis Advisor)

Dr. Yasar Demirel
(Member)

Dr. Ashraf I. Fatehi
(Member)

Dr. Adeniyi W. Lawal
(Member)

Dr. Dulaihan Al-Harbi
(Department Chairman)

Dr. Ala H. Al-Rabeh
(Dean, College of Graduate studies)
Date : 2/7/97

This Thesis is Dedicated to my family
for their love, support and patience

ACKNOWLEDGMENT

Praise and gratitude be to Allah the Almighty, with whose gracious help it was possible to accomplish this work.

Thanks are to *KFUPM, College of Graduate Studies* and *Chemical Engineering Department* for giving me the opportunity to read for my M.S.

I would like to express my appreciation and gratitude to my advisor *Dr. Habib Al-Ali* for his encouragement and support throughout this work.

I would also like to extend my thanks to *Dr. Yasar Demirel* for his invaluable suggestions and comments to my work.

I am also thankful to the other members of my thesis committee, *Dr. Ashraf Fatehi* and *Dr. Adeniyi Lawal.*

I am also very thankful to the department technicians, *Mr. Romeo, Mr. Mahdi* and *Mr. John* for their cooperation and great help during my experimental work.

Thanks are also to my friends and colleges who made my stay at *KFUPM* a memorable experience.

TABLE OF CONTENTS

CHAPTER *PAGE*

LIST OF TABLES....viii

LIST OF FIGURES....ix

ABSTRACT(Arabic)....xiv

ABSTRACT(English)....xv

1. INTRODUCTION 1

1.1 ENHANCED HEAT TRANSFER IN PACKED DUCT AND ITS APPLICATIONS....2

1.2 SIMULATION OF HEAT TRANSFER IN PACKED DUCTS 3

1.3 EFFECTIVE PARAMETERS ON HEAT TRANSFER....4

1.3.1 Geometry of bed, size and type of packing 4

1.3.2 Flow regime and pressure drop.... 4

1.4 RELEVANT PROPERTIES OF AIR AND PACKING PARTICLES 5

1.5 SCOPE AND OBJECTIVES OF THIS STUDY....6

2. LITERATURE REVIEW....9

2.1 INTRODUCTION....9

2.2 BACKGROUND ON PREVIOUS EXPERIMENTAL STUDIES....9

2.2.1 Particle and channel size effects.... 9

2.2.2 Flow regime effects 13

2.2.3 Calculation of Nusselt number 14

2.3 BACKGROUND ON PREVIOUS THEORETICAL STUDIES 16
2.3.1 Simulation of velocity distribution *16*
2.3.2 Simulation of temperature distribution *19*
2.3.3 Simulation of Pressure dr[illegible] *20*
2.3.4 Correlation equation for Nusselt number *22*
3. EXPERIMENTAL APPARATUS AND PROCEDURE 29
3.1 INTRODUCTION 29
3.2 APPARATUS 30
3.2.1 Rectangular channel *30*
3.2.2 Heating Elements *30*
3.2.3 Insulating material *31*
3.2.4 Thermocouples *31*
3.2.5 Flow meter *32*
3.2.6 Manometer *32*
3.3 PACKING TYPE AND MATERIAL 33
3.4 EXPERIMENTAL PROCEDURE 34
4. DEVELOPMENT OF THE MATHEMATICAL MODEL 42
4.1 INTRODUCTION 42
4.2 ASSUMPTIONS 43
4.3 PARAMETERS DEFINITION 43
4.3.1 Bed void fraction *43*
4.3.2 Packing and channel equivalent diameter *44*
4.3.3 Effective thermal conductivity *45*
4.3.4 Modified Reynolds number *46*

4.4 MODEL EQUATIONS 47
4.4.1 pressure drop equation *47*
4.4.2 Continuity and momentum balance equations *49*
4.4.3 Energy balance equation *51*
4.5 NUMERICAL FORMULATIONS AND PROCEDURE 51
4.5.1 Finite difference approximation *51*
4.5.2 Determination of air bulk temperature *53*
4.5.3 Determination of wall to air heat transfer coefficient *54*
5. RESULTS AND DISCUSSION 60
5.1 INTRODUCTION 60
5.2 PACKED CHANNEL EXPERIMENTAL RESULTS 61
5.2.1 Temperature distribution *61*
5.2.2 Pressure drop *78*
5.3 EMPTY CHANNEL EXPERIMENTAL RESULTS 78
5.3.1 Temperature distribution *78*
5.3.2 Pressure drop *89*
5.4 EXPERIMENTAL DATA ANALYSIS 89
5.4.1 Effects of Reynolds number on transverse and axial temperature profiles *89*
5.4.2 Effects of Reynolds number on wall-to-air heat transfer coefficient ... *99*
5.4.3 Comparison between experimental and previous theoretical predictions of packed channel pressure drop *108*
5.5 MODIFIED ERGUN EQUATION 109
5.6 CORRELATIVE EXPRESSION OF NUSSELT NUMBER 116
5.7 SIMULATION RESULTS 117

5.7.1 Velocity distribution *117*
5.7.2 Temperature distribution *121*
5.7.3 Heat transfer coefficient *121*
5.8 COMPARISON BETWEEN EMPTY AND PACKED CHANNEL PERFORMANCE 130
5.8.1 Temperature distribution *130*
5.8.2 Pressure drop *131*
5.8.3 Heat transfer coefficient *131*
6. CONCLUSION AND RECOMMENDATIONS 139
NOMENCLATURE 142
REFERENCES 145
APPENDIX A 151
MAIN PROGRAM AND SUBROUTINES USED 151
APPENDIX B 161
PACKED CHANNEL EXPERIMENTAL DATA ANALYSIS 161
APPENDIX C 165
EMPTY CHANNEL EXPERIMENTAL DATA ANALYSIS 165

LIST OF TABLES

TABLE 2.1 EXPERIMENTAL DATA ON A PACKED CHANNEL WITH ASYMMETRIC HEATING (*6*) 25

TABLE 2.2 CORRELATIONS TESTED FOR HEAT TRANSFER COEFFICIENT (*29*) 26

TABLE 2.3. EMPERICAL CORRELATION FUNCTIONS OF NUSSELT NUMBER 27

TABLE 5.1 EXPERIMENTAL PRESSURE DROP DATA OBTAINED WITH THE PACKED CHANNEL. 80

TABLE 5.2 EXPERIMENTALLY DETERMINED *NU* IN THE PACKED CHANNEL. 106

TABLE 5.3 COMPARISON BETWEEN EXPERIMENTAL AND PREDICTED PRESSURE DROP BY ERGUN EQUATION 112

TABLE 5.4 VISCOUS AND INERTIA FORCES CALCULATED BY THE ORIGINAL ERGUN EQUATION. 113

TABLE 5.5 COMPARISON BETWEEN EMPTY AND PACKED CHANNEL *NU*. 137

LIST OF FIGURES

FIGURE 3.1 EXPERIMENTAL SET-UP 36

FIGURE 3.2 EXPERIMENTAL RECTANGULAR CHANNEL 37

FIGURE 3.3 ARRANGEMENT OF THE RESISTANT-HEATING WIRES 38

FIGURE 3.4 DETAILED DIAGRAM OF THERMOCOUPLES POSITIONS 39

FIGURE 3.5 CONNECTIONS OF THE INCLINED MANOMETER TO THE CHANNEL 40

FIGURE 3.6 PACKING SHAPE AND SIZE 41

FIG. 4.1 GEOMETRY AND COORDINATE SYSTEM OF THE BED. 55

FIG. 4.2 NORMALIZED STAGNANT FLUID THICKNESS δ AS FUNCTION OF THE THERMAL CONDUCTIVITY RATIO K_S/K_G FOR LOOSE PACKING (33). 56

FIG. 4.3 COMPUTER PROGRAME FLOW CHART 57

FIG. 5.1 EXPERIMENTAL AIR TEMPERATURE DISTRIBUTION IN THE PACKED CHANNEL AT Q=55.0 W/M^2 63

FIG. 5.2 EXPERIMENTAL AIR TEMPERATURE DISTRIBUTION IN THE PACKED CHANNEL AT Q=130 W/M^2 64

FIG. 5.3 EXPERIMENTAL AIR TEMPERATURE DISTRIBUTION IN THE PACKED CHANNEL AT Q=230 W/M^2 65

FIG. 5.4 EXPERIMENTAL AIR TEMPERATURE DISTRIBUTION IN THE PACKED CHANNEL AT Q=350 W/M^2 66

FIG. 5.5 EXPERIMENTAL AIR TEMPERATURE DISTRIBUTION IN THE PACKED CHANNEL AT Q=230 W/M^2 67

FIG. 5.6 EXPERIMENTAL AIR TEMPERATURE DISTRIBUTION IN THE PACKED CHANNEL AT Q=350 W/M^2 68

FIG. 5.7 EXPERIMENTAL AIR TEMPERATURE DISTRIBUTION IN THE PACKED CHANNEL AT Q=500 W/M^2 69

FIG. 5.8 EXPERIMENTAL TRANSVERSE AIR TEMPERATURE PROFILES IN THE PACKED CHANNEL AT Q=130 W/M^2 70

FIG. 5.9 EXPERIMENTAL TRANSVERSE AIR TEMPERATURE PROFILES IN THE PACKED CHANNEL AT Q=230 W/M^2 71

FIG. 5.10 EXPERIMENTAL TRANSVERSE AIR TEMPERATURE PROFILES IN THE PACKED CHANNEL AT Q=350 W/M^2 72

FIG 5.11 EXPERIMENTAL AIR BULK TEMPERATURE IN THE PACKED CHANNEL AS FUNCTION OF THE AXIAL DISTANCE AT Q=230 W/M^2 73

FIG 5.12 EXPERIMENTAL AIR BULK TEMPERATURE IN THE PACKED CHANNEL AS FUNCTION OF THE AXIAL DISTANCE AT Q=230 W/M^2 74

FIG. 5.13 EXPERIMENTALLY DETERMINED TEMPERATURE DISTRIBUTION IN THE PACKED CHANNEL AT Q=350 W/M^2 AND Re=3860. 75

FIG. 5.14 EXPERIMENTALLY DETERMINED TEMPERATURE DISTRIBUTION IN THE PACKED CHANNEL AT Q=130 W/M^2 AND Re=1388. 76

FIG. 5.15 EXPERIMENTALLY DETERMINED TEMPERATURE DISTRIBUTION IN THE PACKED CHANNEL AT Q=55 W/M^2 AND Re=2471. 77

FIG. 5.16 EXPERIMENTAL PRESSURE DROP BETWEEN THE TWO ENDS OF THE PACKED SECTION. 80

FIG. 5.17 EXPERIMENTAL AIR TEMPERATURE DISTRIBUTION IN THE EMPTY CHANNEL AT Q=130 W/M^2 82

FIG. 5.18 EXPERIMENTAL AIR TEMPERATURE DISTRIBUTION IN THE EMPTY CHANNEL AT Q=230 W/M^2 83

FIG. 5.19 EXPERIMENTAL TRANSVERS TEMPERATURE PROFILES IN THE EMPTY CHANNEL AT Q=55.0 W/M^2 84

FIG. 5.20 EXPERIMENTAL TRANSVERS TEMPERATURE PROFILES IN THE EMPTY CHANNEL AT Q=130 W/M^2 85

FIG. 5.21 EXPERIMENTAL AIR BULK TEMPERATURE AS FUNCTION OF THE AXIAL DISTANCE IN THE EMPTY CHANNEL AT Q=230 W/M^2 86

FIG. 5.22 EXPERIMENTAL AIR BULK TEMPERATURE AS FUNCTION OF THE AXIAL DISTANCE IN THE EMPTY CHANNEL AT Q=350 W/M^2 87

FIG. 5.23 EXPERIMENTALLY DETERMINED TEMPERATURE DISTRIBUTION IN THE EMPTY CHANNEL AT Q=130 W/M^2 AND MASS FLUX=0.127 KG/M^2S. 88

FIG. 5.24 EMPTY CHANNEL PRESSURE DROP 91

FIG. 5.25 EXPERIMENTAL AIR BULK TEMPERATURE AS FUNCTION OF THE AXIAL DISTANCE IN THE PACKED CHANNEL AT Q=130 W/M^2 92

FIG. 5.26 EXPERIMENTAL DETERMINED AIR BULK TEMPERATURE AS FUNCTION OF THE AXIAL DISTANCE IN THE PACKED CHANNEL AT Q=230 W/M^2 93

FIG. 5.27 EXPERIMENTALLY DETERMINED AIR TEMPERATURE IN THE PACKED CHANNEL AS FUNCTION OF THE AXIAL DISTANCE AT Y=0.02 M. 94

FIG. 5.28 EXPERIMENTALLY DETERMINED AIR TEMPERATURE IN THE PACKED CHANNEL AS FUNCTION OF THE AXIAL DISTANCE AT Y=0.05 M. 95

FIG 5.29 EXPERIMENTALLY DETERMINED AIR BULK TEMPERATURE IN THE PACKED CHANNEL AT X=1.29 M. 96

FIG 5.30 EXPERIMENTALLY DETERMINED AIR BULK TEMPERATURE IN THE PACKED CHANNEL AT X=1.29 M. 97

FIG. 5.31 TRANSVERSE AIR TEMPERATURE PROFILES IN THE PACKED CHANNEL AT X=1.29 M. 98

FIG. 5.32 EXPERIMENTALLY DETERMINED *NU* AS FUNCTION OF *RE* AT X=1.29 M. 101

FIG. 5.33 EXPERIMENTALLY DETERMINED *NU* AS FUNCTION OF *RE* AT X=1.29 M. 102

FIG. 5.34 EXPERIMENTALLY DETERMINED *NU* AS FUNCTION OF *RE* AT X=1.29 M. 103

FIG. 5.35 EXPERIMENTALLY DETERMINED *NU* AS FUNCTION OF *RE* AT X=1.29 M. 104

FIG. 5.36 LOCAL *NU* AS FUNCTION OF THE AXIAL DISTANCE IN THE PACKED CHANNEL. 105

FIG. 5.37 LOCAL *NU* AS FUNCTION OF THE AXIAL DISTANCE IN THE PACKED CHANNEL. 106

FIG. 5.38 COMPARISON BETWEEN THE EXPERIMENTAL PACKED CHANNEL PRESSURE DROP AND ERGUN'S PREDICTIONS. 111

FIG. 5.39 COMPARISON BETWEEN EXPERIMENTAL AND PREDICTED PRESSURE DROP BY BOHN CORRELATION. 112

FIG. 5.40 BEST FIT VALUES OF THE PRESSURE DROP IN THE PACKED SECTION AS FUNCTION OF THE AIR SUPERFICIAL VELOCITY. 115

FIG. 5.41 BEST FIT VALUES FOR THE *NU* AS FUNCTION OF *RE*. 118

FIG. 5.42 FULLY DEVELOPED VELOCITY PROFILES IN THE PACKED CHANNEL AS FUNCTION OF THE TRANSVERSE DISTANCE 119

FIG. 5.43 FULLY DEVELOPED VELOCITY PROFILES IN THE PACKED CHANNEL AS FUNCTION OF THE TRANSVERSE AT DIFFERENT *RE*. 120

FIG. 5.44 EXPERIMENTAL AND PREDICTED AIR TEMPERATURE PROFILES IN THE PACKED CHANNEL AT Q=230 W/M^2 123

FIG. 5.45 EXPERIMENTAL AND PREDICTED AIR TEMPERATURE PROFILES IN THE PACKED CHANNEL AT Q=230 W/M^2 124

FIG. 5.46 EXPERIMENTAL AND PREDICTED TRANSVERSE AIR TEMPERATURE PROFILES IN THE PACKED CHANNEL AT Q=230 W/M^2 125

FIG. 5.47 EXPERIMENTAL AND PREDICTED TRANSVERSE AIR TEMPERATURE PROFILES IN THE PACKED CHANNEL AT Q=230 W/M^2 126

FIG. 5.48 EXPERIMENTAL AND PREDICTED AIR BULK TEMPERATURE AS FUNCTION OF THE AXIAL DISTANCE. 127

FIG. 5.49 EXPERIMENTAL AND PREDICTED FULLY DEVELOPED NU AT X=1.29 M. 128

FIG. 5.50 EXPERIMENTAL AND PREDICTED FULLY DEVELOPED NU AT X=1.29 M. 129

FIG. 5.51 COMPARISON BETWEEN THE EXPERIMENTAL AXIAL AIR TEMPERATURE PROFILES IN THE EMPTY AND PACKED CHANNEL AT Y=0.05 , Q=130 W/M^2 133

FIG. 5.52 EXPERIMENTAL TRANSVERSE AIR TEMPERATURE PROFILES IN THE EMPY AND PACKED CHANNEL AT X=1.29 M, Q=230 W/M^2 134

FIG 5.53 COMPARISON BETWEEN EMPTY AND PACKED CHANNEL AIR BULK TEMPERATURE AT Re=2471 135

FIG. 5.54 COMPARISON BETWEEN EMPTY AND PACKED CHANNEL PRESSURE DROP. 136

FIG. 5.55 COMPARISON BETWEEN Nu OBTAINED IN THE EMPTY AND PACKED CHANNEL AT Y=1.29 M. 137

خلاصة الرسالة

اسم الطالب : ياسر طه مكاوى

عنوان الدراسة : تقصى انتقال الحرارة فى الاوعية المحشوة من خلال امدادها بكمية حرارة ثابتة

التخصص : الهندسة الكيميائية

تاريخ الرسالة : يونيو ١٩٩٥م

تم اجراء تجربه على انتقال الحرارة بالحمل فى وعاء مستطيل كبير الحجم محشو بحلقات اسطوانية من البلاستيك المقوى. التجربة اجريت بامداد السطح العلوى للوعاء بكمية حرارة ثابتة تتراوح ما بين ٥٠ الى ٥٥٠ واط/م٢ و رقم رينولدز يتراوح ما بين ١٠٠٠ الى ٥٥٠٠ في وعاء كبير الحجم بنسبة عرض/ارتفاع=٨ . فى التجربة تم قياس كمية الحرارة الموجهة, كمية الهواء الداخل, انخفاض الضغط و توزيع درجة حرارة الهواء داخل الوعاء. كما تم اجراء تجارب اخرى و تحت نفس الظروف فى وعاء خالى للمقارنة بين الاداء الحرارى للوعاء المحشو و الخالى معا.

من خلال التجارب تم ملاحظة ان قيمة رقم نسلت تزيد زيادة ملحوظة بزيادة رقم رينولدز. بنا على نتائج التجارب فى الوعاء المحشو تم استنباط علاقة رياضية تربط ما بين رقم رينولدز و رقم نسلت. ايضا تم ملاحظة ان قيمة رقم نسلت فى الوعاء المحشو تزيد حوالى ٦ مرات عن ما هى عليه فى الوعاء الخالى.

فى هذا البحث تم اعداد علاقات رياضية لمحاكاة انخفاض الضغط, توزيع سرعة و درجة حرارة الهواء داخل الوعاء المحشو. كما تم مقارنة نتائج درجة حرارة الهواء و معامل انتقال الحرارة بين الحائط و الهواء المستنبطة من حل العادلات الرياضية مع نتائج التجارب حيث ثبتت فعالية العلاقات الرياضية فى محاكاة الاداء الديناميكى و الحرارى للوعاء المحشو فى حدود الظروف المستخدمة فى التجارب.

درجة الماجستير فى العلوم

جامعة الملك فهد للبترول و المعادن

الظهران, المملكة العربية السعودية

يونيو ١٩٩٥م

THESIS ABSTRACT

NAME OF STUDENT *: YASSIR T. MAKKAWI*

TITLE OF STUDY *: Investigation of heat transfer in a rectangular packed Duct with constant heat flux and asymmetrical wall temperatures*

MAJOR FIELD *: Chemical Engineering*

DATE OF DEGREE *: June, 1995*

An experiment has been Carried out for forced convection of air in a rectangular packed duct with large Rashig rings hard plastic packing. The experiments were conducted for a constant heat flux ranging from 50 to 550 W/m^2 *and Reynolds number ranging from 1000 to 5500 in a large rectangular channel of an aspect ratio* $W/H = 8$ *. Heat supplied, air mass flow rate, pressure drop and temperature distribution inside the channel were measured. Experiments under the same operating conditions and without packing has been carried out for comparison between empty and packed channel thermal performance.*

It is found that the value of Nu increases considerably in the packed channel as Re increases in the range of operating conditions considered in the study. Based on the experimental results, a correlative equation for Nu in terms of Re has been obtained as, $Nu = 0.8334\, Re^{0.6836}$ *. It is also found that the value of Nu is about 6 times higher in the packed channel than in the empty one.*

For predicting the pressure drop, velocity and temperature distribution in the packed channel a numerical simulation model has been developed. The comparison between the experimental and the predicted results for the air temperature distribution and Nu has shown a good agreement within the range of operating conditions considered in the study.

MASTER OF SCIENCE DEGREE
KING FAHD UNIVERSITY OF PETROLEUM AND MINERALS
DHAHRAN, SAUDI ARABIA
JUNE, 1995

CHAPTER 1

INTRODUCTION

The fluid dynamics and heat transfer behavior of fluid flow through packed tube and channel is of special interest because of the wide applications of such geometry in chemical engineering processes. As the heat transfer coefficient from wall to air is small compared with those obtained for liquids, radial heat transfer in wall heated or cooled tubular reactors and other heat transfer equipments is very low. Although air is a fluid that provides easy operating conditions, direct use of heat recovered, and less corrosion and hence longer useful life for heat transfer equipment, low heat transfer rate creates a major drawback for air as a heat transporting fluid.

One of the best ways of increasing the heat transfer from wall to air is to introduce a suitable packing into the air passage. The packing cause mixing and prevents the build up of a slow moving layers of fluid next to the wall and therefore increases the wall-to-air heat transfer coefficient. This increase reaches a maximum at a certain ratio of packing to channel diameter and flow regime (*1,2*). This indicates the real effect of these two factors on the thermal performance of such system.

1.1 Enhanced heat transfer in packed duct and its applications

Packed ducts and tubes have been widely used in the chemical industry and for energy storage purposes. Due to their high performance, a number of investigations have been conducted in order to analyze the thermal behavior of packed channels (*3,4*). As early as *1931* Colburn (*5*) found that forced convection heat transfer through a packed tube is about eight times higher than that of an empty bed while recently it is reported as three times only (*6*). Experimental investigation of heat transfer in a rectangular heated channel has also shown a considerable increase in the wall-to-fluid heat transfer coefficient by using packing in the flow passage (*1,2*). The substantial increase in the heat transfer rate has been attributed to the mixing of fluid owing to the presence of the solid matrix. During the last five decades, experiment has been reported on the forced convection of air through cylindrical and annular packed columns with different duct to particle diameter ratio and different flow regimes (*4,6*).

Among the most common applications of a rectangular heated channel are heat exchangers, catalytic reactors, adsorption and desorption operations, automotive catalytic converters, nuclear reactors, solar air heat collectors, oil extraction and the manufacturing of numerous products in chemical industry.

These diverse applications have made it essential that the thermal engineering community focus its research interest on the fundamentals of packed bed processes. The accumulation impact of these studies is twofold: first to improve the performance of existing packed ducts media related thermal systems, and second to generate new ideas and explore new avenues with respect to the use of packing material in heat transfer applications.

1.2 Simulation of heat transfer in packed ducts

The simulation of heat transfer in a packed duct has been the subject of many recent studies, due to the increasing need of better understanding the associated transport process in a packed duct or tube (*7,8,9,10*). A major problem with such simulation is the difficulties associated with the prediction of the thermal behavior with respect to operating conditions, geometry of duct, size and type of packing. For such a simulation, a good mathematical model is needed, capable of accurately predicting the temperature profiles, given a certain packed channel design (such as length, width, particle diameter and shape) and operating conditions (such as gas flow rate, inlet temperature and pressure, and heat supplied). This is usually done by numerically solving the continuity and momentum equations together with the energy balance for the packed duct. To validate the mathematical model, the predicted temperature

profile and wall-to-air heat transfer coefficient are usually compared with the experimental results.

1.3 Effective parameters on heat transfer

1.3.1 Geometry of bed, size and type of packing

As the packing size decreases, the distance over which each mixing process occurs is decreased. On the other hand there are a large number of more or less stagnate films between the air and the packing that heat must cross in reaching the opposite wall. This shows the importance of carefully choosing the particle to channel diameter ratio and the flow regime.

Previous investigations on the effect of type and shape of packing on the thermal performance of a packed channel has shown that by choosing nontoxic, noncorrosive Raschig ring type of packing (hollow cylinder) the heat transfer rate can be increased considerably without excessive cost (*1,2,11*).

1.3.2 Flow regime and pressure drop

Transferring of heat to air flowing through a packed bed has been of industrial importance. The main reason behind this is the large surface area of the packing material and the better mixing of air which provides a rapid

increase of heat exchange. However, the higher heat transfer to the flowing air in any packed bed is associated with high pressure drop. It is necessary to ascertain that the pressure drop across the packed bed is large enough to ensure good flow distribution across the bed ; On the other hand, it is necessary to keep the pressure drop very low so that energy spent in air pumping through the bed is low enough to make the system cost effective (*11*).

Recent studies have shown an increase in the overall heat transfer coefficient in packed channel within some limited range of *Re* (*1,6*). It is of vital important to determine the increase of heat transfer within different flow regimes.

1.4 Relevant properties of air and packing particles

Raschig ring type of packing (hollow cylinders) made of hard plastic (*PVC*) is used as the packing material inside the flow passage for the present study. This type of packing is specially preferred to produce a reasonable pressure drop along the channel, beside its cheap cost. All the physical properties of air and solid packing are taken to be constant and calculated at the inlet temperature and pressure of the air provided that temperature and

pressure variations are insufficient to cause any considerable change in the properties of the medium.

1.5 Scope and objectives of this study

Literature review on heat transfer on packed beds reveals that the mathematical modeling in terms of the Nusselt number, Reynolds number, and packing to channel diameter ratio is the latest trend in this area.

To provide some experimental data, wall-to-air heat transfer coefficient has been measured in the packed bed with unequal wall temperatures. Steady state measurements were taken to investigate the effect of packing and the air flow rate on the heat transfer coefficient. Experimental results are used to validate the mathematical model and the analytical expression of the heat transfer coefficient. As the most of the existing studies are for cylindrical geometry, the property of the one sided heating is another unique side of this investigation beside the large scale of the experimental equipment used.

The primary objective of this work is to present an experimental study of forced convection heat transfer in a large scale packed rectangular duct with unequal wall temperatures, also to present a mathematical model to simulate the thermal behavior of such system and compare the calculated results with the experimental measurements. Very few studies on forced convection

through a packed rectangular channel is experimental, even fewer have compared modeling with experimental results.

The following items constitute the specific objectives of the experimental part of this work,

1. Measurement of air and wall temperatures at different positions.

2. Measurement of pressure drop caused by the presence of the packing material inside the channel.

3. Operate under different mass flow rate of air to explore the effect of flow rate on heat transfer rate.

The following items constitute the specific objectives of the modeling part of this work

1. For the mathematical model of air flow through a packed rectangular channel, a model that accurately predict the dynamic and thermal behavior of the system has been employed. The pressure drop was calculated by using a modified Ergun equation then by Using the finite difference the momentum equation was solved to determine the velocity field distribution.

2. The flow field was introduced into the energy equation and using implicit finite difference technique the temperature distribution was determined.

3. Calculated temperature distribution and wall-to-air heat transfer coefficient were compared with the ones obtained from the measurements. This accuracy check was the crucial evaluation of the mathematical model.

CHAPTER 2

LITERATURE REVIEW

2.1 Introduction

The problem of thermally developing forced convection flow in a packed channel with asymmetric heating has been studied intensively during the last five decades. One of the pioneers in this area was Colburn (*5*) who reported in *1931* that wall-to-fluid heat transfer can be increased about eight times than in empty tubes by using packing inside the flow passage. Theoretical studies have shown that the geometry of bed and the size of packing are the two important parameters along with the flow conditions which will determine the increase in heat transfer. In terms of non dimensional groups this may be expressed as relationship between *Nu*, *Re* and the ratio of packing size to equivalent diameter of the channel .

2.2 Background on previous experimental studies

2.2.1 Particle and channel size effects

The influence of the particle and channel diameter, as well as their ratio and the packing shape, on the thermal performance of packed tubes and channels has been studied in literature. This is usually done by changing the

packing size at the same channel diameter. It is worth noting that most of the existing experimental and theoretical studies are carried out under small scale dimensions, unlike the present work which to my knowledge is the first to be carried out in such a large scale experimental equipment.

Hwang et al (*6*) carried out an experimental study on forced convection in a packed rectangular channel with asymmetric heating using Freon-*13* as the working fluid. The experiments were conducted in a channel of *660.4 mm* length, *203.2 mm* width and *304.8 mm* depth, the cross-sectional flow area of the channel was *50.8* X *152.4 mm* . Glass spheres of diameter ranging from *3-6.35 mm* were used as the packing material. Both the heat flux to the wall and transverse temperature profiles inside the channel were measured. It was found that the *Nu* increase in the range of flow considered. It was also found that heat transfer in a packed channel is approximately three times higher than that in an empty channel.

Demirel (*1*), presented an experimental study on the influence of size and type of packing on the heat transfer rate in a rectangular packed empty channel with asymmetrical wall temperatures, in his study an experimental data on a *255* X*80*X *675 mm* channel with different type and size of particle were presented. The maximum value of heat transfer coefficient of a packed

channel (h_p) was found to be at maximum when packing to channel diameter ratio (D_p/D_e)=*0.0975*, while smith (*12*) reported that it is maximum at D_p/D_e =*0.15* in a packed tube. In a similar study by Demirel and Kunc (*2*) it was also shown that (h_p) has a maximum at (D_p/D_e)=*0.15*. According to these studies it was obvious that the packing size is an important factor, and heat transfer by convection dominate the other mechanism of conduction and radiation for the air flow rates and packing size considered in the measurements, no serious effect of packing material has been observed (*1*).

In an experimental work by Dixon (*13*), the effective thermal conductivity and apparent heat transfer coefficient for a packed tube were experimentally determined for beds of spheres, full cylinders and hollow cylinders, for tube to particle diameter ratios ranging from *5* to *12*. Both the Peclet number (Pe) and the Biot number (B_i) showed significant dependence on tube to particle diameter ratio over the operating conditions considered .

Experiments conducted in a rectangular packed channel with an aspect ratio (*width/hight*) greater than *4* are very rare in literature. While experimental studies conducted for effective channel to packing diameter ratio (De/D_p of greater than *7* are reported in literature. As an example, Chou et al

(*14*) studied experimentally the effect of (De/D_p) on the thermal performance of a rectangular packed channel made of *65 cm*X*9.5 cm*X*9.5 cm* stainless steel using water as a working fluid. The ratio of equivalent hydraulic diameter to sphere diameter significantly affects the Nusselt number when the Peclet number (*Pe*) is high, this was mainly attributed to the thermal dispersion effects (*14*).

Borking and Westerterp (*15*) studied experimentally the influence of the tube and particle diameter and shapes, as well as their ratio on the radial heat transfer in packed tube. It was found that the Bodestien number (Bo_h) for fully developed turbulent flow was strongly influenced by the shape of the packing

(glass spheres, alumina cylinders, and alumina Raschig rings). For the same packing, no significant influence was found of the tube diameter on the effective radial conductivity.

The efficiency of packed air flow passage as function of packing diameter and shape has been studied by Choudary and Garg (*11*). In their study it was clear that smaller diameter of packing result in higher efficiency as well as large pumping cost of air, however, in air heaters with ring-shaped, there seems no much rise of pumping power cost.

The above brief survey on channel and packing size effect reveals that channel and packing size as well as their ratio must be taken into consideration in the design of a packed heated channel.

2.2.2 Flow regime effects

The fluid dynamics and heat transfer behavior of fluid flow through packed tubes and channels is of special interest because of the considerable effects of the flow regime on the design of such system. Experimental data for the *Nu* as function of *Re* in packed channels often shows considerable disagreement from one study to the next, with discrepancies as large as 100 % being reported (*16,17*).

In an experimental study by Hwang et al (*6*) it is shown that as the value of *Re* is increased, the value of average Nusselt number ($\overline{Nu}$) varies gradually from horizontal line where conduction is pre-dominant to an inclined straight line where convection becomes pre-dominant. Results for temperature distribution at different flow regimes were also shown.

Demirel (*1*) investigated experimentally the effect of flow regime on heat transfer rate using air as the working fluid in an asymmetrically heated channel. The value of *Nu* shows a maximum at *Re* (based on superficial velocity and equivalent channel diameter) of about *650*. In a similar

experiment, Choudhry and Garg (*11*) investigated the performance of air heating collectors with packed air flow passage with different mass flow rates. Large air mass flow rate has shown a considerable increase in the system efficiency, but higher pressure drop and hence higher pumping power cost.

2.2.3 Calculation of Nusselt number

In chemical reactor and packed bed engineering literature the *Nu* is usually defined in terms of particle diameter D_p, heat transfer coefficient h_w, and the thermal conductivity of the fluid k_f. Thus the *Nu* is defined as

$$\mathrm{Nu} = \frac{\mathrm{h_w\, D_p}}{\mathrm{k_f}} \qquad (2.1)$$

In a rectangular heated channel, Hwang et al (*6*), calculated *Nu* experimentally based on the plate separation distance *H* and the stagnate thermal conductivity instead of the particle diameter and the thermal conductivity of the fluid respectively, while Chou et al (*14*) and Demirel (*1*), reported an experimental *Nu* based on the effective channel diameter D_e.

Wall-to-air heat transfer coefficient is generally defined as local values representative of a cross-sectional through the bed by the following relation,

$$dQ = h_{loc}(b\,\mathrm{dx})\,(T_w(x) - T_b(x) \qquad (2.2)$$

in which $b\,dx$ is the available heated surface area, Q is the heat flow to the fluid, $T_w(x)$ and $T_b(x)$ are the temperatures of the wall and bulk fluid at x respectively.

Frequently experimental data reported average heat transfer coefficient based upon an arbitrarily defined temperature differences, the most two common being used are as follows (18),

$$Q_{\ln} = \frac{h_{lm}\, A\,(\Delta t_{in} - \Delta t_{out})}{\ln(\Delta t_{in}/\Delta t_{out})} \tag{2.3}$$

$$Q_{am} = \frac{h_{am}\, A\,(\Delta t_{in} - \Delta t_{out})}{2} \tag{2.4}$$

where h_{ln} and h_{am} are average heat transfer coefficients based upon the logarithmic mean temperature and the arithmetic average temperature respectively. The coefficient h_{ln} is preferable for most calculation, however it is not universally used (*19*). On the other hand, most experiments report only the average heat transfer coefficient ($\overline{h_w}$), which is more easily measured, however h_{loc} is more informative than $\overline{h_w}$ because it shows how the heat flux is distributed inside the packed channel.

Experimental calculation of wall-to-air heat transfer coefficient can also be expressed in terms of net air enthalpy rise as follows (*19*),

$$h_{loc} = \frac{-\dot{m}C_p}{b}\left(\frac{dT_b}{dx}\right)\left(\frac{1}{T_w(x) - T_b(x)}\right) \qquad (2.5)$$

were $\dot{m}$ is the flow rate of the fluid and C_p is the specific heat of the fluid at constant pressure.

2.3 Background on previous theoretical studies

The simulation of heat transfer in a packed bed has been the subject of many recent studies, due to the increasing need for better understanding of the associated transport process in a packed channel, beside the difficulties and expenses which may be associated with the experimental work such as the scale up of the experimental equipment and the operation under different conditions.

The numerical solution usually involve the simultaneous solution of the continuity, momentum and energy equations along with the boundary and initial conditions consistent with the heat transfer system.

2.3.1 Simulation of velocity distribution

In mathematical modeling of convective heat transfer in a packed channel the knowledge of the velocity distribution inside the bed is necessary.

The flow is generally governed by the requirement of mass conservation which provides the continuity equation,

$$\Delta G = 0 \tag{2.6}$$

were G is the mass flow rate. The momentum equation, which for incompressible fluid is usually expressed in the form of Ergun equation (*19*),

$$-\nabla P = (f_1 + f_2|\upsilon|)\upsilon \tag{2.7}$$

were υ is the superficial velocity vector, f_1 and f_2 account for the viscous and inertia effects respectively, and are defined as follows,

$$f_1 = \frac{150(1-\varepsilon)^2}{\varepsilon^3 D_p^{\,2}}\mu \tag{2.8}$$

$$f_2 = \frac{1.75(1-\varepsilon)\rho}{\varepsilon^3 D_p} \tag{2.9}$$

Despite Ergun equations attractive simplicity the most serious drawback is the lack of parameters characterizing the structure of the packed bed.

Cheng et al (*21*), presented a mathematical model simulation of fluid flow inside a channel with asymmetric heating. The momentum equation applied for the flow distribution was based on the Brinkman-Darcy-Ergun model (*22*),

$$\frac{\mu\upsilon}{K} + \frac{\rho F}{\sqrt{K}}\upsilon^2 = -\frac{dP}{dx} + \frac{\mu}{\varepsilon}\frac{d^2\upsilon}{dy^2} \tag{2.10}$$

the two parameters K and F which depend on the packing diameter and void fraction of the bed were defined as follows,

$$K = \frac{\varepsilon^3 D^2_p}{150(1-\varepsilon)^2} \tag{2.11}$$

$$F = \frac{1.75}{\sqrt{150}\,\varepsilon^{3/2}} \tag{2.12}$$

the velocity profile was assumed to be symmetric about the centerline of the channel, so only half of the packed channel was considered in their solution.

Polkakes and Renken (*7*) presented a similar mathematical model for a rectangular channel in which the developed flow field was described by the following x-momentum equation,

$$0 = -\frac{1}{\rho}\frac{dP}{dx} + \mu\frac{d}{dy}\left(\frac{d\upsilon}{dy}\right) - \frac{\mu}{K}\upsilon - A\upsilon^2 \tag{2.13}$$

were A and K are empirical functions which depend on the structure of the packed bed and defined as follows,

$$K = \frac{\varepsilon^3 D^2_p}{175(1-\varepsilon)^2}$$
$$A = \frac{1.75(1-\varepsilon)}{\varepsilon^3 D_p} \tag{2.14}$$

Borkink and westerterp (*15*) has presented a theoretical and experimental study on the influence of tube and particle diameter on heat transport in packed beds, in their analysis the mathematical model was based

. on constant velocity over the radius based on the superficial velocity. It is worth noting that the same assumption has been considered by the same workers in other recent reported studies (*9,23*).

2.3.2 Simulation of temperature distribution

The heat transfer characteristic of steady state thermally developing forced convection flow in a packed channel heated asymmetrically has been analyzed by many workers in the last five decades.

Cheng et al (*21*) reported a mathematical model of heat distribution in a packed channel with asymmetric heating. The thermally developing flow has been analyzed by the following two dimensional equation,

$$\rho C_p \upsilon \frac{\partial T}{\partial x} = \frac{\partial}{\partial y}\left(k_e \frac{\partial T}{\partial y}\right) \qquad (2.15)$$

the effective thermal conductivity k_e was taken to be as function of the bed structure and the fluid flow distribution (*21*). In a similar study by Chou et al (*14*) a steady state thermally developing flow has been simulated by a three dimensional model including the dispersion of heat in the three directions *x, y, z* as follows,

$$w\frac{\partial \theta}{\partial z} = \frac{\partial}{\partial x}\left(\frac{k_e}{k_f}\frac{\partial \theta}{\partial x}\right) + \frac{\partial}{\partial y}\left(\frac{k_e}{k_f}\frac{\partial \theta}{\partial y}\right) + \frac{1}{Pe^2}\frac{\partial}{\partial z}\left(\frac{k_e}{k_f}\frac{\partial \theta}{\partial z}\right) \qquad (2.16)$$

Young et al (*24*) reported a theoretical study on the inclusion of axial dispersion of heat in a two dimensional modeling of heat transfer in a cooled or heated tubular reactor, their results has shown a significant effect on the predicted temperature profile. Although recently Borking and Westerterp (*23*) have shown the temperature profile to be relatively insensitive to the value of the effective axial dispersion if the correct radial inlet temperature profile is used and the *Re* based on particle diameter exceeds *50* (*23*). Also extensive recent computer simulations showed axial dispersion of heat to be of minor importance for practical conditions (*25,26*).

Polkakes and Renken (*7*) reported an energy equation describing the temperature distribution inside a heated channel with neglected axial conduction term as follows,

$$\upsilon \frac{\partial T}{\partial x} = \alpha_e \left(\frac{\partial^2 T}{\partial y^2} \right) \qquad (2.17)$$

noting that the effective thermal diffusivity, that is denoted by α_e, is taken to be constant (*7*).

2.3.3 Simulation of Pressure drop

The ability to predict a reliable pressure drop through packed beds is of great significance since pumping cost are directly related to pressure drop of

the system in question. When pressure drop and flow information is required for a wide range of *Re* in packed bed configuration, the Ergun equation (*19*) has been the favorite choice amongst literature correlation. Ergun equation effectively accounts for simultaneous inertia and viscous energy losses, and a fair amount of pressure drop flow data have been correlated by it for beds with various geometrically shaped particles, however Ergun's equation has a serious drawback since it is generally good for void fraction less than *0.5* (*19*).

It is for this reason a modified Ergun equation has been proposed by different studies in literature. Recently Foumeny et al (*20*) have reported an experimental study on the effects of the confining wall of a tubular packed channel on the pressure drop. The two constants *150* and *1.75* were replaced respectively by *A* and *B* which are defined as follows (20),

$$A = 130$$

$$B = \left(\frac{\left(D_t / D_p\right)}{0.335\left(D_t / D_p\right) + 2.28} \right) \qquad (2.18)$$

There are other Ergun based equations in the literature which mainly cast doubt on the universal constants *150* and *1.75* in the original equation.

Handley and Heggs (*27*) proposed a constant *368* and *1.24*, instead of the respective values *150* and *1.75* as proposed by Ergun (*19*).

Bohn and Swanson (*28*) reported a correlation expression relating the friction factor to the *Re*, the resulting expression was as follows,

$$f_{\cdot} = 6.508\left(\mathrm{Re}_{g}\right)^{-0.241} \qquad (2.19)$$

This expression has been obtained by a least square curve fit procedure to the experimental result in a packed tube of *150 mm* (ID) column with *610 mm* hight and filled with metal rings. Air was taken as the working fluid in the rang 0f *0.3* to *1.4* kg/m^{2}s.

It is worth noting that most of the reported experimental results of pressure drop were taken in a packed channel of void fraction of less or equal to *0.6*.

2.3.4 Correlation equation for Nusselt number

The purpose of the early studies was to obtain the appropriate heat transfer parameters for the numerical simulation of the performance of wall cooled or heated catalytic reactor and packed heating systems. For this purpose correlation equations of the average wall-to-air heat transfer

coefficient as function of dimensionless parameters were needed. The most common definition of *Nu* is,

$$\mathrm{Nu} = \frac{h_w D_p}{k_f} \tag{2.20}$$

In a recent review on the packed bed heat transfer performance Cheng (*21*) have attributed the disparity of the Nusselt number correlation equation to the fact that the heat transfer rate was not measured directly, and to the methods used for the determination of *Nu* in the heated or cooled flow passage.

Hwang et al (*6*) has reported a correlation equation of the *Nu* based on the experimental results obtained in a packed and empty channel with asymmetric heating, (see table *2.1*). The following correlation equation for the packed channel *Nu* based on the separation distance *H* was obtained as,

$$Nu = 0.31(\mathrm{Re}_h)^{0.814}(e)^{-1.638\gamma} \tag{2.21}$$

were $\gamma = \frac{D_p}{H}$, the above equation is valid for forced convection of Freon-113 at $400 \le \mathrm{Re}_h \le 1700$, $0.06 \le \gamma \le 0.13$, and $\mathrm{L/H} = 9$ (*6*).

Li and Finlayson (*29*) presented different correlation expressions of h_w according to different experimental data on heat transfer in packed tubes. The

correlative expression obtained for *Nu* is valid in the range of *Re* $(=\frac{\rho \upsilon D_p}{\mu})$ ranging from *20* to *800* and D_p/D_e from *0.03* to *0.2* . The following correlation for *Nu* obtained for cylindrical packed bed with constant heat flux was obtained,

$$\frac{h_w d_p}{k_f} = 0.16\left(Gd_p/\mu\right)^{0.93} \tag{2.22}$$

Other forms of correlations tried in their study are shown in table (*2.2*) with the average deviation from the experimental data.

Dixon (*13*) reported a study on the wall and particle effects on heat transfer in packed beds, and constructed new correlation of *Nu* which is related to the *Re* , *Pr* and D_p/D_e by,

$$Nu = 0.523\left(1 - D_p/D_t\right)(\mathrm{Pr})^{0.33}(\mathrm{Re})^{0.783} \tag{2.23}$$

the dependence of *Nu* on the Prandtl number is just an assumption, no reported study used a range of fluid that would prove or disprove the one-third power which appears in the above equation (*13*). Mainly it was found that the exponent of the *Re* number in the correlation equation for the *Nu* varies widely from *0.33* to *1*.

There is a question of how far it is worthwhile to refine prediction formula such as those reviewed above and also how accurate is the measurement of these parameters. As Bohn and Swanson (*28*) suggested that the testing at a large scale is required before the correlation equation can be fully validated. This point is one of the main concern in this study.

Many other forms of correlations have also been proposed in the literature. Table (*2.3*) shows a summarized review on these correlations.

Table 2.1 Experimental data on a packed channel with asymmetric heating (*6*)

Run No.	GPM	T_h-T_c (^oC)	q_w (W/m^2)	Re_h	Nu_h
6.35 mm chrome steel beds, ε=0.3423, γ=0.125, k_d=1.324 W/mK					
r261	2.07	16.11	4110	2148	174
r272	3.98	16.23	5131	4130	216
r280	5.94	15.31	7039	6164	314
r286	8.0	15.40	8280	8301	367
r291	9.96	15.26	10009	10335	448
r295	12.0	14.80	11238	12452	519
r299	14.01	14.67	13094	14537	609
r302	15.97	14.23	14110	16571	677
Empty channel, kf=0.0744 W/mk					
pr16	5.19	15.70	2541	5385	111
pr18	7.67	15.46	1930	7959	129
pr10	10.05	15.39	3489	10428	155
pr20	12.02	14.38	3734	12472	177
pr12	14.07	16.54	5142	14600	212
pr22	15.90	14.62	5122	16498	239
pr24	17.86	13.99	4913	18532	240
pr27	19.80	13.85	5503	20545	271
pr28	21.85	15.56	6050	22672	165

Table 2.2 Correlations tested for heat transfer coefficient (*29*)

Correlation	a	b	average deviation %	R^2
h_w, Spherical packing				
$Nu = a\,\mathrm{Re}_p^b$	0.17	0.79	14	0.98
$Nu = a + b\,\mathrm{Re}_p\,\mathrm{Pr}$	10.7	0.033	73	0.94
$Nu_m = a\,\mathrm{Re}_m^b$	0.029	0.94	21	0.97
$Nu = a\left(\mathrm{Re}_p\,\mathrm{Pr}\right)^{0.33} + b\,\mathrm{Re}_p^{0.8}\,\mathrm{Pr}^{0.4}$	1.33	0.14	38	0.98
h_w, Cylinderical packing				
$Nu = a\,\mathrm{Re}_p^b$	0.16	0.93	33	0.85
$Nu = a + b\,\mathrm{Re}_p\,\mathrm{Pr}$	5.21	0.126	62	0.76
$Nu_m = a\,\mathrm{Re}_m^b$	0.03	1.06	39	0.85
$Nu = a\left(\mathrm{Re}_p\,\mathrm{Pr}\right)^{0.33} + b\,\mathrm{Re}_p^{0.8}\,\mathrm{Pr}^{0.4}$	0.36	0.38	49	0.79

Table 2.3. Emperical correlation functions of Nusselt number .

Dimensionless form of working equation	Range of applicability	Channel type	References
$Nu_D=o.536(x^2Re_p+Pr_e\tau_w)^{1/3}$	$Re > 50$	Rectangle	Polkakos and Renken (3)
$Nu_p=(1-d_p/d_t)(Pr)^{0.33}(Re_p)^{0.6}$	$Re > 50$	Tube	Anthony Dixon (13)
$Nu_p=0.155(Re_p)^{0.75}(Pr)^{1/3}$	$Re > 50$	Tube	Areov and Uminik (30)
$Nu_p=0.2(Re_p)^{0.8}(Pr)^{1/3}$	$10 < Re_p < 250$	Tube	Dixon and Cresswel (31)
$Nu_D=7+0.025(RePr)^{0.8}$	$Re_p > 10$	Tube	R. N. Lyon (32)
$Nu_D=0.8+0.1N^{1/3}\{1+2.1N^{1/3}(\mu/\mu)^{0.14}\}$ $N=RePrD/L$	$N > 100$	Rectangle	Robert H. Perry and Don Green (18)

CHAPTER 3

EXPERIMENTAL APPARATUS AND PROCEDURE

3.1 Introduction

The purpose of the early experimental studies on heat transfer in packed channels was to obtain the appropriate heat transfer parameters for the numerical simulation of the performance of the system considered. Usually experiments for this purpose are carried out by forcing a fluid through a heated or cooled packed channel with different operating conditions (*1,2,6*), such as the flow regime, and the amount of heating supplied to the system. The appropriate heat transfer parameters are then calculated from the experimental data obtained under steady state condition. On the other hand the experimental data are used to validate and check the accuracy of the mathematical model. A line diagram of the experimental arrangement used in this study is shown as Figure (*3.1*)

3.2 *Apparatus*

3.2.1 Rectangular channel

The experimental heated channel is shown in Figure (*3.2*). The rectangular flow passage is of *180 cm* long which includes three sections, namely the entrance, packing, and exit section, each of *10, 160, 10 cm* long respectively and a cross-sectional area of *80X10 cm*. The rectangular flow passage which is horizontally oriented is made of *10 mm* thick phelexy glass while the top heated plate is made of stainless steel of *1.0 mm* thick. Two distributor plates are placed at the inlet and outlet sections of the channel to get a better distribution of the incoming air flow and support the packing. All the side walls, top and bottom are insulated from surrounding to minimize heat losses.

3.2.2 Heating Elements

Two electric heating elements hanged on the bottom of a galvanized mild steel plate were used to provide uniform heat flux along the air flow passage. Each heating element could provide a maximum of *1000 W*. Two adjustable electric power input (rheostat) were used to provide the adjustable

uniform heat flux. Figure (*3.3*) shows the arrangement of the resistance-heating wires on the bottom of the galvanized mild steel sheet.

3.2.3 Insulating material

The top heating element insulated with a Vermiculite insulating material that is of *5.0 cm* thick and *0.12* $W/m^{o}c$ thermal conductivity. All the side walls, bottom and top plates were insulated. Experimental results has shown an estimated heat losses of about *30* percent through the top plate and about 8 percent of the total heat supplied through the bottom plate.

3.2.4 Thermocouples

Thirty K-type thermocouples of accuracy ± *0.1°C* were used for temperature readings. Twelve thermocouples which are inserted inside the channel from one side wall are located *24, 40 and 60 mm* away from the heated top plate and *30, 63, 96 and 129 cm* away from inlet distributor plate, beside, *2* thermocouples were placed at the inlet and outlet sections of the flow passage, *4* thermocouples were placed on the bottom plate at *30, 63, 96 and 129 cm* away from the inlet distributor plate. Six thermocouples were placed over the top heated plate at *15, 41, 67, 93, 119 and 134 cm* away from the inlet distributor plate. Details of the thermocouples distribution are shown

in Figure (*2.4*). For measuring the heat losses to the surrounding through the top plate, *6* thermocouples were placed over and bellow the top Vermiculite insulating sheet at *40, 80 and 120 cm* away from the inlet distributor plate. All the Thermocouples placed at the top and bottom plates were covered with Silicon material so as to reduce radiation effects from surrounding. Three selector switches each of *12* channel were connected to a digital displayer for temperature readings.

3.2.5 Flow meter

Air flow rate from the main air line compressor was calculated by measuring the incoming air velocity through the inlet pipe. Calibrated Anometer of the type *HHF710* which have a range of *0.3 to 35.0 m/s* was used for air velocity measurement. Air filter with a pressure regulator was placed in the same line and before the Anometer to retain any moisture or oil from the air compressor. The Anometer has an accuracy of *± 1%* of reading *(± 1 digit)*, and a resolution of *0.01 m/s*.

3.2.6 Manometer

A sensitive inclined manometer filled with red Merium liquid *(0.8 s.g)* was used for measuring the inlet pressure and the pressure drop caused by the

packing. The two ends of the Manometer were connected to the heated channel through *2* holes on the side wall, the holes were placed exactly at the two ends of the packed section (between the two distributor plates). Figure (*3.5*) shows the details of the Manometer and its connections to the channel.

3.3 Packing type and material

Raschig ring type of packing (hollow cylinders) with the following properties was used :

Material : Polyvinyl chloride plastic (PVC)

inside diameter : *4.0 cm*

outside diameter : *4.8 cm*

Height : *4.8 cm*

Thermal conductivity : *1.18 w/m^{o}c*

Density : *1320 kg/m^{3}*

specific heat capacity : *825.0*

Number of units : *910*

The packing was filled randomly through the top movable plate. Fig (*3.6*) shows the packing shape and dimensions.

3.4 Experimental procedure

Experiments were first conducted for forced convection of air in a packed heated channel under different air mass flux ranging from *0.05 to 0.5* $kg/m^2 s$, and different heat flux ranging from *50 to 550* W/m^2, by this we were able to evaluate the thermal performance of the system under varying operating conditions. Both the transverse temperature profiles and heat flux to the top plate were measured at a particular *Re*. Experiments were then conducted for forced convection of air in the same channel and under the same operating conditions with empty flow passage, by that we were able to compare between the thermal performance of the channel in both cases of packed and empty flow passage. For each run, the inlet pressure and the pressure drop were measured.

All measurements were carried out on a consistent basis once steady state hydrodynamic and thermal condition were reached, temperature, flow rate, inlet pressure, pressure drop, as well as current and voltage for each strip heater were recorded when a complete set of temperature data showed no differences to within the experimental accuracy of $\pm$ *0.2* ^oC for *30 min.* Experimental observations For different operating conditions has shown a

steady state conditions satisfied within an average time ranging from *4 to 6 hr.* The experiments were carried out within an average top plate temperature ranging from *35 to 85* ^{o}C. Each set of experiment was carried out for *2* runs, which makes a total of *40* experimental runs for packed flow passage beside *12* experiments conducted in the empty channel under the same operating conditions.

Special *30* experimental runs were carried out for measring the pressure drop, of which, *20* experiments were in the packed channel and *10* experiments in the empty channel. Measurements were tacken under varying mass flux rate ranging from *0.05 to 0.5* kg/m^2 *s.*

1. Valve	5.Thermocouples	9.Exit section	13.Rheostate
2.Air filter	6.Selector switch	10.Circit boards	14.Power supply
3.Flow meter	7.Inclined manometer	11.Ammeter	
4.Entrance section	8.Strip heaters	12.Voltmeter	

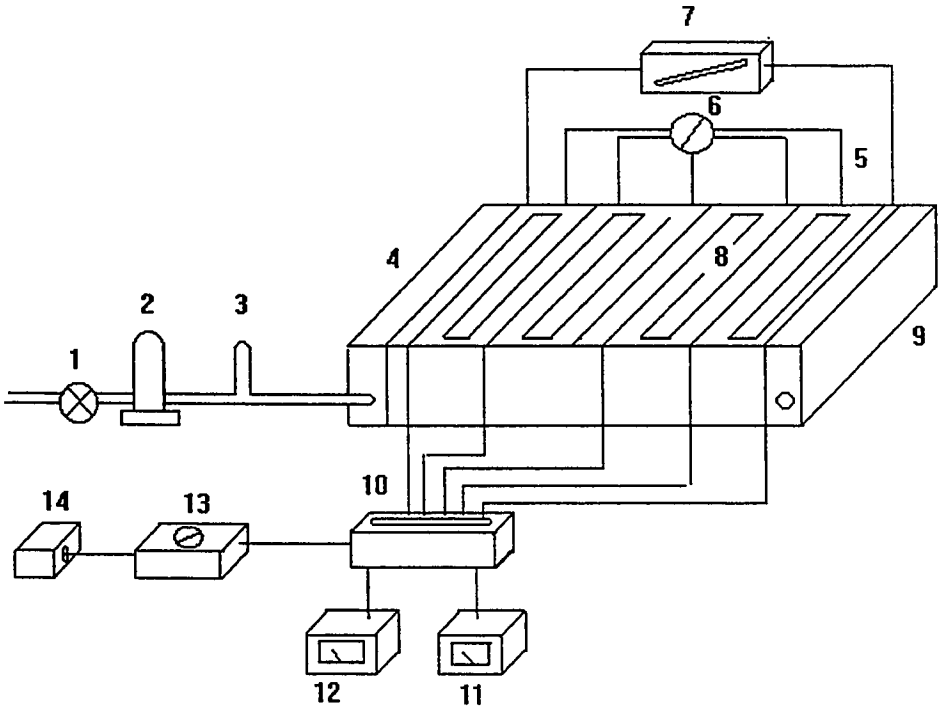

FIGURE 3.1 EXPERIMENTAL SET-UP

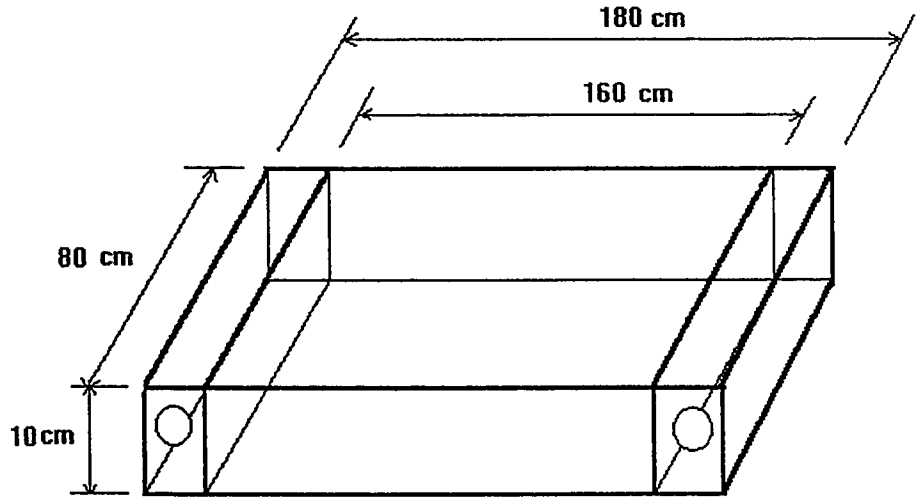

FIGURE 3.2 EXPERIMENTAL RECTANGULAR CHANNEL

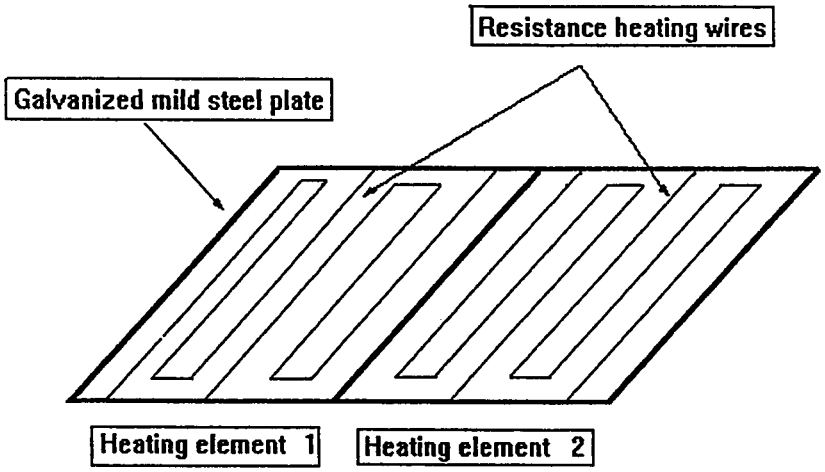

FIGURE 3.3 ARRANGEMENT OF THE RESISTANT-HEATING WIRES

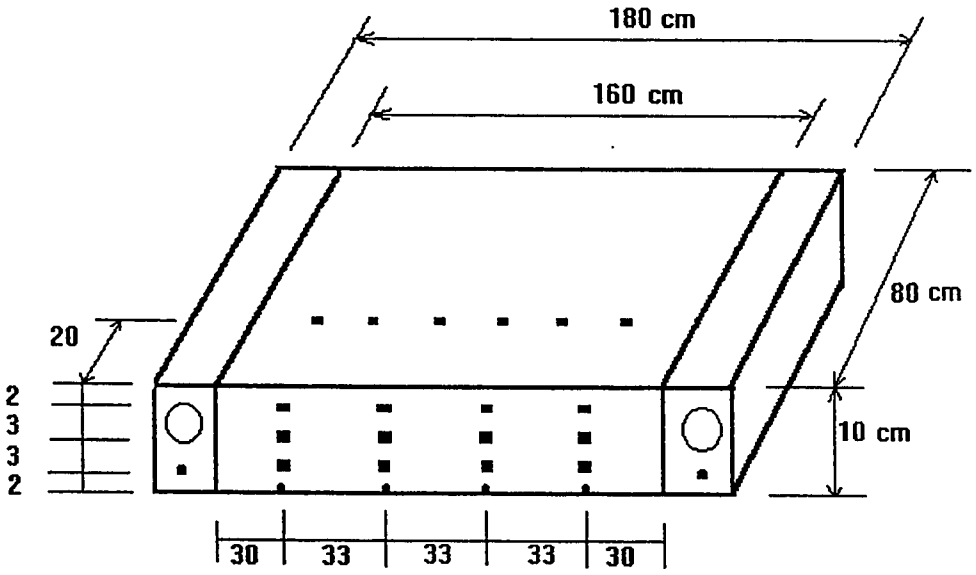

FIGURE 3.4 DETAILED DIAGRAM OF THERMOCOUPLES POSITIONS .

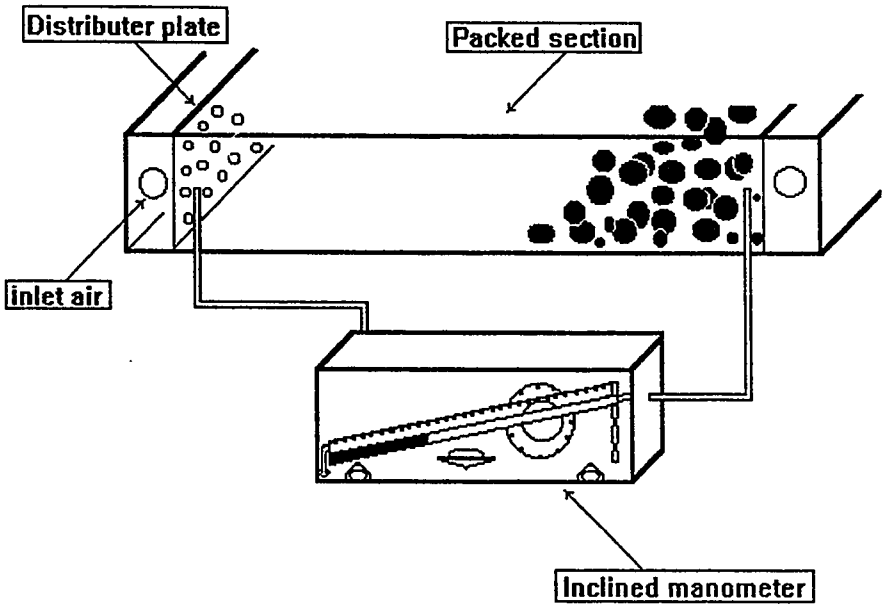

FIGURE 3.5 CONNECTIONS OF THE INCLINED MANOMETER TO THE CHANNEL

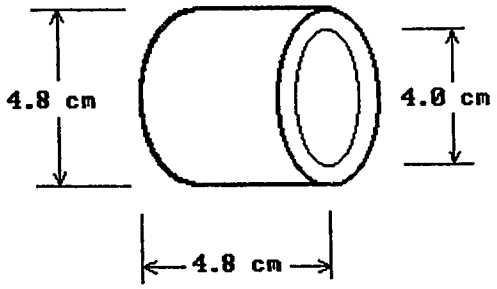

FIGURE 3.6 PACKING SHAPE AND SIZE

CHAPTER 4

Development of the mathematical model

4.1 Introduction

Mathematical simulation of packed channel heat transfer has proven to be an effective and important tool for studying the thermal performance of such system. Mathematical simulation provides good prediction with the ability to validate concepts and theories used in connection with experimental studies. Most of the previous theoretical studies has concentrated on heat and fluid flow in tubular packed channel with small scale flow passage and packing size, in contrast to these studies, the present model considers a rectangular flow passage with large scale of channel with asymmetrical wall temperatures and focuses on the effects of different flow regimes on the thermal performance of the system.

The objective of this part of the study is to develop a simple and efficient, time-independent mathematical model to simulate the thermal behavior of a rectangular packed channel with asymmetric heating. This is done by simultaneously satisfying the momentum and energy equations

together with the boundary conditions of the system. Figure *4.1* shows the geometry and coordinate system of the channel.

4.2 Assumptions

The mathematical model is based on the following assumptions:

1. The system is at steady state and no reaction takes place.
2. Air and solid packing are in local thermal equilibrium.
3. The air flow is considered as fully developed incompressible flow.
4. There is no radiation effects.
5. Thermal dispersion of heat in the x direction (main flow) is negligible in the energy equations.
6. Void fraction is constant in all directions.
7. Variation of the pressure drop with direction of flow is constant.
8. Physical properties of the air and solid packing are constant calculated at the inlet conditions.

4.3 Parameters definition

4.3.1 Bed void fraction

The actual void fraction of the rectangular packed channel in question was estimated based on the following definition,

$$\varepsilon = \frac{Total\ channel\ volume - Total\ packing\ volume}{Total\ channel\ volume}$$

The total volume of packing was calculated according to the actual shape, dimensions and number of the Raschig ring type of packing used in the packed section. Based on the total number of Raschig ring packing (*N= 910*) and the dimensions of the rectangular packed section (length=*1.6 m*, width=*0.8 m*, and hight=*0.1 m)* the void fraction was found to have a value of *0.81* .

4.3.2 Packing and channel equivalent diameter

For non spherical packing, the equivalent particle diameter D_p is commonly defined by the following equation(*18*),

$$D_p = \frac{6(1-\varepsilon)}{\phi_s S} \qquad (4.1)$$

where S=specific surface area, or area of particle per unit volume of bed $=S_o(1-\varepsilon)$, m^2/m^3; and S_o=area of particle surface per unit volume of solid, m^2/m^3. The shape factor ϕ_s which is defined as the quotient of the area of a sphere equivalent to the volume of the particle divided by the actual surface of the particle has a value of about *0.3* for Raschig rings type of packing (*18*). According to this definition the equivalent particle diameter has been found to have a value of *0.0369 m.*

For rectangular channels of an aspect ratio *W/H>3*, the following method is given by Normand (*33*). The channel is treated as though it were a round pipe having an equivalent diameter D_e defined as follows:

$$D_e = \left(2.55K \frac{(WH)^2}{W+H} \right) \tag{4.2}$$

were K is a constant of a value $=1.4$ for a rectangular channel of an aspect ratio $W/H=8$. According to the above definition the equivalent channel diameter was found to have a value $D_e=0.29\ m$.

4.3.3 Effective thermal conductivity

The effective thermal conductivity k_e is a convenient engineering concept in packed bed systems. In a rectangular packed channel heated asymmetrically the effective transverse thermal conductivity is an important parameter, since this corresponds to the direction of heat flux. For the present model, the following expression is used,

$$k_e = k_{st} + k_{dy} \tag{4.3}$$

the stagnant thermal conductivity (k_{st}) is defined as the contribution to heat transfer in a packed channel due to conduction in case of stagnant fluid and is given as by (*34*),

$$k_{st} = k_g\left(\varepsilon + (1-\varepsilon)\left(\frac{\beta}{\delta + \frac{2}{3}\frac{k_g}{k_s}}\right)\right) \tag{4.4}$$

were $\beta = 1$ for the case of loose packing and δ is taken as *0.18* (see figure *4.2*). k_s and k_g are the thermal conductivity of solid and gas respectively. The dynamic contribution k_{dy} that is due to fluid flow is approximated by (*34*),

$$k_{dy} = \frac{0.0025}{1+46\left(\frac{D_p}{D_t}\right)^2}\mathrm{Re} \tag{4.5}$$

where *Re* is defined as

$$\mathrm{Re} = \frac{GD_p}{\mu} \tag{4.6}$$

4.3.4 Modified Reynolds number

The modified *Re* for the packed bed used in the course of this study is defined as follows,

$$\mathrm{Re} = \frac{\rho \upsilon D_p}{\mu(1-\varepsilon)} \tag{4.7}$$

were υ is the superficial velocity (this is the average linear velocity the air would have in the channel if no packing were present). (*10,19*)

4.4 Model equations

4.4.1 pressure drop equation

Most available studies on modeling packed channels pressure drop rely on Ergun equation (*35*). Generally speaking, there have been two main theoretical approaches for studding pressure drop through packed beds. In one method the packed bed is regarded as bundle of tangled tubes of weird cross-section ; the theory is then developed by applying the previous results for single straight tubes to the collection of crooked tubes. In the second, which is applied by Ergun, the packed channel is visualized as a collection of submerged objects and the pressure drop is calculated by summing up the resistance of the submerged particles.

Analysis of great deal of data in laminar flow regime has lead to the following equation (*19*),

$$\frac{P_0 - P_L}{L} = C_1 \frac{\mu \upsilon (1-\varepsilon)^2}{D_p^2 \varepsilon^3} \qquad (4.8)$$

which is the Bulk-Kozeny equation valid for $Re < 10$ $(Re = \frac{\rho \upsilon D_p}{\mu(1-\varepsilon)})$, the C_1 was found to be 150 .

In turbulent flow regime, experimental data indicated that correlation of pressure drop takes the following form (*19*),

$$\frac{P_0 - P_L}{L} = C_2 \frac{\rho \upsilon^2 (1-\varepsilon)}{D_p \varepsilon^3} \tag{4.9}$$

which is the Burke-Plummer equation valid for $Re > 1000$. The constant C_2 was found to be 1.75.

When the Blake-Kozeny equation for laminar flow and the Burke-Plummer equation for turbulent flow are simply added together the result is

$$\frac{P_0 - P_L}{L} = C_1 \frac{\mu \upsilon (1-\varepsilon)^2}{D_p^2 \varepsilon^3} + C_2 \frac{\rho \upsilon^2 (1-\varepsilon)}{D_p \varepsilon^3} \tag{4.10}$$

which is the full Ergun equation(*35*).

For values of $Re>1000$, which is our concern in this study, the viscous resistance, that is the first term on the right hand side of equation (4.10), represent less than *10%* of the total flow resistance and may be neglected. For values of $Re<10$ the inertia resistance, that is the second term on the right side of equation (4.10), becomes negligibly small (*10*).

It is worth noting that Ergun equation is generally good for void fraction of less than *0.5* and for small packing to channel diameter ratio (*19*). In applying Ergun equation to the present simulation of the pressure drop,

special modification was carried out to the constant C_2 by fitting the experimental pressure drop data obtained with our packed channel which is of void fraction *0.81*.

4.4.2 Continuity and momentum balance equations

We consider fully developed, incompressible flow in a rectangular channel, the geometry and coordinate system are shown in figure (*4.1*). The time independent *x*-momentum equation based on the Brinkman-Ergun model is as follows (*22*),

$$\frac{dP}{dx} = \frac{\mu}{\varepsilon}\frac{d^2\upsilon}{dy^2} - C_1\frac{\mu\upsilon(1-\varepsilon)^2}{D_p^2\varepsilon^3} - C_2\frac{\rho\upsilon^2(1-\varepsilon)}{D_p\varepsilon^3} \qquad (4.11)$$

The boundary effects accounted for by the Brinkman friction term, which is the first term on the right hand side of equation (*4.11*), makes it possible to satisfy the no-slip condition on a solid boundary. The inertia term which is the last term on the right hand side of equation (*4.11*) represent the inertia forces, which are significant for fast flows *(Re >1000)*. The viscous term, that is the second term on the right hand side of equation (*4.11*) represent lass than *10%* of the total resistance forces for *Re >1000* (*10*).

In the course of this study the fluid flow regime is in the range of $Re > 1000$, so the viscous term was neglected. The momentum balance of equation (*4.11*) reduces to the following final form,

$$\frac{dP}{dx} = \frac{\mu}{\varepsilon}\frac{d^2\upsilon}{dy^2} - C_2\frac{\rho\upsilon^2(1-\varepsilon)}{D_p\varepsilon^3} \qquad (4.12)$$

with the following boundary conditions,

$$\begin{aligned} &\upsilon = 0 && \text{at } y = 0 \\ &\frac{d\upsilon}{dy} = 0 && \text{at } y = \frac{H}{2} \end{aligned} \qquad (4.13)$$

The requirements of the mass conservation provides the following continuity equation,

$$\frac{dG}{dx} = 0 \qquad (4.14)$$

since the density is considered to be constant in this study, then equation (*4.14*) reduces to the following form,

$$\frac{d\upsilon}{dx} = 0 \qquad (4.15)$$

It is worth noting that if the pressure drop due to the flow of gas through a packed channel causes a density variation of less than *10 %,* compared to the inlet density, then the flow is considered to be an incompressible (*18*).

4.4.3 Energy balance equation

The heat transfer characteristics of a thermally developing forced convection flow in a packed tube or channel has been analyzed in many previous studies (*7,21,23*). For a two dimensional, time-independent with negligible axial dispersion of heat model, the energy equation reduces to the following,

$$(\rho C_p)\upsilon \frac{\partial T}{\partial x} = k_e\left(\frac{\partial^2 T}{\partial y^2}\right) \tag{4.16}$$

where $(\rho\, c_p)$ is the heat capacity of the air calculated at the inlet conditions. equation (4.16) was solved with the following boundary conditions,

$$\begin{aligned} \frac{\partial T}{\partial y} &= \frac{q}{k_e} && \text{at} \quad y = 0 \\ \frac{\partial T}{\partial y} &= -\frac{q_{loss}}{k_e} && \text{at} \quad y = H \end{aligned} \tag{4.17}$$

were q_{loss} is the heat lost to the surroundings through the bottom plate. It is worth noting that the numerical calculation of heat loss through the bottom plate has shown a maximum of about 8 % loss of the total heat supplied.

4.5 Numerical formulations and procedure

4.5.1 Finite difference approximation

The momentum equation was solved based on the finite difference and following an iterative process. The initial guess of the velocity distribution,

together with the boundary conditions transform into a set of algebraic equations. The set of equations were then solved using Tridiagonal-Matrix algorithm *(TDMA)*. To obtain the correct velocity distribution the iteration process was repeated until convergence was achieved.

Equation (*4.12*) is written in a finite difference form as follows,

$$0 = u_{i-1} - u_i(2+F_1 u_i)+u_{i+1}+F_2 \qquad (4.18)$$

were

$$F_1 = \frac{C_1 \rho(1-\varepsilon)}{D_p \varepsilon^2 \mu}(\Delta y)^2$$
$$F_2 = \left(\frac{P_o - P_L}{L}\right)\left(\frac{\varepsilon}{\mu}\right)(\Delta y)^2 \qquad (4.19)$$

The above set of equations *(i=0 to N/2)* were solved iteratively using *Newton Raphson* method.

The energy equation was discritized using implicit finite difference method, namely the Cranck-Nicolson method, as follows,

$$Tnew_{i-1}(F)-Tnew_i(2F+1)+Tnew_{i+1}(F)=Told_{i-1}(-F)+Told_i(2F-1)+Told_{i+1}(-F) \qquad (4.20)$$

were F is defined as follows,

$$F = \frac{k_e(\Delta x)}{2\rho \upsilon C_p(\Delta y)^2} \qquad (4.21)$$

The above set of equations *(I=0 to N)* were developed using Tridiagonal-Matrix algorithm *(TDMA)*.

Since the present work pertains to forced convection with the assumption of constant physical properties, the momentum equation was solved independently to yield the velocity field. With the velocity field in hand, the temperature field was obtained from the energy equation. Flow chart of the computer program is shown in figure *4.3*. Main computer program and subroutines used in the numerical simulation are shown in appendix A

4.5.2 Determination of air bulk temperature

Once the temperature distribution inside the channel is known, one can get the average fluid temperature. The average bulk temperature commonly used in connection with flow of fluids with essential constant ρ and C_p is as follows (*36*),

$$T_b(x) = \frac{\int_A \upsilon(y) T(y,x) dA}{\int_A \upsilon(y) dA} \qquad (4.22)$$

The bulk temperature T_b is the temperature one would measure if the channel was chopped off at x and if the air issuing forth were collected in a container and thoroughly mixed (hence this average temperature is sometimes refereed to as the "Cup-mixing temperature" or the average temperature).

Numerical calculation of the integral form of equation (*4.22*) was approximated by using Simpson integral scheme (*37*).

4.5.3 Determination of wall to air heat transfer coefficient

In chemical reactor and packed bed engineering literature the local heat transfer coefficients is usually defined in the following form (*21*),

$$h_i = \frac{(q_w)_i}{(T_w - T_b)_i} \tag{4.23}$$

with T_b defined as in equation (*4.22*), q_w is represented numerically by the following differential form,

$$q_w = k_e \frac{\partial T}{\partial}\Big|_{y=0} \tag{4.24}$$

For the present problem with asymmetric heating, the local Nu for the thermally developing flow in terms of the effective channel diameter and the thermal conductivity of air is given by (*21*),

$$Nu_i = \frac{h_i D_e}{k_f} \tag{4.25}$$

It is worth noting that other forms of the Nu in terms of the effective particle diameter D_p (*1,14*) or the effective thermal conductivity k_e (*38*) are reported in literature instead of the effective channel diameter D_e and the fluid thermal conductivity k_f.

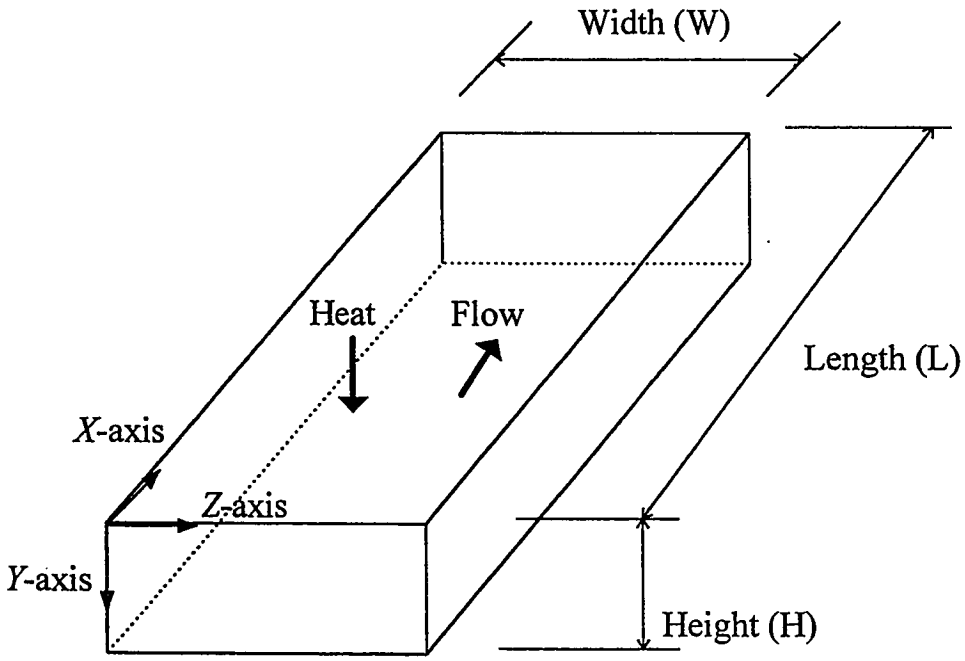

FIG. 4.1 GEOMETRY AND COORDINATE SYSTEM OF THE BED.

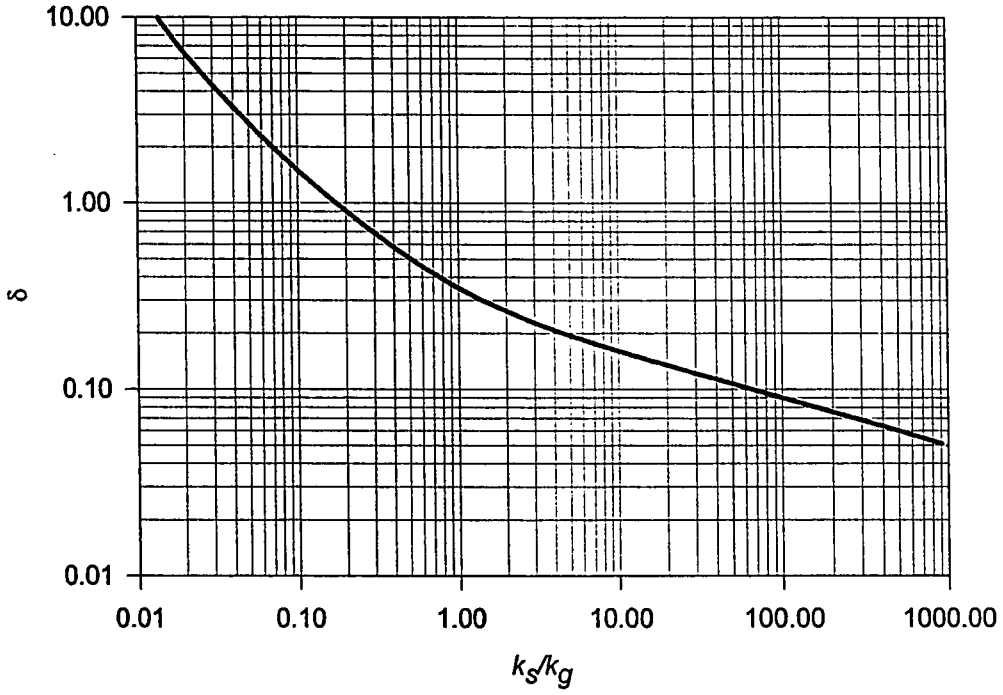

FIG. 4.2 NORMALIZED STAGNANT FLUID THICKNESS δ AS FUNCTION OF THE THERMAL CONDUCTIVITY RATIO K_S/K_G FOR LOOSE PACKING (33).

FIG. 4.3 COMPUTER PROGRAME FLOW CHART

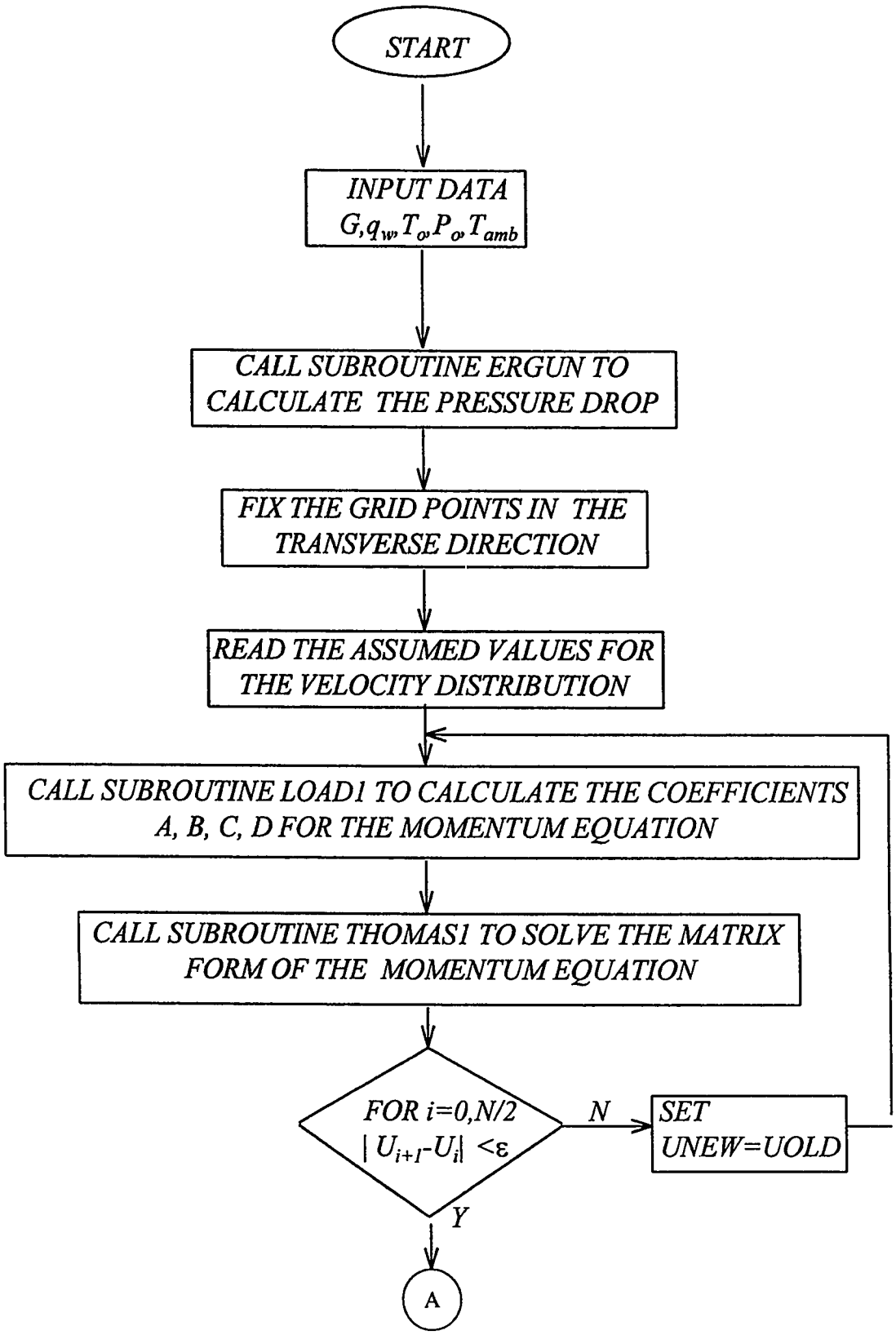

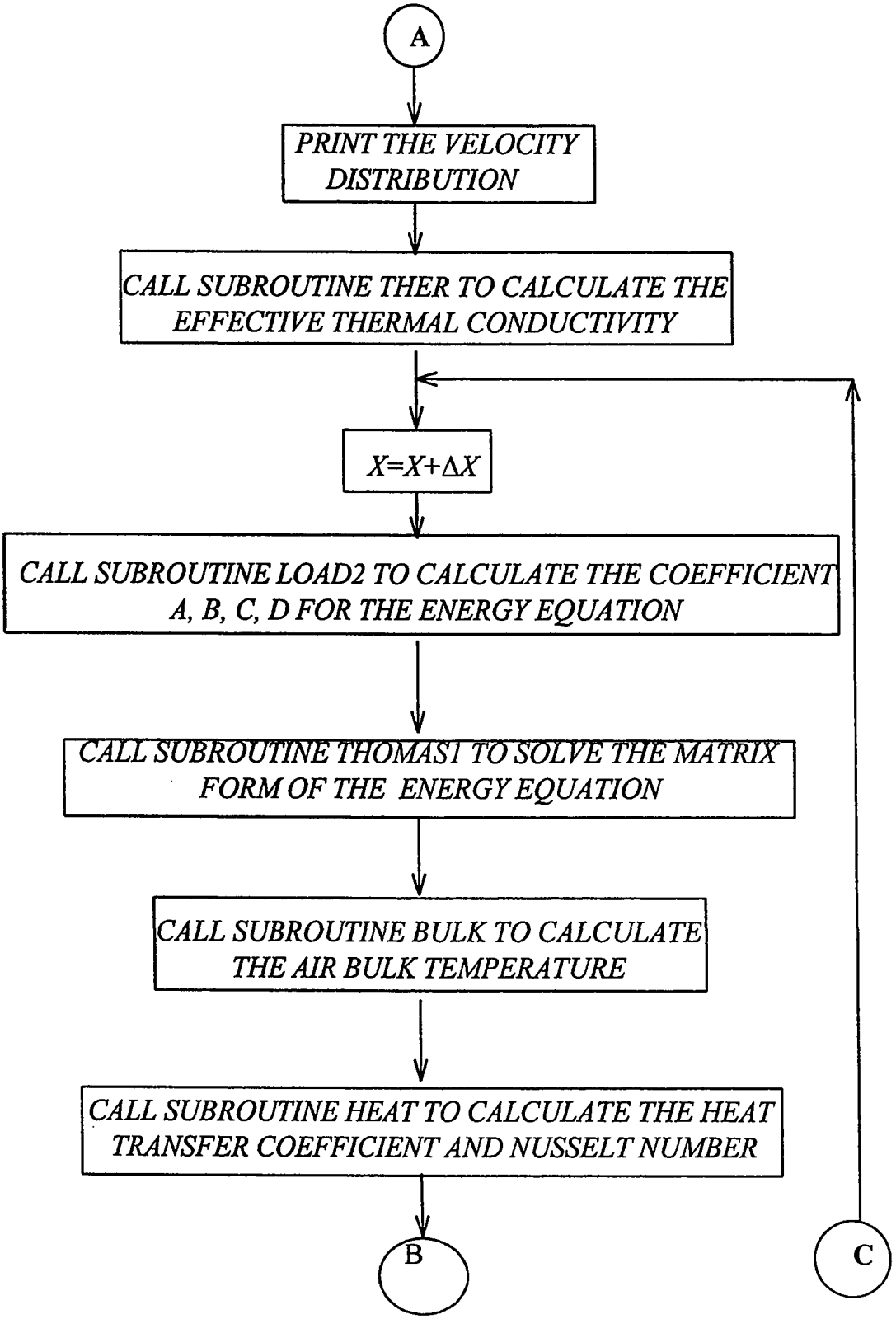
A
PRINT THE VELOCITY DISTRIBUTION
CALL SUBROUTINE THER TO CALCULATE THE EFFECTIVE THERMAL CONDUCTIVITY
X=X+ΔX
CALL SUBROUTINE LOAD2 TO CALCULATE THE COEFFICIENT A, B, C, D FOR THE ENERGY EQUATION
CALL SUBROUTINE THOMAS1 TO SOLVE THE MATRIX FORM OF THE ENERGY EQUATION
CALL SUBROUTINE BULK TO CALCULATE THE AIR BULK TEMPERATURE
CALL SUBROUTINE HEAT TO CALCULATE THE HEAT TRANSFER COEFFICIENT AND NUSSELT NUMBER
B
C

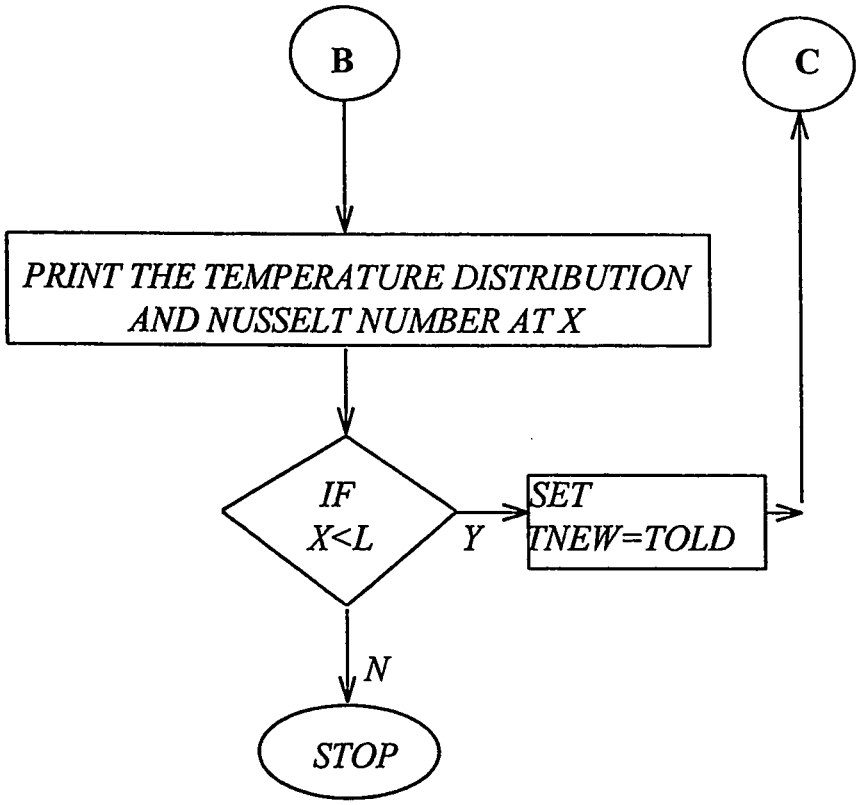
B
C
PRINT THE TEMPERATURE DISTRIBUTION AND NUSSELT NUMBER AT X
IF X<L
Y
SET TNEW=TOLD
N
STOP

CHAPTER 5

Results and discussion

5.1 Introduction

The main objectives of the present work are to investigate experimentally the thermal behavior of air flow in a rectangular packed channel with constant heat flux, beside the development of a reliable mathematical model to simulate the thermal and dynamic behavior of the system. The experimental set up and procedure was presented in chapter 3 and a detailed discussion on the model development was presented in chapter 4. The unique sides of the present work is that it is the first to be conducted in such a large scale experimental equipment.

In this chapter a new correlative expression for *Nu* based on the experimentally determined results on the packed channel is presented. A comparison between the empty and packed channel performance are also shown especially in terms of *Nu*. In the modeling part the mathematical simulation results for the packed channel were compared with the experimental data. Appendices B and C shows a summaries experimental data analysis for the packed and empty channel respectively.

5.2 *Packed channel experimental results*

5.2.1 Temperature distribution

Air temperature distribution inside the packed channel at different heat flux at *Re=2471* are shown in figures *5.1-5.4*. The air enters the channel from one side of the packed section and a heat transfer process occurs between the top heated plate and the flowing air. Figures *5.5-5.7* shows the air temperature distribution at different heat flux and at *Re=5137*.

The packed channel transverse temperature profiles at *Re=1388* and at different heat flux are shown in figures *5.8* and *5.10* . The air is heated by a constant heat flux from the top heated plate at *y=0*. The air temperature shows a steep gradient near the top heated plate, at the core region a linear temperature profile occurs, and at the region close to the bottom plate a slight decrease in the air temperature is observed.

The experimental air bulk temperature at each axial position was calculated by the integral form of equation *4.22* for the local transverse temperatures at *y=0.02, y=0.05, y=0.08 m* from the top heated plate. The bulk temperature profiles as function of axial distance at *Re=1881* and *3860* and at a constant heat flux of *230* W/m^2 are shown in figures *5.11* and *5.12*

respectively. As the air goes through the packed section in the axial direction the temperature was considerably increased.

The air temperature distribution inside the packed section as function of the axial and transverse distance are shown in a three dimensional plot in figures *5.13-5.15*.

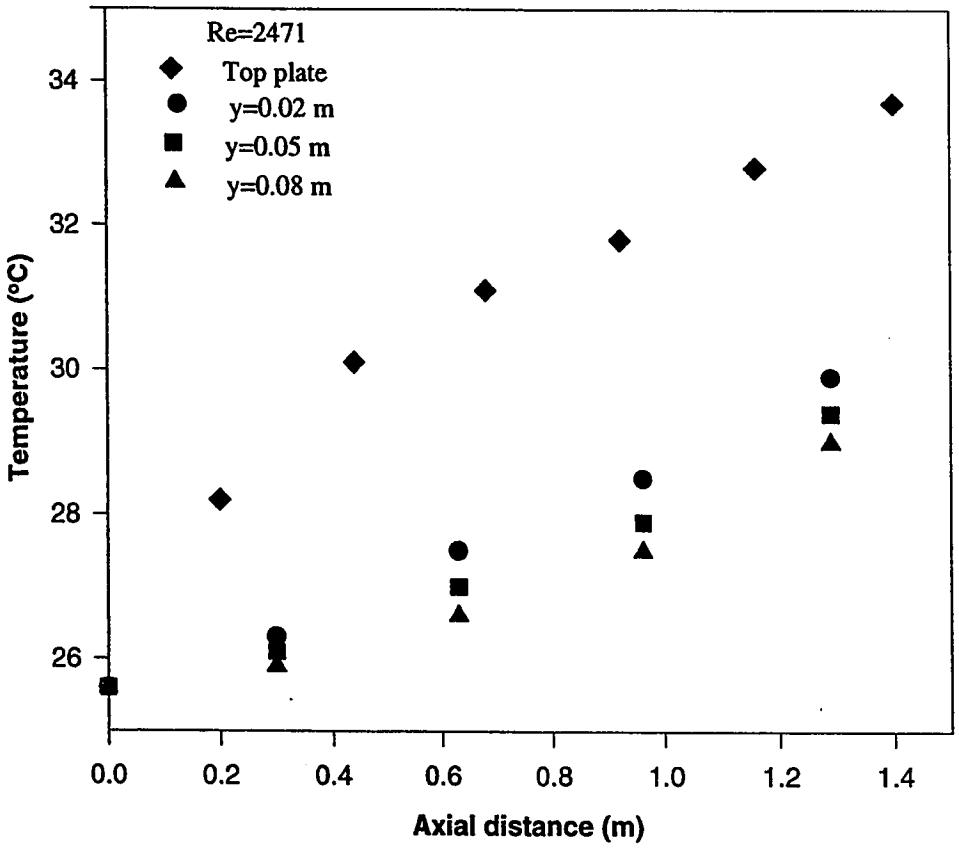

FIG. 5.1 EXPERIMENTAL AIR TEMPERATURE DISTRIBUTION IN THE PACKED CHANNEL AT Q=55.0 W/m^2

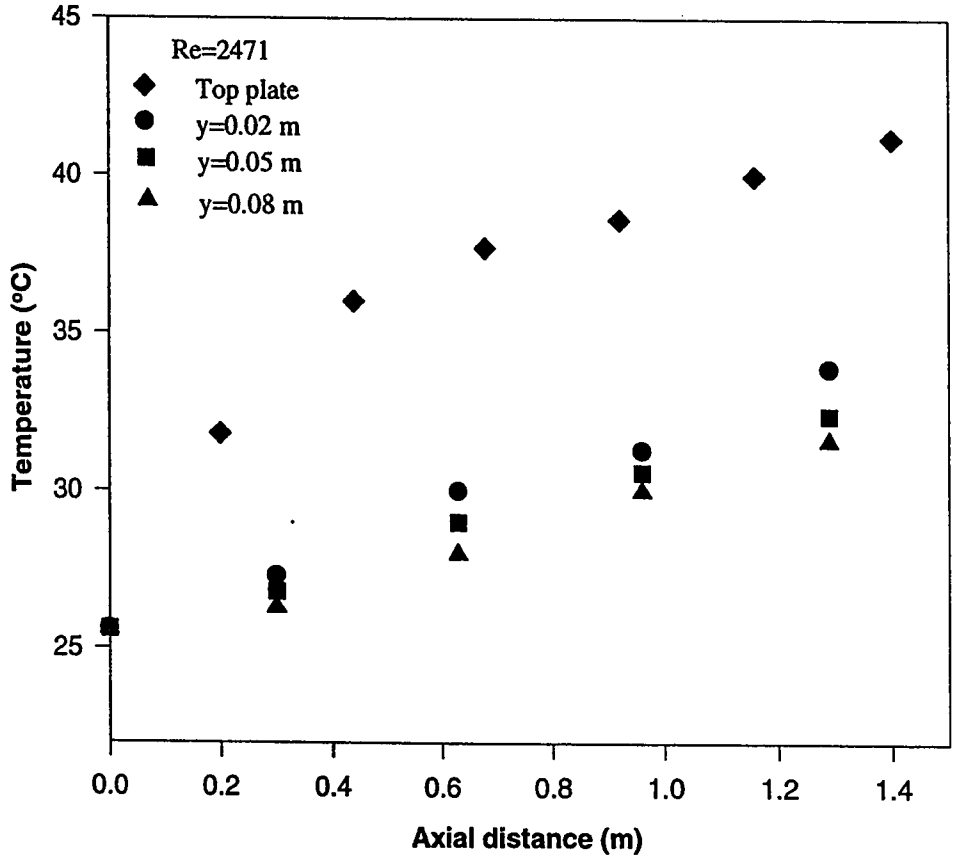

FIG. 5.2 EXPERIMENTAL AIR TEMPERATURE DISTRIBUTION IN THE PACKED CHANNEL AT Q=130 W/m^2

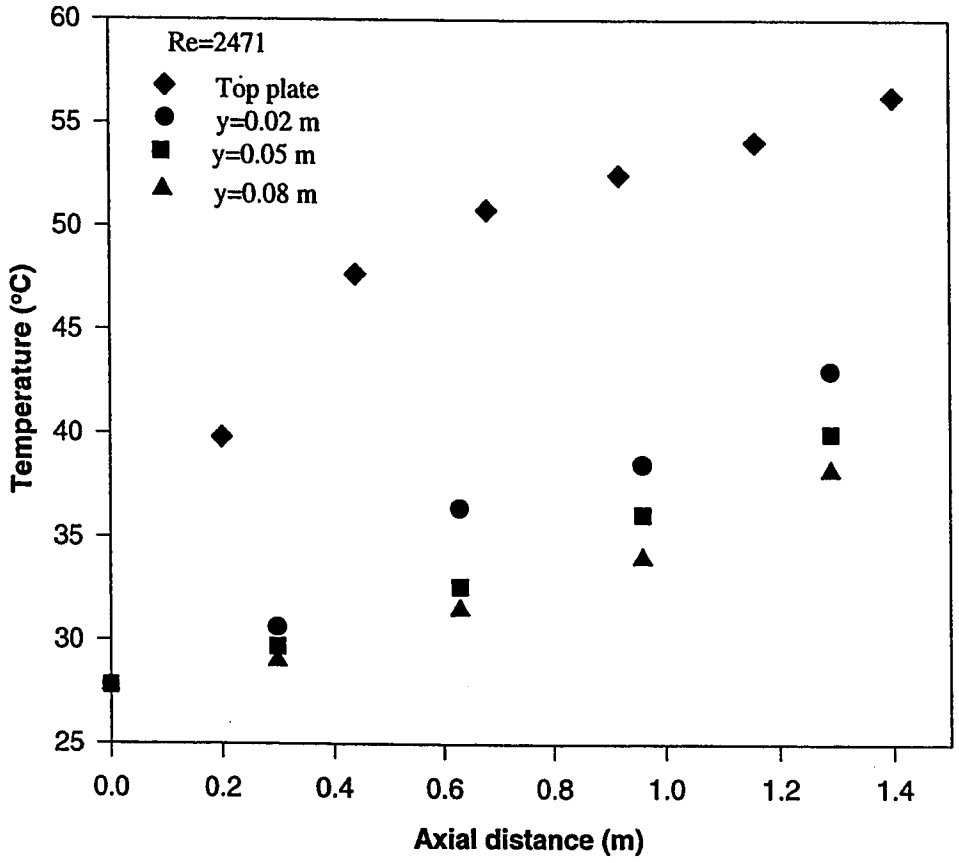

FIG. 5.3 EXPERIMENTAL AIR TEMPERATURE DISTRIBUTION IN THE PACKED CHANNEL AT Q=230 W/m^2

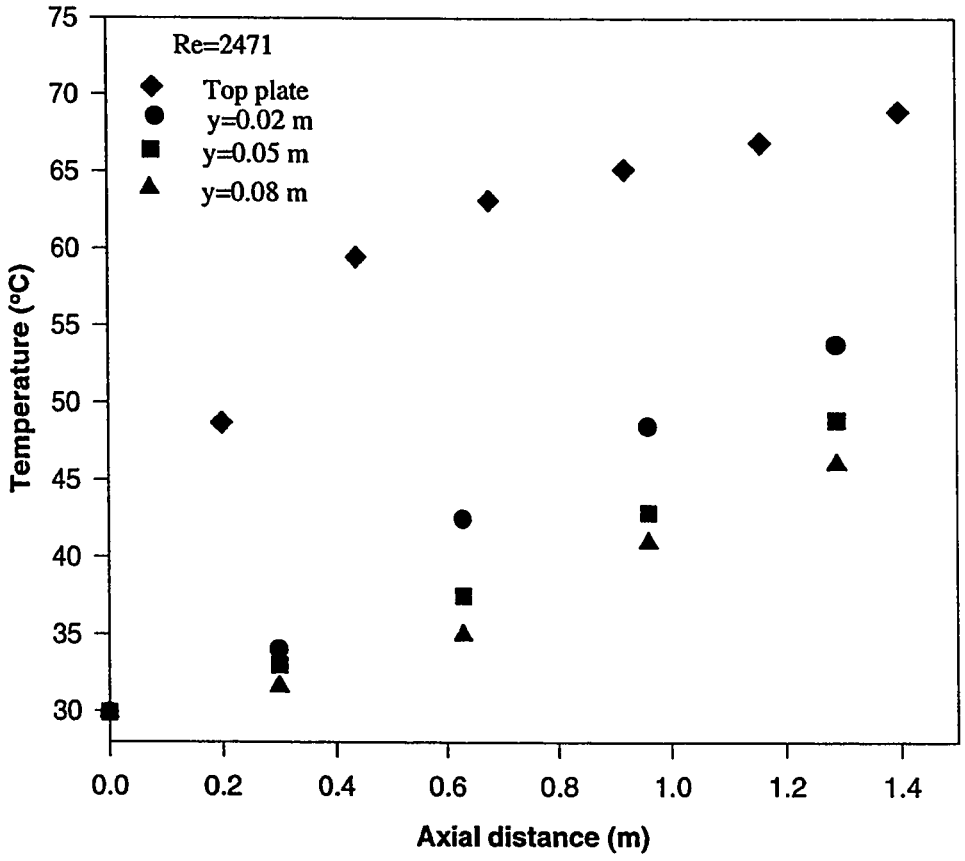

FIG. 5.4 EXPERIMENTAL AIR TEMPERATURE DISTRIBUTION IN THE PACKED CHANNEL AT Q=350 W/m^2.

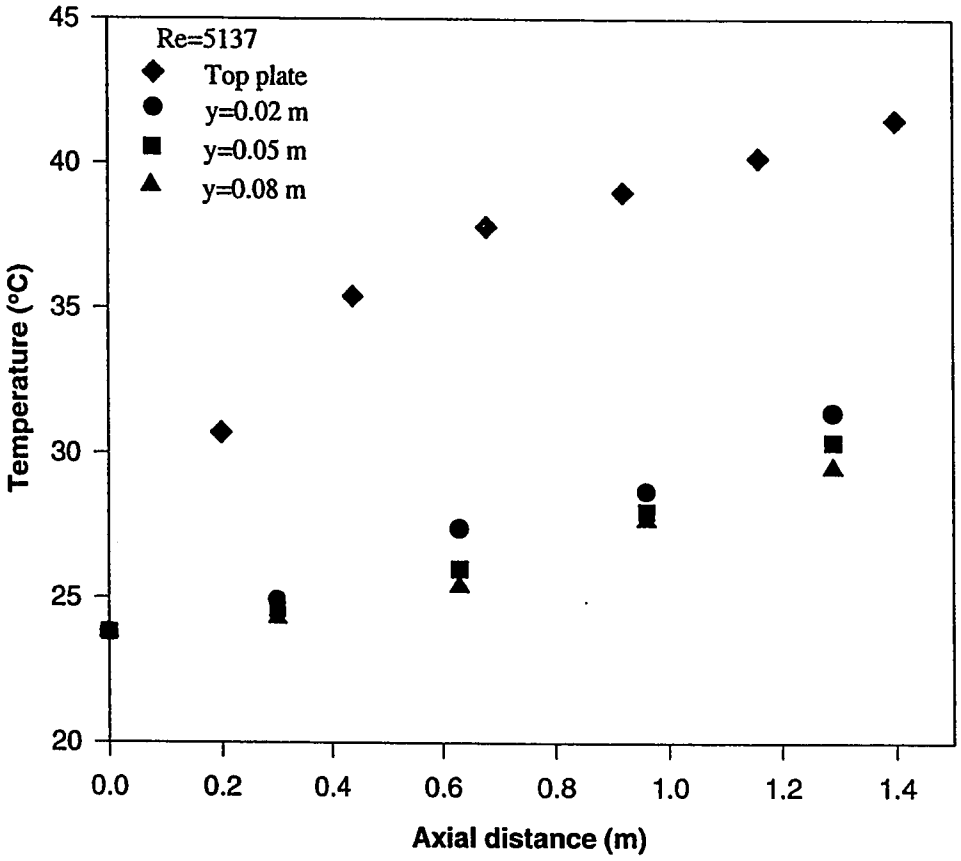

FIG. 5.5 EXPERIMENTAL AIR TEMPERATURE DISTRIBUTION IN THE PACKED CHANNEL AT Q=230 W/m^2

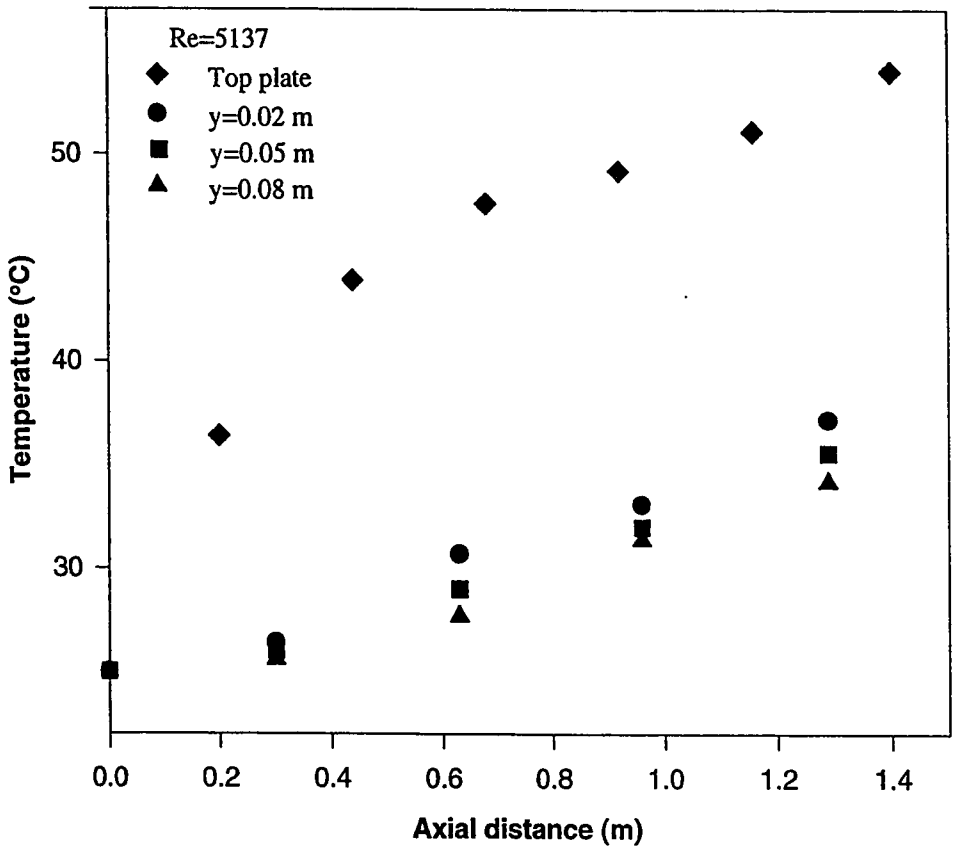

FIG. 5.6 EXPERIMENTAL AIR TEMPERATURE DISTRIBUTION IN THE PACKED CHANNEL AT Q=350 W/m^2

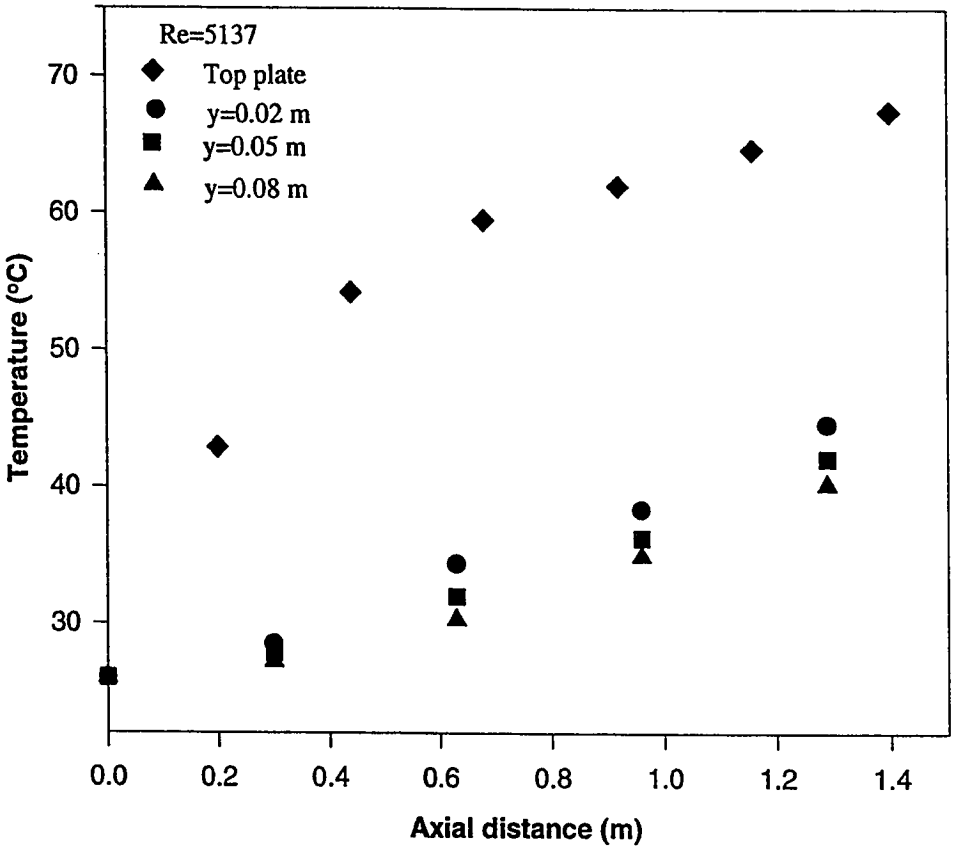

FIG. 5.7 EXPERIMENTAL AIR TEMPERATURE DISTRIBUTION IN THE PACKED CHANNEL AT Q=500 W/m^2

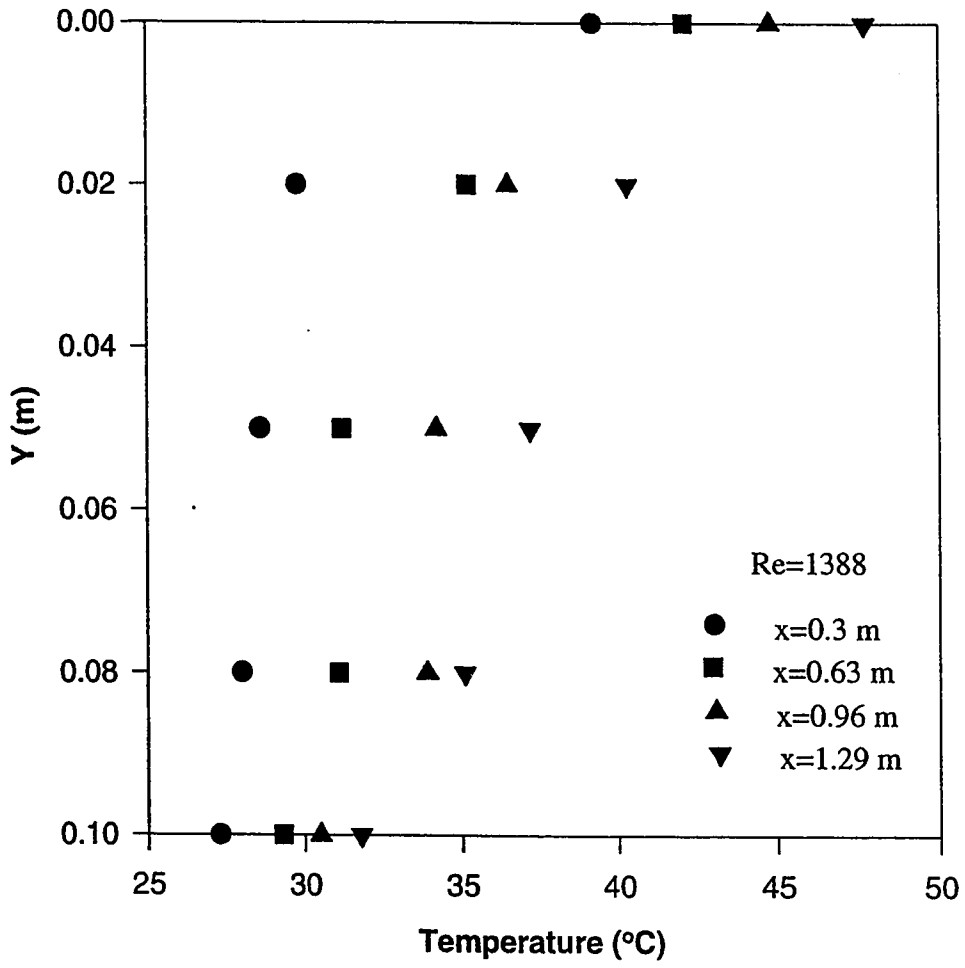

FIG. 5.8 EXPERIMENTAL TRANSVERSE AIR TEMPERATURE PROFILES IN THE PACKED CHANNEL AT Q=130 W/m^2

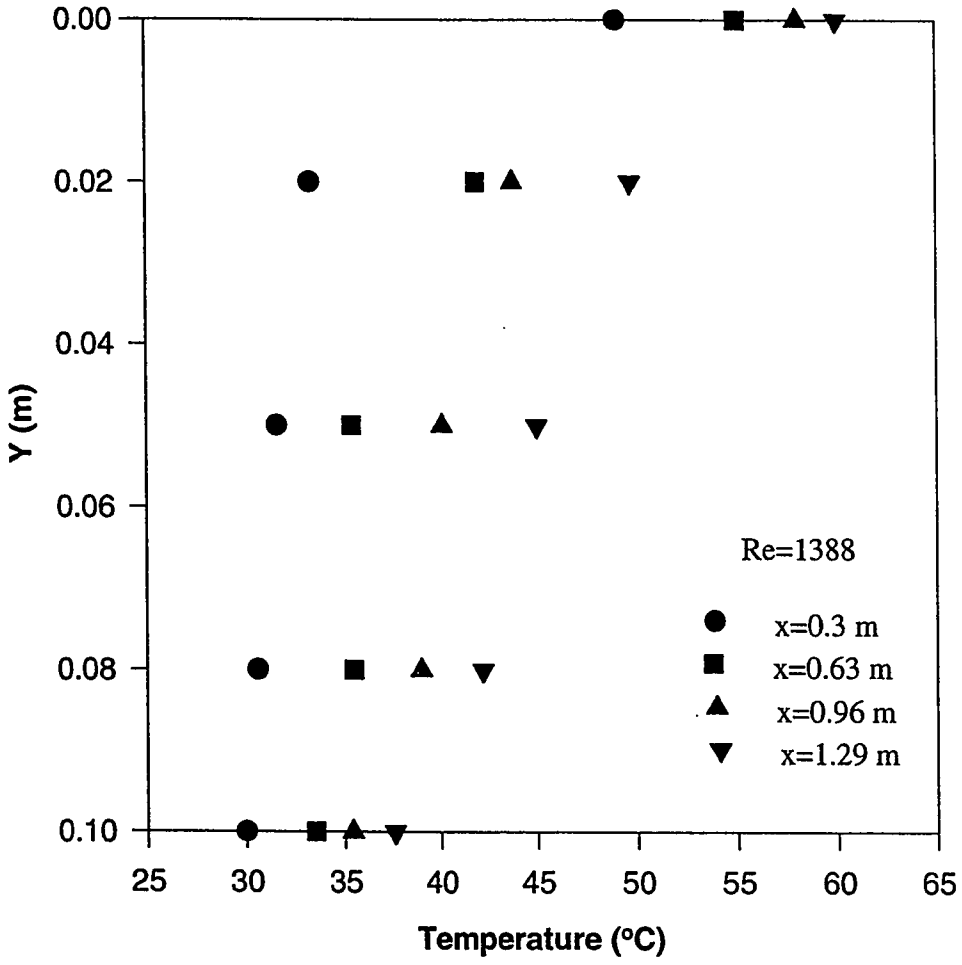

FIG. 5.9 EXPERIMENTAL TRANSVERSE AIR TEMPERATURE PROFILES IN THE PACKED CHANNEL AT Q=230 W/m^2

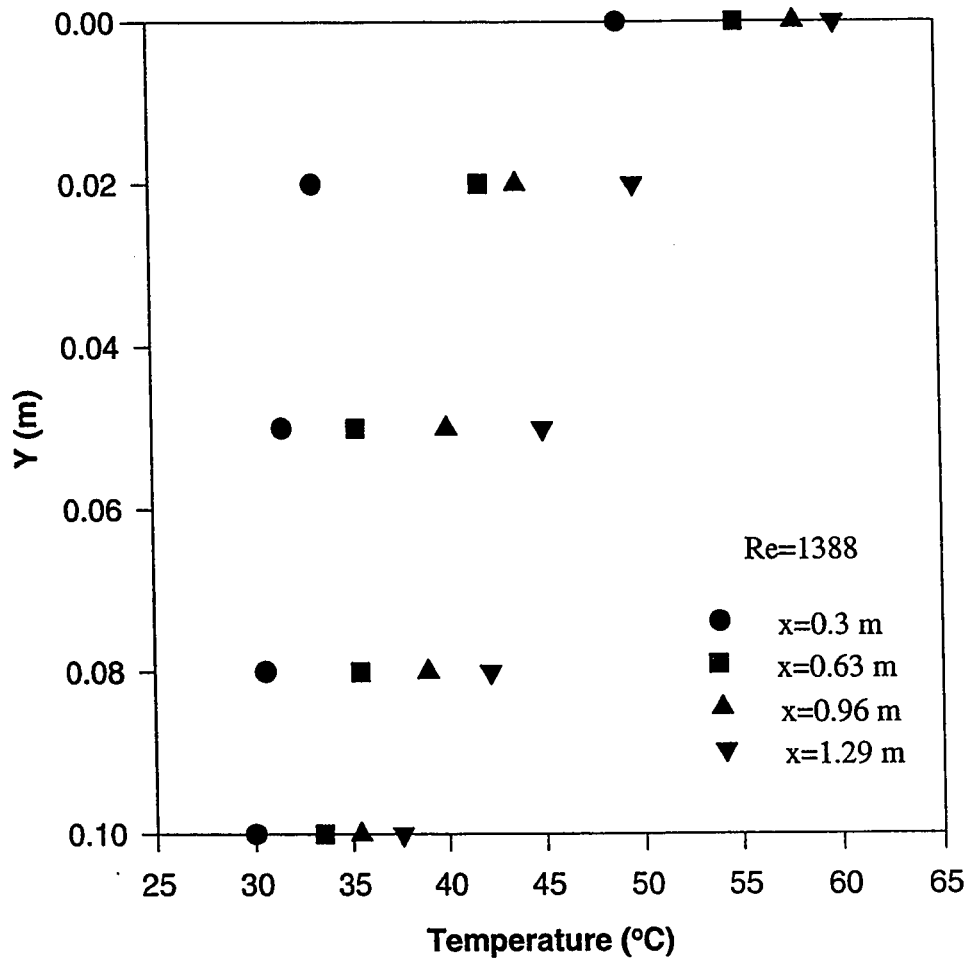

FIG. 5.10 EXPERIMENTAL TRANSVERSE AIR TEMPERATURE PROFILES IN THE PACKED CHANNEL AT Q=350 W/m^2

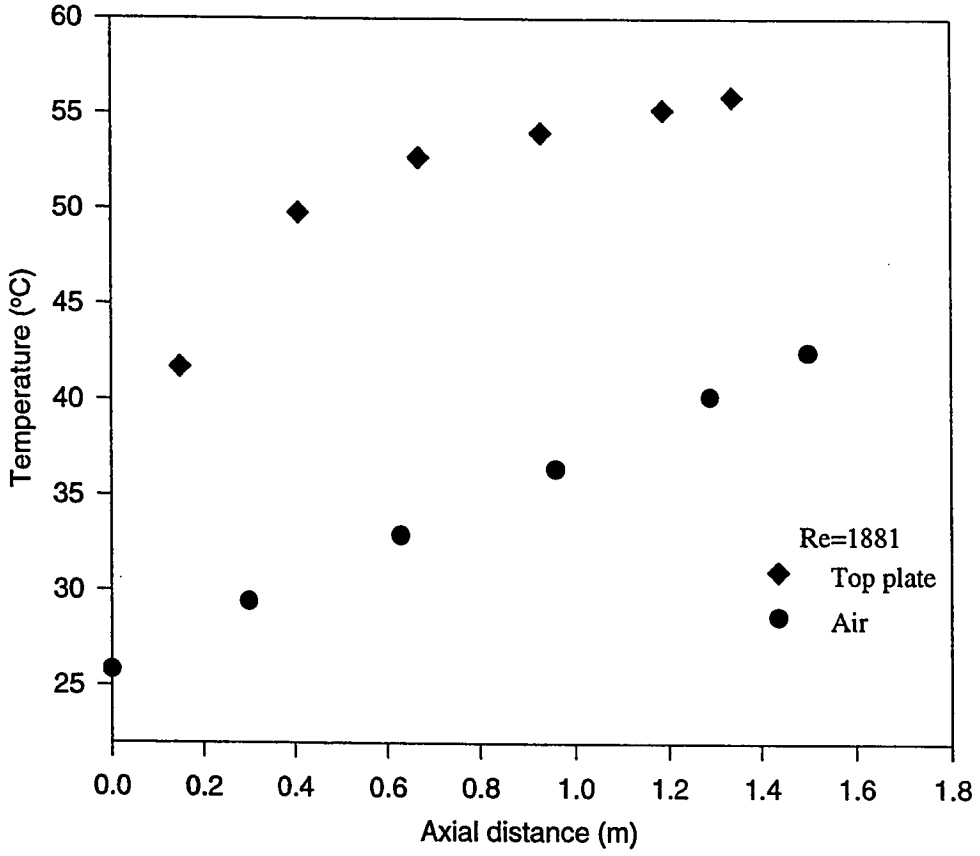

FIG 5.11 EXPERIMENTAL AIR BULK TEMPERATURE IN THE PACKED CHANNEL AS FUNCTION OF THE AXIAL DISTANCE AT Q=230 W/m^2

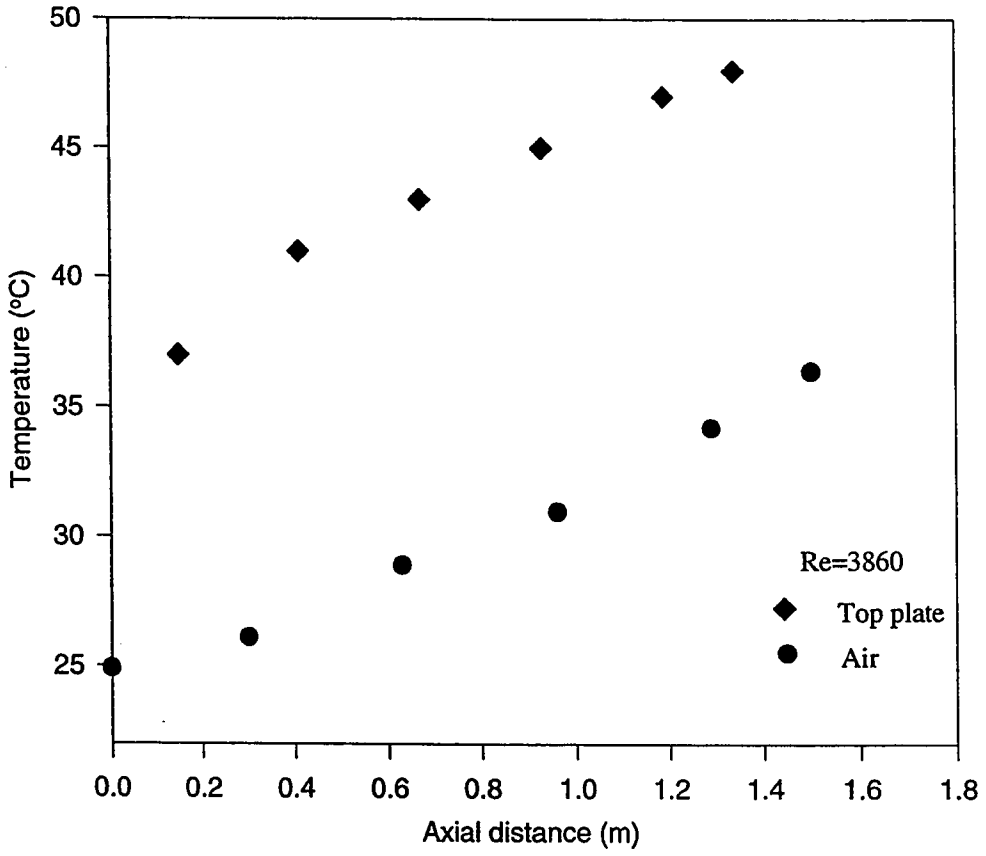

FIG 5.12 EXPERIMENTAL AIR BULK TEMPERATURE IN THE PACKED CHANNEL AS FUNCTION OF THE AXIAL DISTANCE AT Q=230 W/m^2

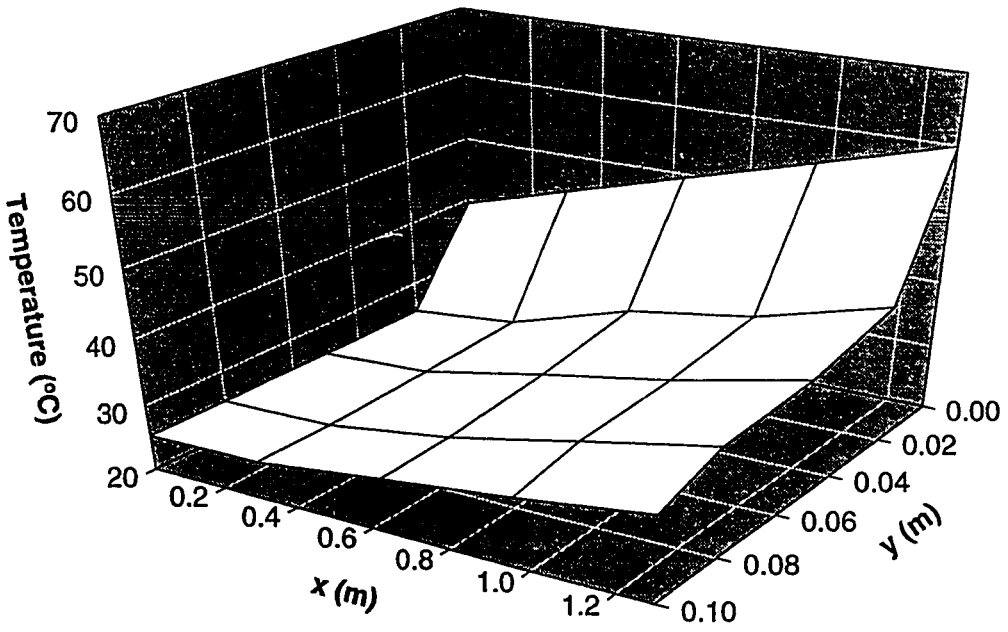

FIG. 5.13 EXPERIMENTALLY DETERMINED TEMPERATURE DISTRIBUTION IN THE PACKED CHANNEL AT Q=350 W/m^2 AND *Re*=3860.

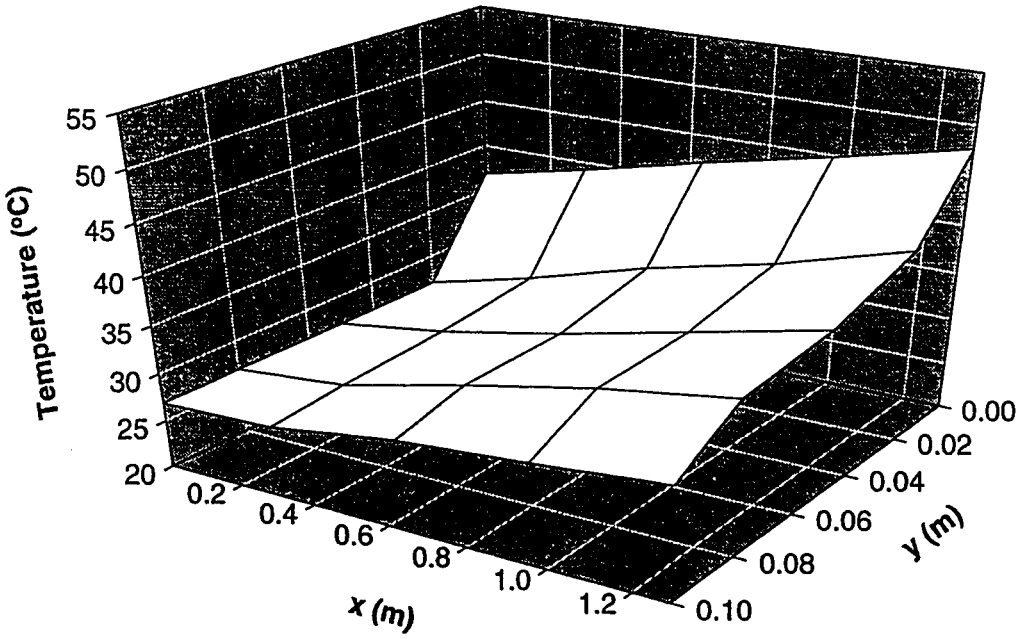

FIG. 5.14 EXPERIMENTALLY DETERMINED TEMPERATURE DISTRIBUTION IN THE PACKED CHANNEL AT Q=130 W/m^2 AND *Re*=1388.

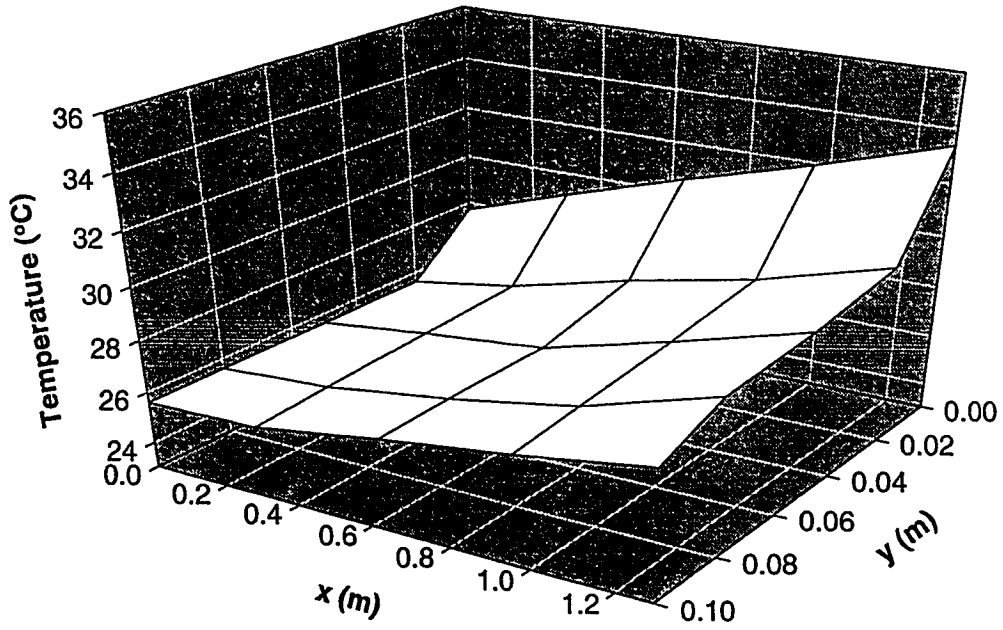

FIG. 5.15 EXPERIMENTALLY DETERMINED TEMPERATURE DISTRIBUTION IN THE PACKED CHANNEL AT Q=55 W/m^2 AND *Re*=2471.

5.2.2 Pressure drop

Experimental packed pressure drop data in *mm* H_2o were taken over a wide range of flow rate ranging from *0.05* to *0.5* kg/m^2s. The results obtained within the packed section as function of the air superficial velocity are shown in figure *5.16*. The *20* experimental measurements were taken at an average air temperature of *25* ^oC and without heat flux. Table *5.1* shows the experimental data of the pressure drop. It is clear that due to the large void fraction of the packed section the pressure drop is very low compared to other packed bed systems.

5.3 Empty channel experimental results

5.3.1 Temperature distribution

A total number of *12* experimental runs were conducted in the empty channel with asymmetric heating for comparison with the packed channel thermal performance. The air temperature distribution inside the empty channel as function of the axial distance is shown in figures *5.17* and *5.18*. These figures show that the temperature near the top heated plate ($y=0.02$ *m*) is considerably heated compared to the temperature at the lower half section of the channel, this is mainly attributed to the fact that the air mixing process for the empty channel is very limited. A selected data for The transverse air

temperature profiles are shown in figures *5.19* and *5.20*. It is clear that the air temperature drops rapidly from the top wall (*y=0*) as it attains a linear profile in the bulk region. The bottom plate temperature has shown a slight increase compared to the temperature of air at y=*0.08 m*.

Figures *5.21* and *5.22* shows the air bulk temperature as function of the axial distance. The air temperature profile almost takes a linear shape as the air moves towards the exit section of the channel. A three dimensional plot shows the shape of the air temperature distribution inside the empty channel is presented in figure *5.23*.

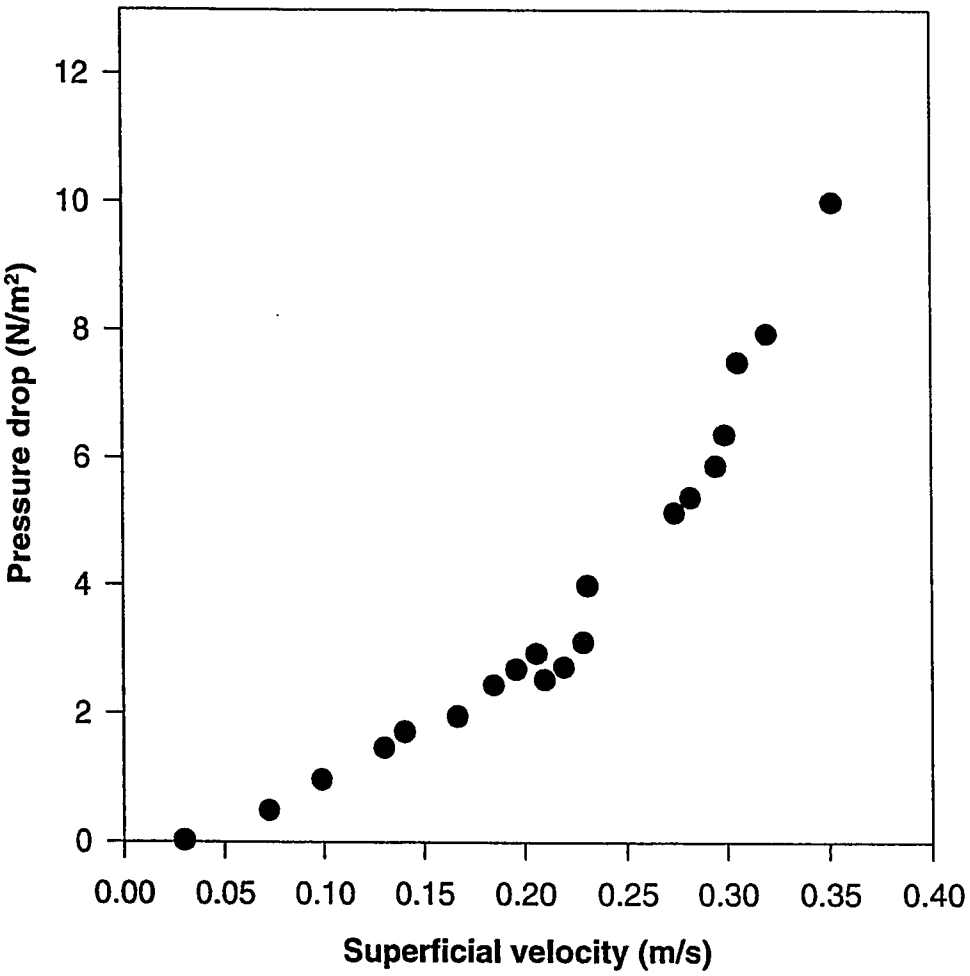

FIG. 5.16 EXPERIMENTAL PRESSURE DROP BETWEEN THE TWO ENDS OF THE PACKED SECTION.

Table 5.1 Experimental pressure drop data obtained with the packed channel.

Superficial velocity (m/s)	Pressure drop (N/m^2)
0.030	0.12
0.071	0.49
0.099	0.97
0.130	1.47
0.140	1.72
0.167	1.96
0.185	2.45
0.196	2.69
0.206	2.94
0.210	5.53
0.219	2.73
0.228	3.12
0.231	4.00
0.274	5.14
0.282	5.39
0.295	5.88
0.299	6.37
0.305	7.50
0.320	7.95
0.352	9.75

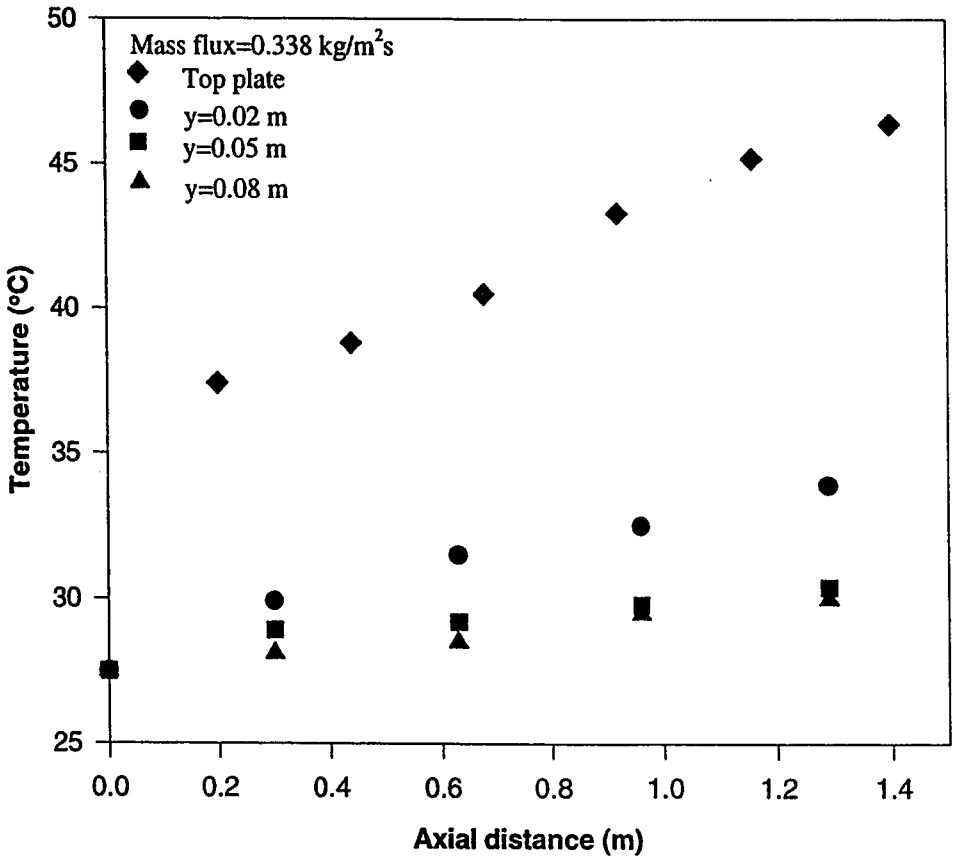

FIG. 5.17 EXPERIMENTAL AIR TEMPERATURE DISTRIBUTION IN THE EMPTY CHANNEL AT Q=130 W/M^2

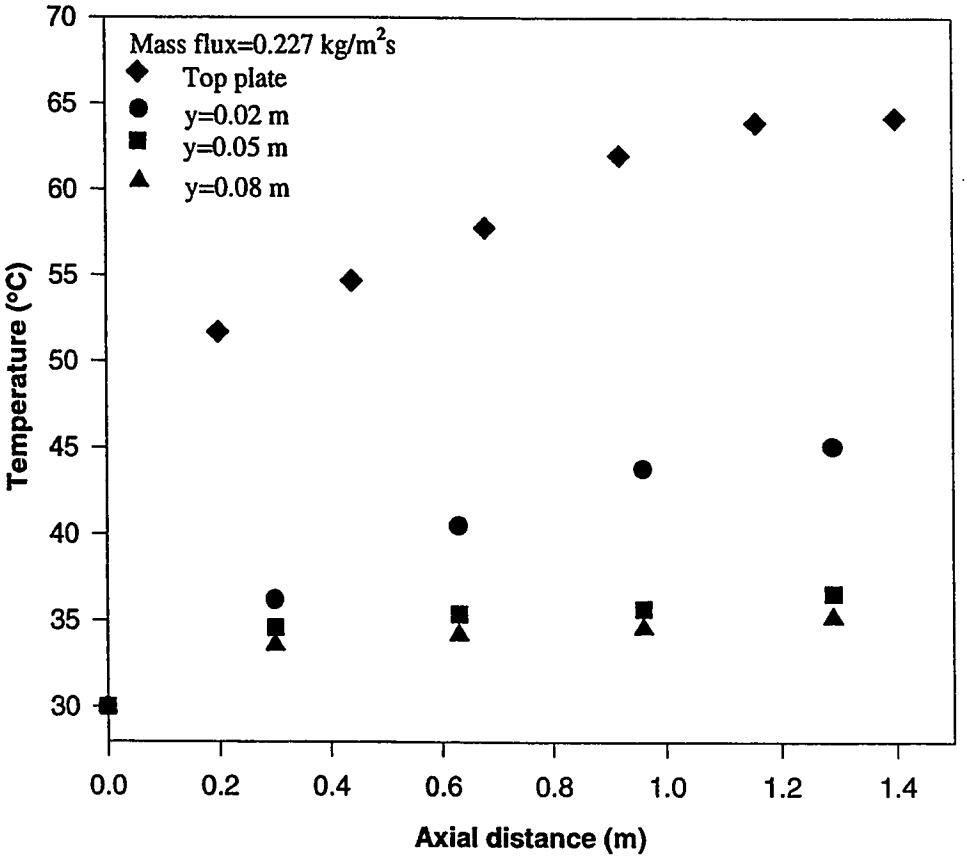

FIG. 5.18 EXPERIMENTAL AIR TEMPERATURE DISTRIBUTION IN THE EMPTY CHANNEL AT Q=230 W/M^2

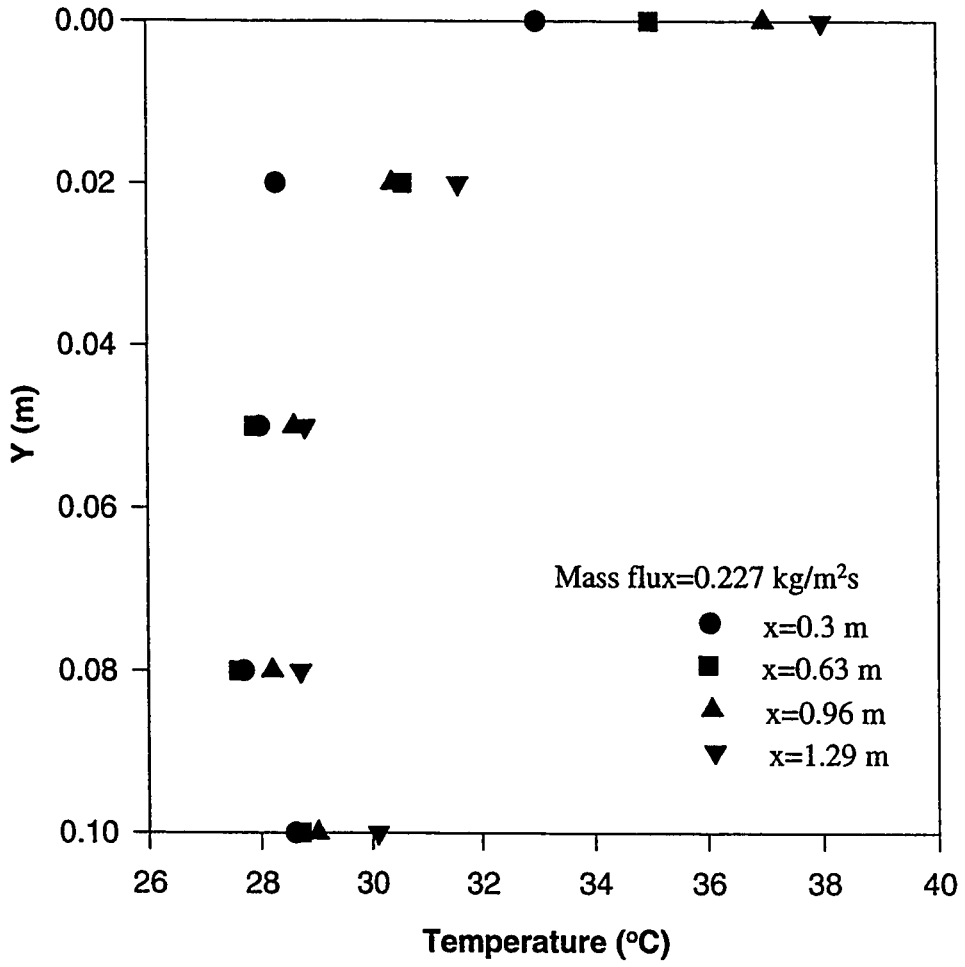

FIG. 5.19 EXPERIMENTAL TRANSVERS TEMPERATURE PROFILES IN THE EMPTY CHANNEL AT Q=55.0 W/M^2

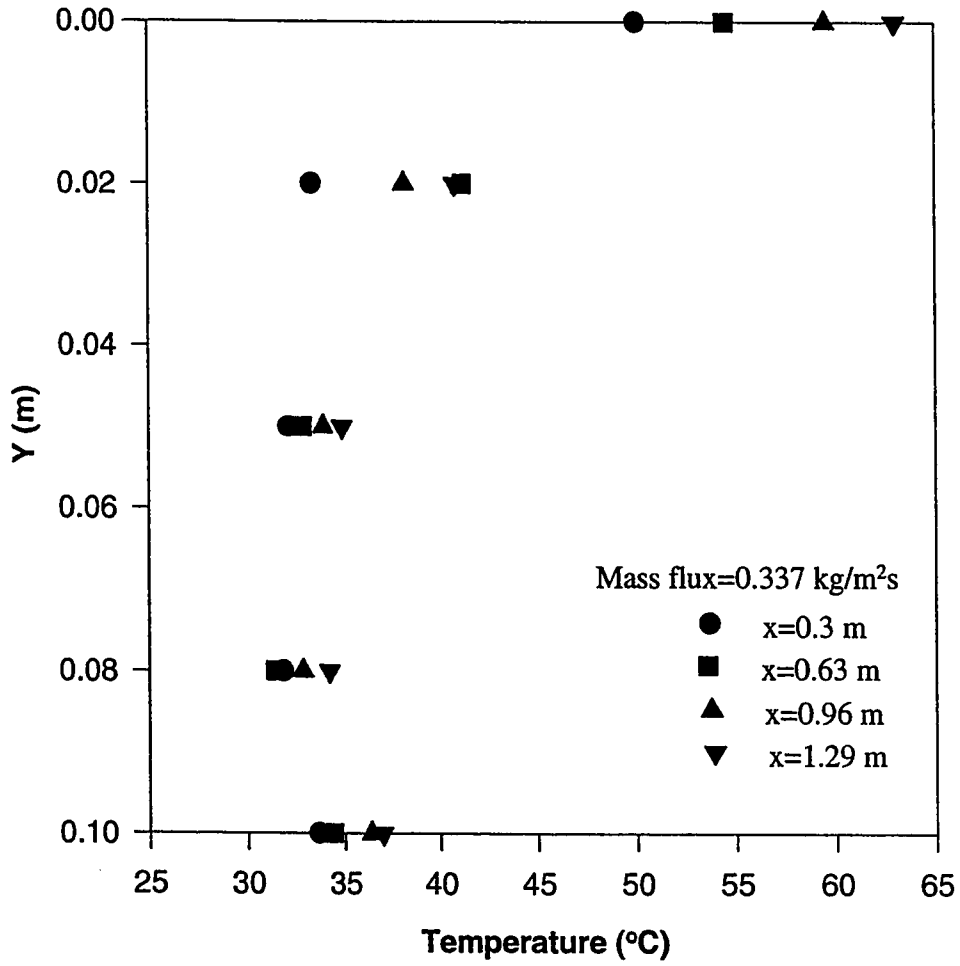

FIG. 5.20 EXPERIMENTAL TRANSVERS TEMPERATURE PROFILES IN THE EMPTY CHANNEL AT Q=130 W/M^2

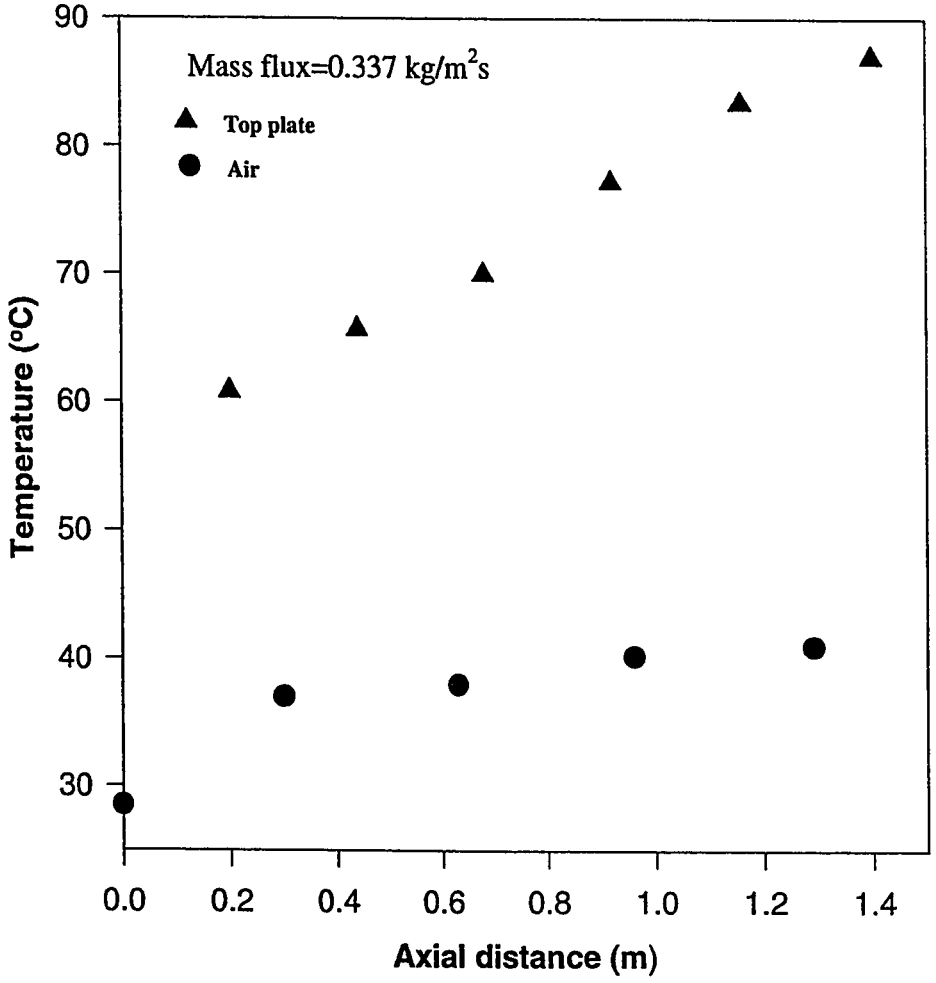

FIG. 5.21 EXPERIMENTAL AIR BULK TEMPERATURE AS FUNCTION OF THE AXIAL DISTANCE IN THE EMPTY CHANNEL AT Q=230 W/M^2

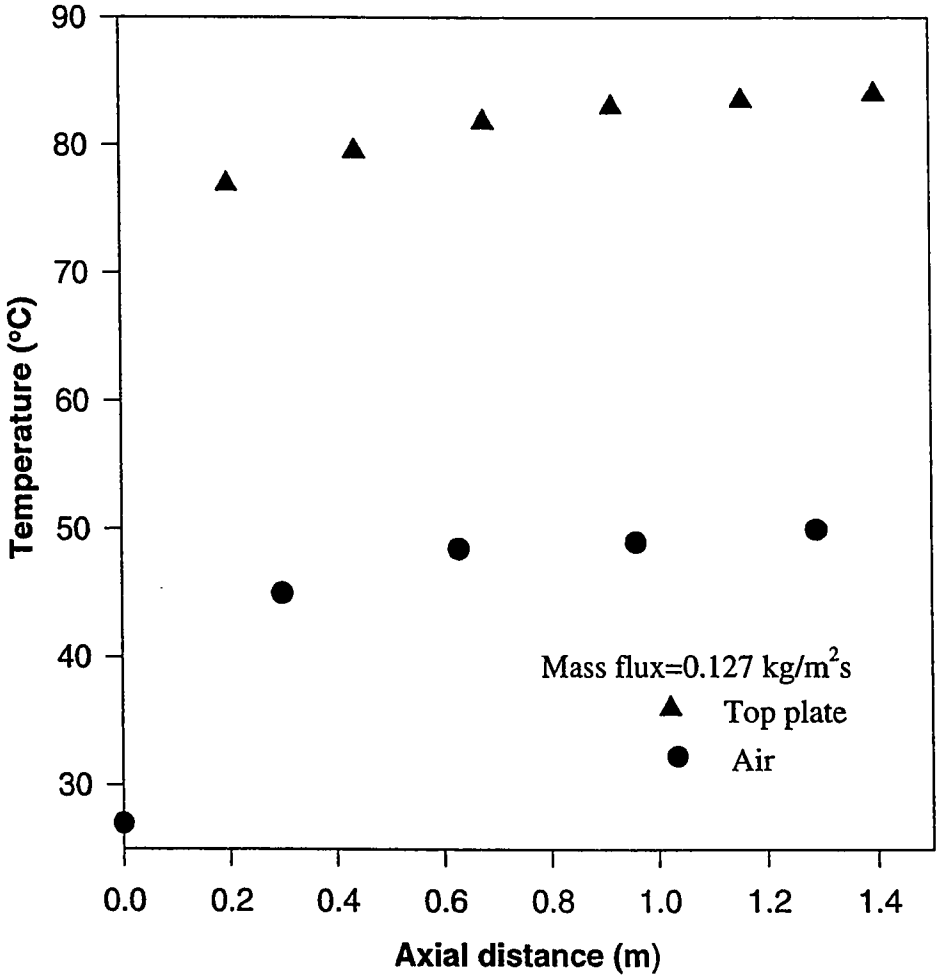

FIG. 5.22 EXPERIMENTAL AIR BULK TEMPERATURE AS FUNCTION OF THE AXIAL DISTANCE IN THE EMPTY CHANNEL AT Q=350 W/M^2

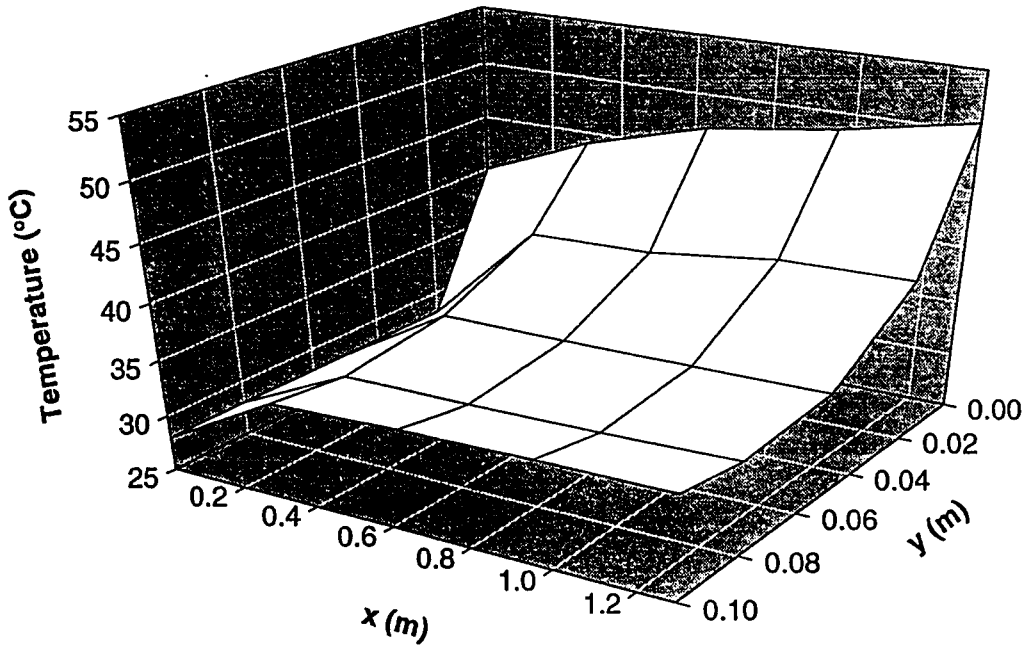

FIG. 5.23 EXPERIMENTALLY DETERMINED TEMPERATURE DISTRIBUTION IN THE EMPTY CHANNEL AT Q=130 W/M^2 AND MASS FLUX=0.127 KG/M^2S.

5.3.2 Pressure drop

Eight experiments were conducted in the empty channel for measuring the pressure drop. The experimental results for the empty channel pressure drop as function of the air superficial velocity are shown in figure *5.24*. The data was collected with an air flow ranging from *0.1* to *0.5* kg/m^2s and without heat supply for comparison with the packed channel pressure drop. The average air inlet temperature was about 25^oC.

5.4 Experimental data analysis

5.4.1 Effects of Reynolds number on transverse and axial temperature profiles

The thermally developing air temperature profiles inside the packed channel has shown a great dependence on the air flow rate. for each set of experimental runs different flow rates ranging from *0.05* to *0.5* kg/m^2s were tested. The experimentally determined air bulk temperatures for the thermally developing flow as function of axial distance at different *Re* are shown in figure *5.25-5.26* . It is observed that the air temperature takes longer to develop thermally in the axial direction as *Re* decreased. This observation can be seen more clear at higher heat supplied to the flowing air as shown in

figures *5.27* and *5.28* for the air temperature at $y=0.02\ m$ and $y=0.05\ m$ respectively.

Figures *5.29* and *5.30* shows the relationship between the increase in air bulk temperature and the *Re* at different heat fluxes. In these figures, the air bulk temperature at $x=1.29\ m$ is plotted against *Re*. As shown in the previous figures it is observed that as the *Re* decreases the air outlet temperature increases, this is mainly due to the existence of large number of slow moving layers of air between the packing and the increase in the residence time of air inside the packed section. This result may not hold for smaller size of packing in which the mixing process counterbalances the slow moving layers effects.

The effects of *Re* on the transverse air temperature profiles is shown in figure *5.31*. In this figure, The temperature profiles at the last section of the channel ($y=1.29\ m$) are plotted against the transverse distance from the top heated plate ($y=0$) at different *Re*. It is observed that as the *Re* increases the temperature profiles at the bulk reigon takes a linear shape and the temperature gradient at the wall decreases. This is mainly attributed to the mixing effects which becomes significant at high *Re*, But still the slow moving layers effects are dominant.

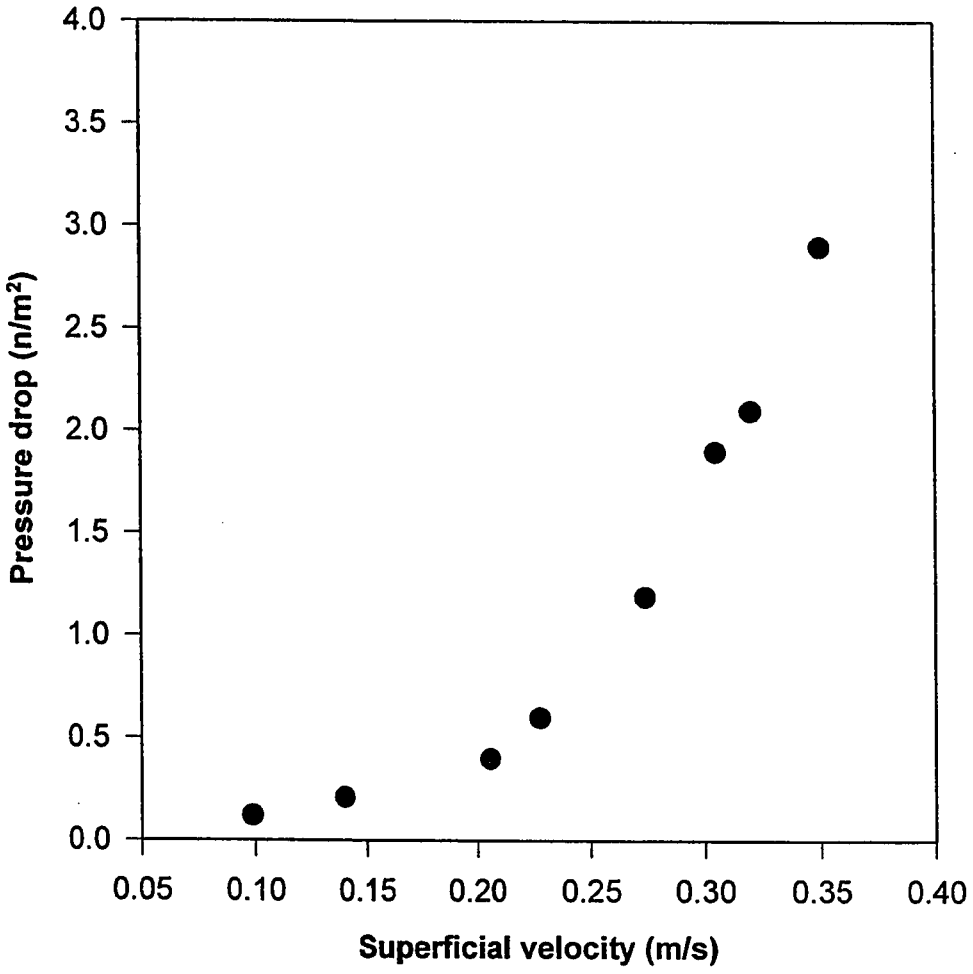

FIG. 5.24 EMPTY CHANNEL PRESSURE DROP.

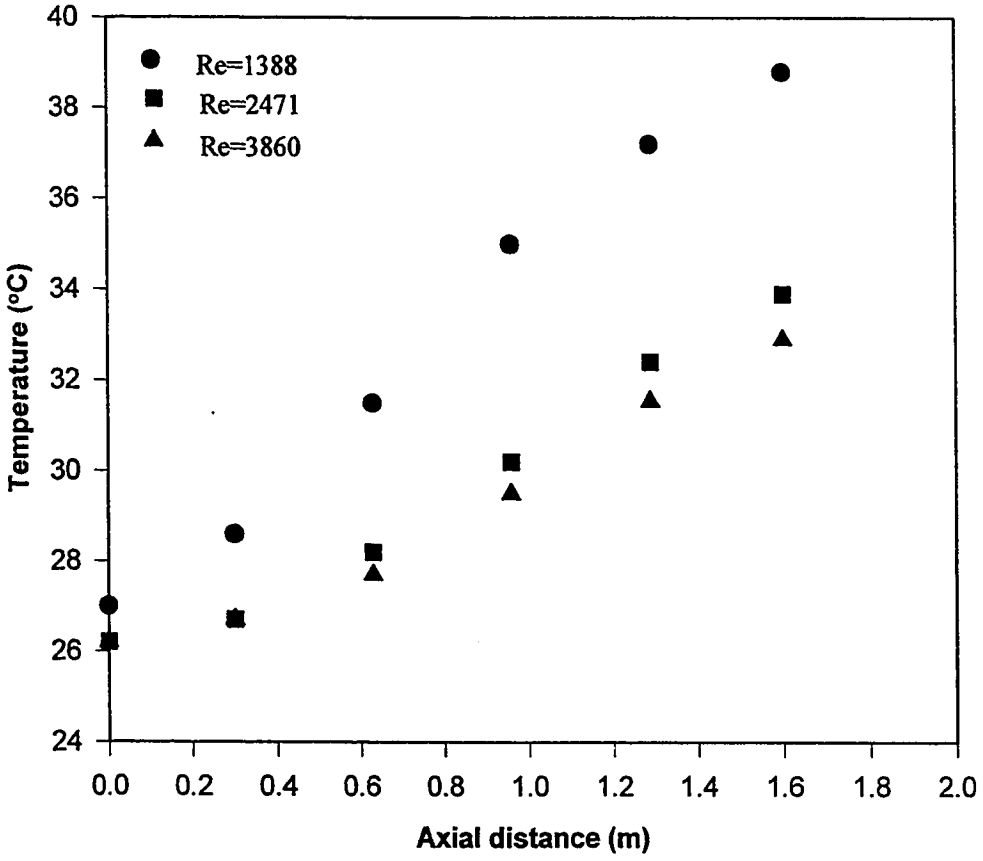

FIG. 5.25 EXPERIMENTAL AIR BULK TEMPERATURE AS FUNCTION OF THE AXIAL DISTANCE IN THE PACKED CHANNEL AT Q=130 W/m^2

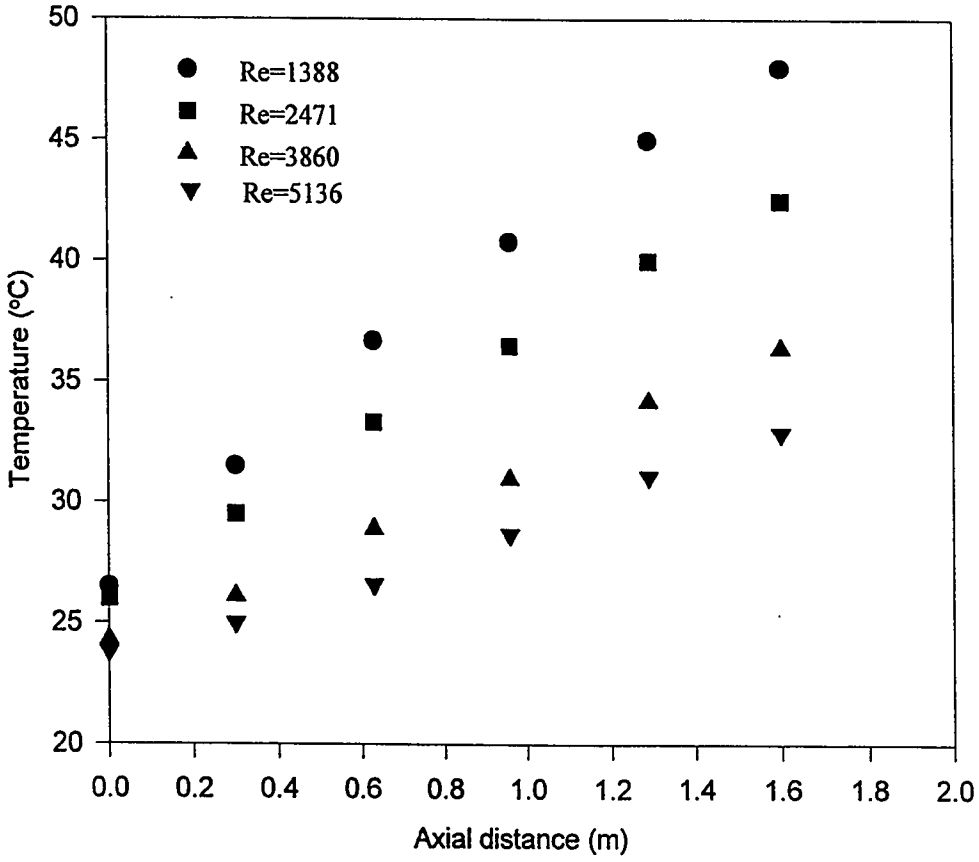

FIG. 5.26 EXPERIMENTAL DETERMINED AIR BULK TEMPERATURE AS FUNCTION OF THE AXIAL DISTANCE IN THE PACKED CHANNEL AT Q=230 W/m^2

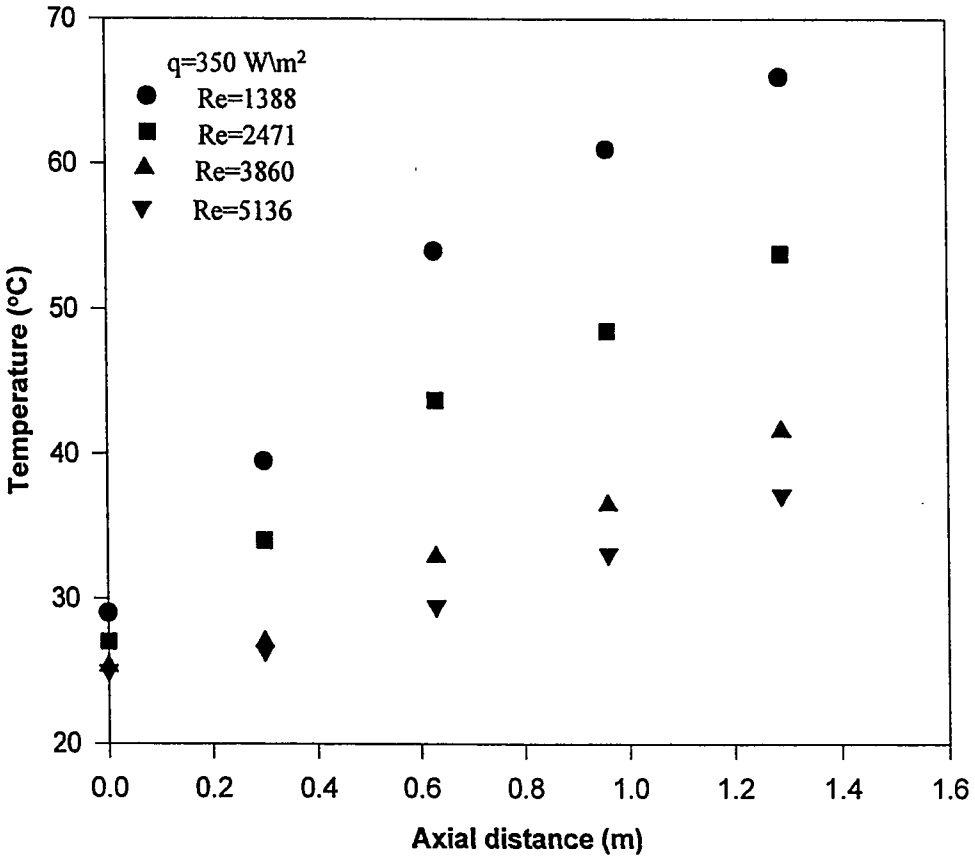

FIG. 5.27 EXPERIMENTALLY DETERMINED AIR TEMPERATURE IN THE PACKED CHANNEL AS FUNCTION OF THE AXIAL DISTANCE AT Y=0.02 m.

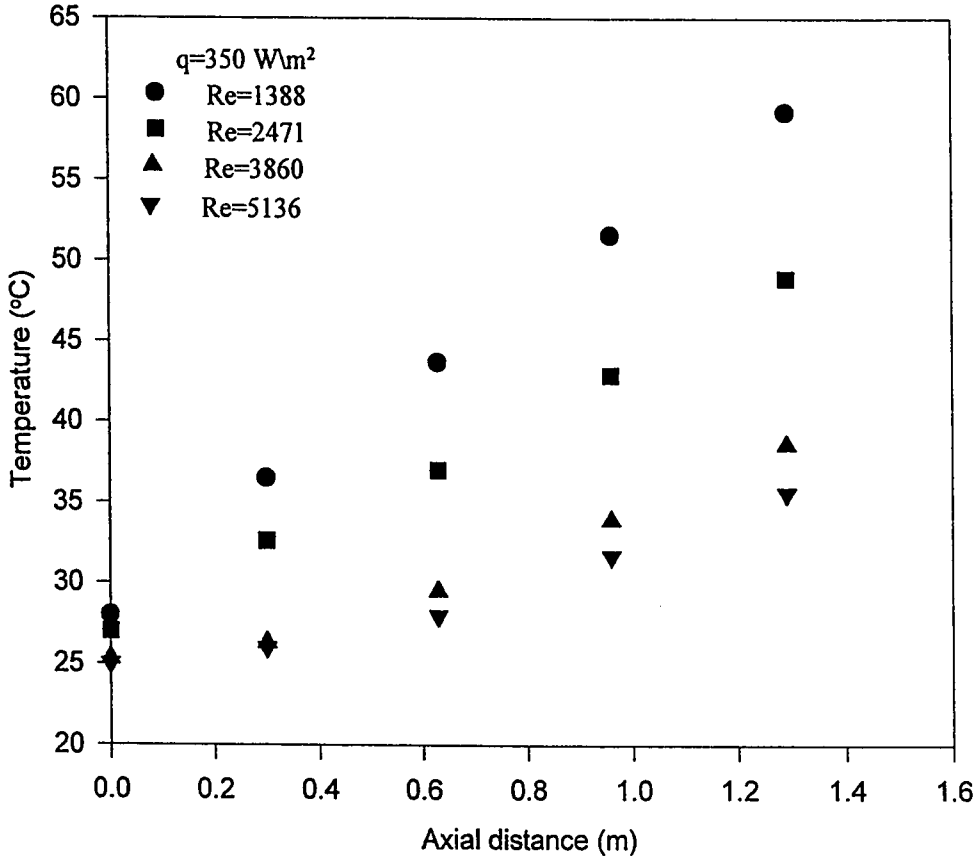

FIG. 5.28 EXPERIMENTALLY DETERMINED AIR TEMPERATURE IN THE PACKED CHANNEL AS FUNCTION OF THE AXIAL DISTANCE AT Y=0.05 m.

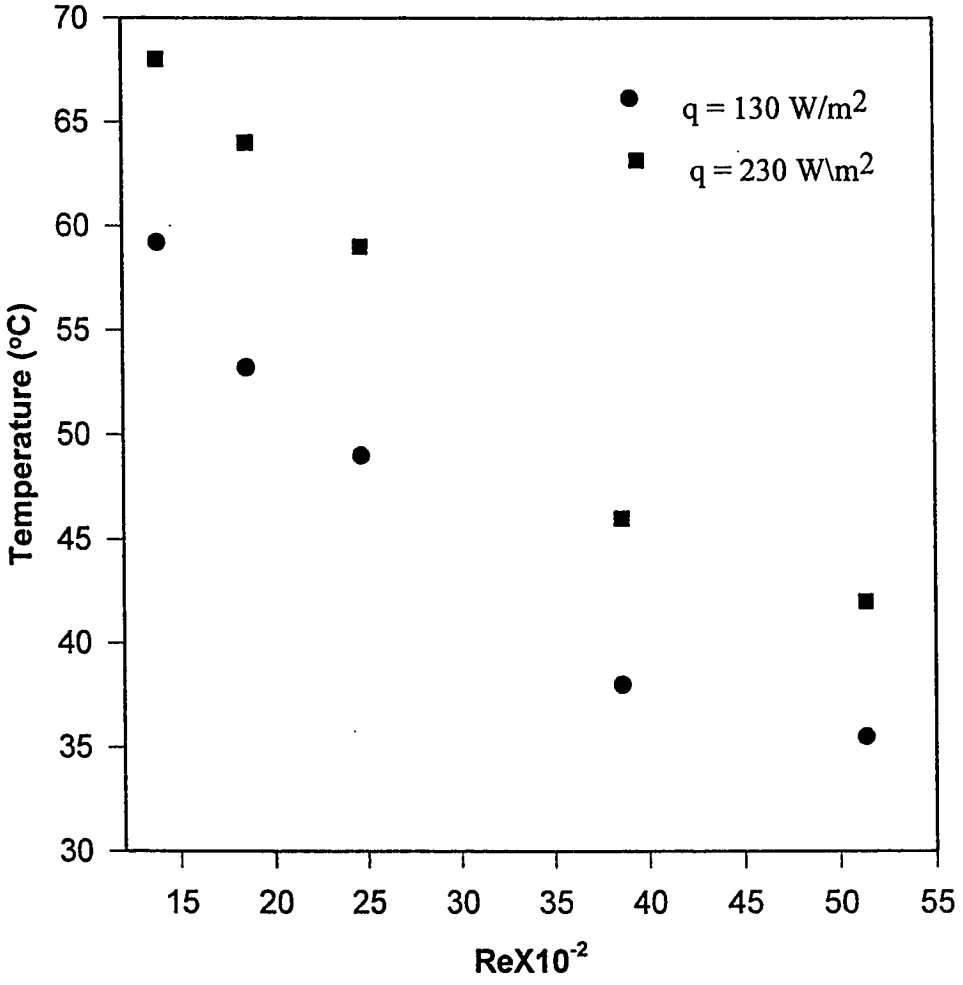

FIG 5.29 EXPERIMENTALLY DETERMINED AIR BULK TEMPERATURE IN THE PACKED CHANNEL AT X=1.29 m.

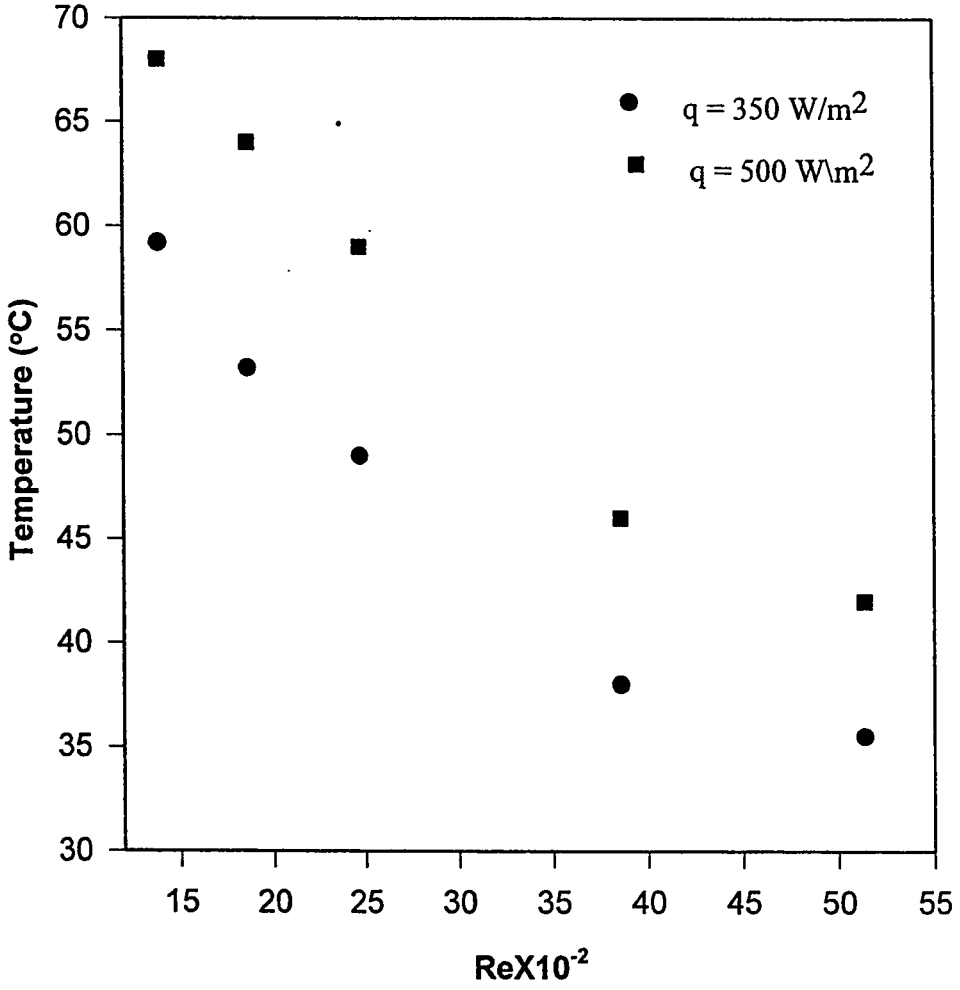

FIG 5.30 EXPERIMENTALLY DETERMINED AIR BULK TEMPERATURE IN THE PACKED CHANNEL AT X=1.29 m.

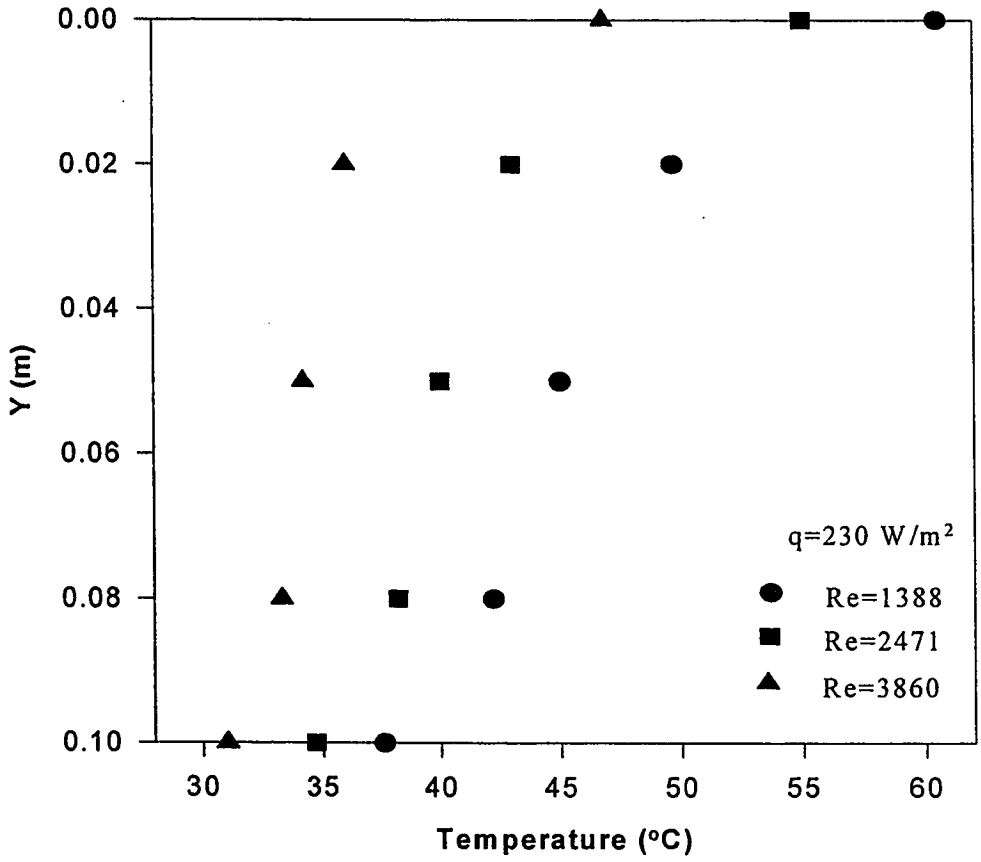

FIG. 5.31 TRANSVERSE AIR TEMPERATURE PROFILES IN THE PACKED CHANNEL AT X=1.29 m.

5.4.2 Effects of Reynolds number on wall-to-air heat transfer coefficient

In this section the local wall-to-air heat transfer coefficient with asymmetric heating for the fully developed air flow are calculated based on the experimental air temperature data and the mass flow rate by the following formula,

$$h_{loc} = \frac{mC_p(T_b - T_o)_i}{A_i(T_w - T_b)_i} \qquad (5.1)$$

The local heat transfer coefficient is presented in terms of Nusselt number. The *Nu* is defined based on the effective channel diameter and the air thermal conductivity as,

$$Nu_{loc} = \frac{h_{loc}D_e}{k_f} \qquad (5.2)$$

A plot of *Nu* calculated at *x=1.29 m* against *Re* are shown in figures *5.32-5.35* for a constant heat flux of *130, 230, 350 and 500 W/m*^{2} respectively. It shows that the value of *Nu* increases considerably in the range of *Re* considered. This increase is mainly attributed to the convection process, which is predominant at this flow regime. However figures *5.32* and *5.35* shows that at *Re>4500* the curve shows a slight decrease in the value of *Re* compared to figures *5.33* and *5.34*.

The values of local Nusselt as function of axial distance and different *Re* are shown in figure *5.36*. From this figure, it can be seen that *Nu* has almost a linear profile at low flow rates (*Re* < *1881*) as the air flows towards the exit section of the packed channel. It is noteworthy that the effects of *Re* on the local *Nu* becomes significant at *Re* >*1881* as shown in figure *5.37*. This result can be explained from a physical standpoint: The mixing of local air streams yield a significant effect on the process of heat transfer, it can also be seen that the entrance effects is relatively week as the flow rate decreases.

The experimentally determined fully developed *Nu* obtained with the packed channel at different flow regimes is shown in table *5.2*.

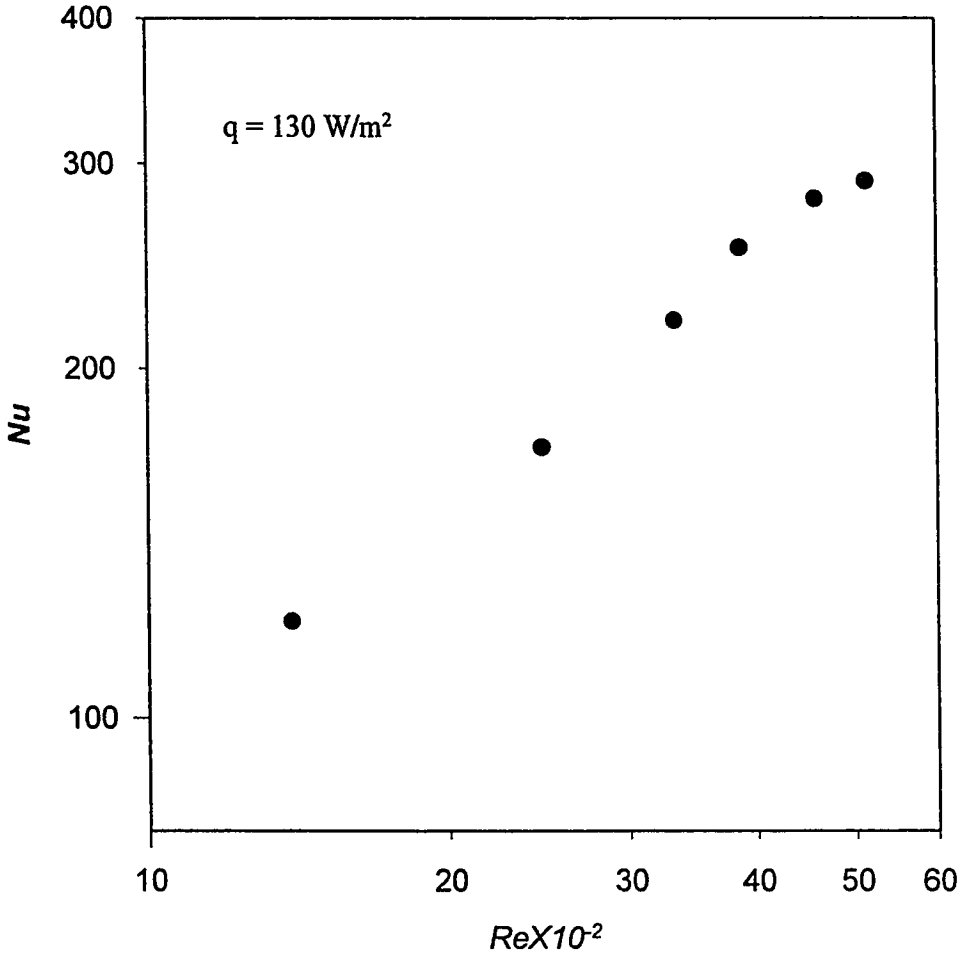

FIG. 5.32 EXPERIMENTALLY DETERMINED *Nu* AS FUNCTION OF *Re* AT X=1.29 m

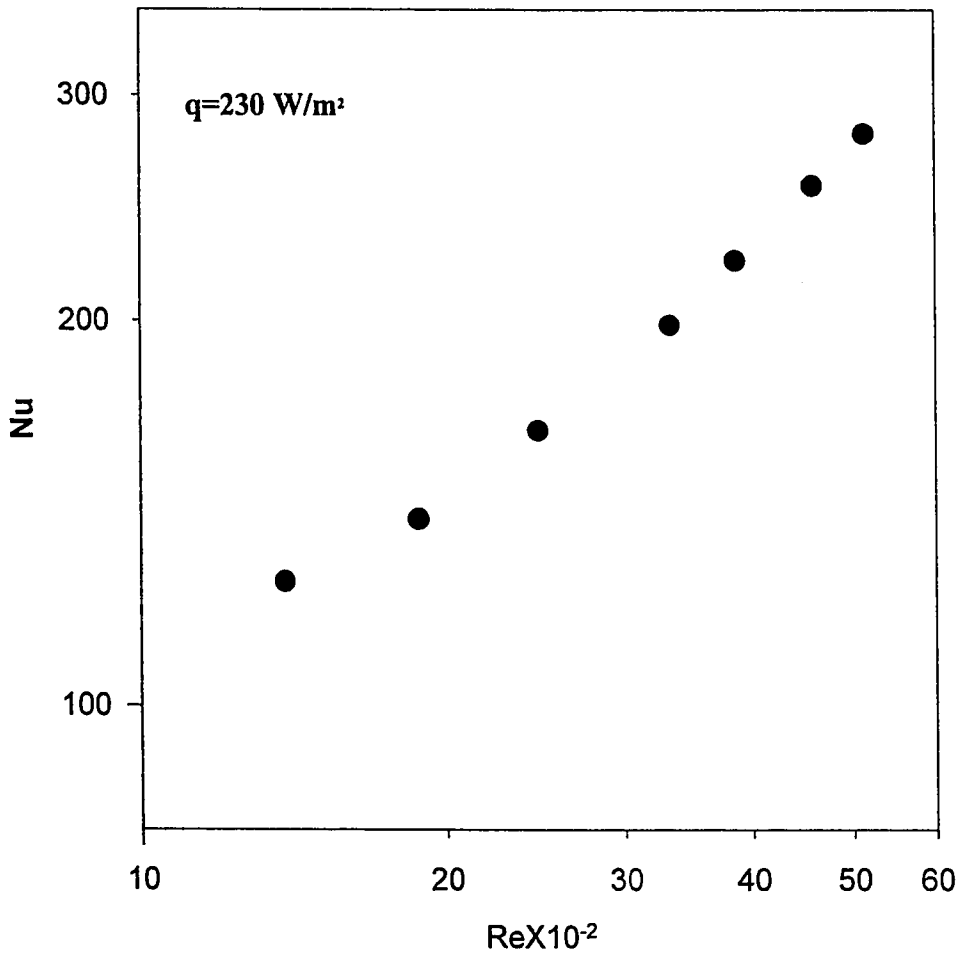

FIG. 5.33 EXPERIMENTALLY DETERMINED *Nu* AS FUNCTION OF *Re* AT X=1.29 m.

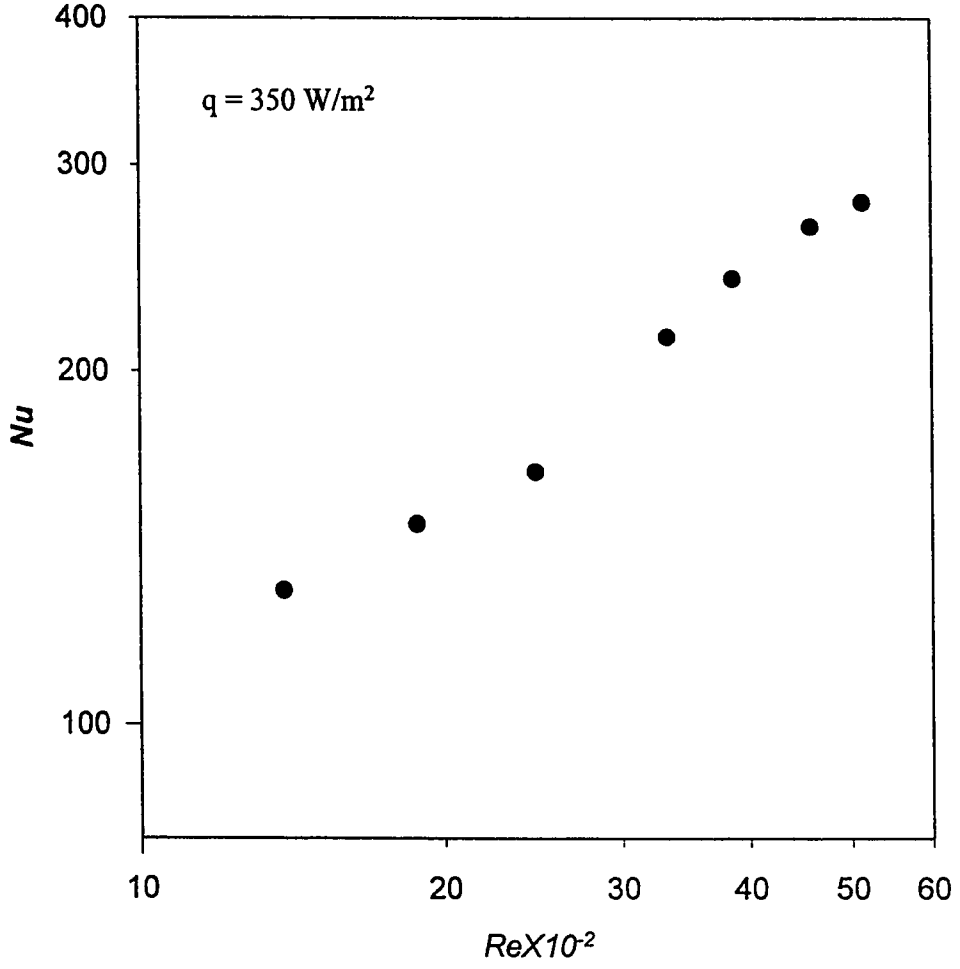

FIG. 5.34 EXPERIMENTALLY DETERMINED *Nu* AS FUNCTION OF *Re* AT X=1.29 m.

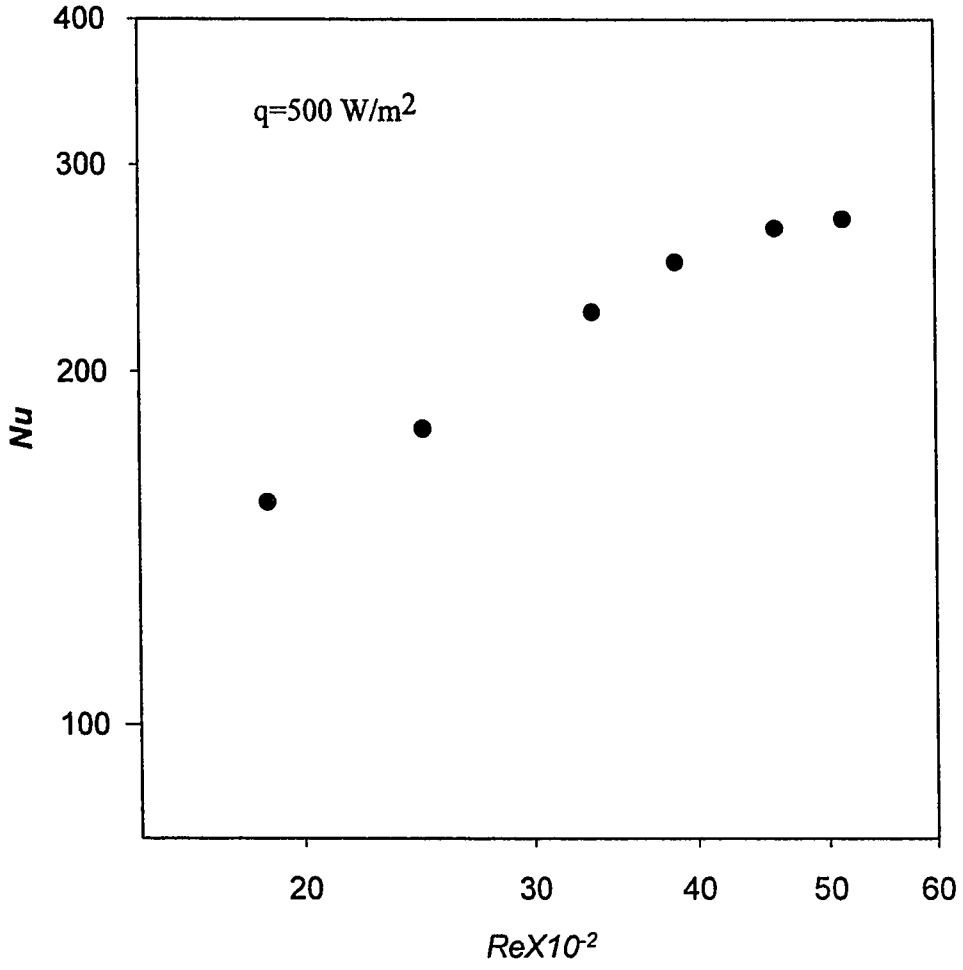

FIG. 5.35 EXPERIMENTALLY DETERMINED *Nu* AS FUNCTION OF *Re* AT X=1.29 m.

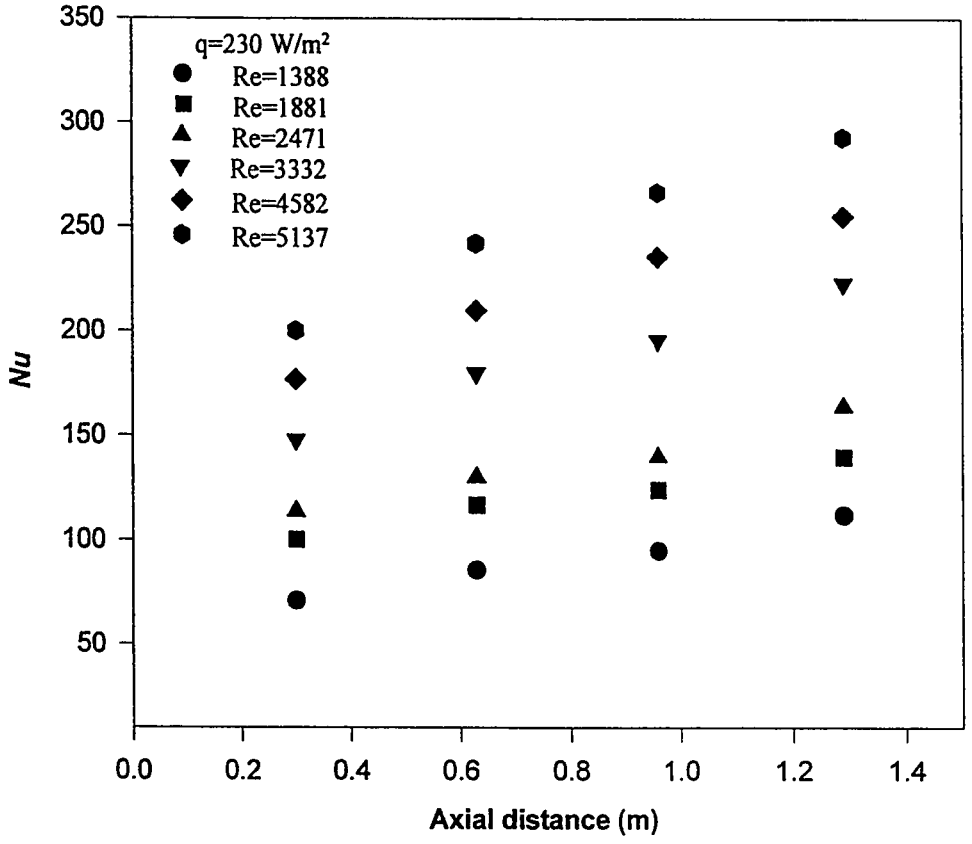

FIG. 5.36 LOCAL *Nu* AS FUNCTION OF THE AXIAL DISTANCE IN THE PACKED CHANNEL.

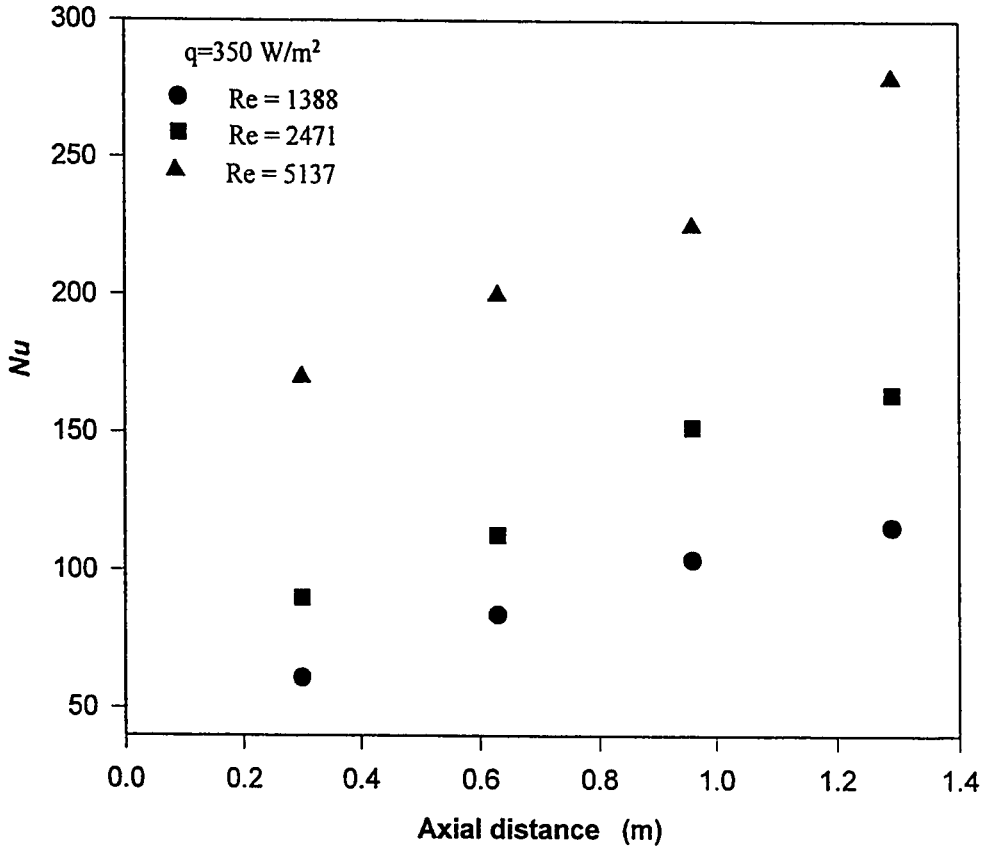

FIG. 5.37 LOCAL *Nu* AS FUNCTION OF THE AXIAL DISTANCE IN THE PACKED CHANNEL.

Table 5.2 Experimentally determined *Nu* in the packed channel.

Heat supplied (W/m^2)	Nusselt number						
	Reynolds number						
	1388	**1881**	**2471**	**3332**	**2860**	**4582**	**5137**
130	121	130	171	231	254	276	290
230	125	139	164	198	223	255	293
350	117	148	164	214	194	266	279

5.4.3 Comparison between experimental and previous theoretical predictions of packed channel pressure drop

Ergun equation is one of the most reliable model for the prediction of pressure drop in packed beds. It is generally good for void fraction of less than *0.5* (*19*). The experimental results for the pressure drop obtained in our system which is of void fraction *0.81* has shown a great difference from Ergun's equation predictions.

Many previous studies on related packed bed systems has cast doubt on the constants presented in ergun equation. Figure *5.38* shows a comparison between the present experimental pressure drop data and that which would be obtained by Ergun equation. It is observed that the Ergun equation is under estimating the pressure drop, the differences between the experimental and Ergun prediction increases considerably as the flow rate decreases. The percentage error in Ergun prediction reaches a value of *68 %* at a superficial velocity of about *0.07 m/s*.

In a recent experimental study by Bohn (*28*) a new correlative expression for the friction factor in packed beds as function of *Re* was presented as,

$$f_o = 6.508\,\mathrm{Re}^{-0.241} \qquad (5.3)$$

This expression was obtained by a least square fit to the experimental data obtained in a pall ring tubular packed bed of void fraction *0.947* and at an average air temperature of about *250 °C*. Figure *5.39* shows a comparison between the present experimental data and that which would be obtained by Bohn Correlation. It is shown that the Bohn correlation is over estimating the pressure drop with an error of about *65 %* at a superficial velocity of *0.03 m/s*.

5.5 Modified Ergun equation

Due to the nature of the rectangular shape of the present experimental equipment and the large void fraction used in this study, a modification to Ergun equation proved to be necessary to obtain a reliable pressure drop. Table *5.3* shows the experimental and the predicted pressure drop by Ergun equation along with the percentage error.

The predictive pressure drop model presented by Ergun is as follows,

$$\frac{P_o - P_L}{L} = C_1 \frac{G\mu(1-\varepsilon)^2}{D_p{}^2 \rho} + C_2 \frac{G^2(1-\varepsilon)}{D_p \rho \varepsilon^3} \qquad (5.4)$$

with C_1=*150* and C_2=*1.75*.

For values of *Re > 1000* the viscous forces, that is the first term on the right hand side of equation (*5.4*) represent less than *10 %* of the total flow

resistance, and therefore may be neglected, for values of $Re < 10$ the inertia forces, that is the second term on the right hand side of equation (*5.4*) become negligibly small (*10*). Table *5.4* shows the percentage of viscous and inertia forces of the total flow resistance that calculated by the original Ergun equation in the range of *Re* considered in this study. As shown the viscous forces represent a maximum of *5 %* of the total flow resistance at the lowest *Re* considered in the experimental study. So in the present modified equation the viscous forces were neglected.

The experimental data and a least squares curve fit procedure was used to evaluate the fitting parameter C_2 which appears in equation (5.4) by relating the experimental packed channel pressure drop results to the superficial velocity. Based on the *20* experimental data listed in table *5.1*, the following modified Ergun equation for the range of *Re* considered is,

$$\frac{P_o - P_L}{L} = 4.275 \frac{G^2(1-\varepsilon)}{D_p \rho \varepsilon^3} \qquad (5.5)$$

Figure *5.40* shows the experimental and the predicted packed channel pressure drop by the present modified equation. The maximum deviation is *9 %*, the standard error is *0.09*.

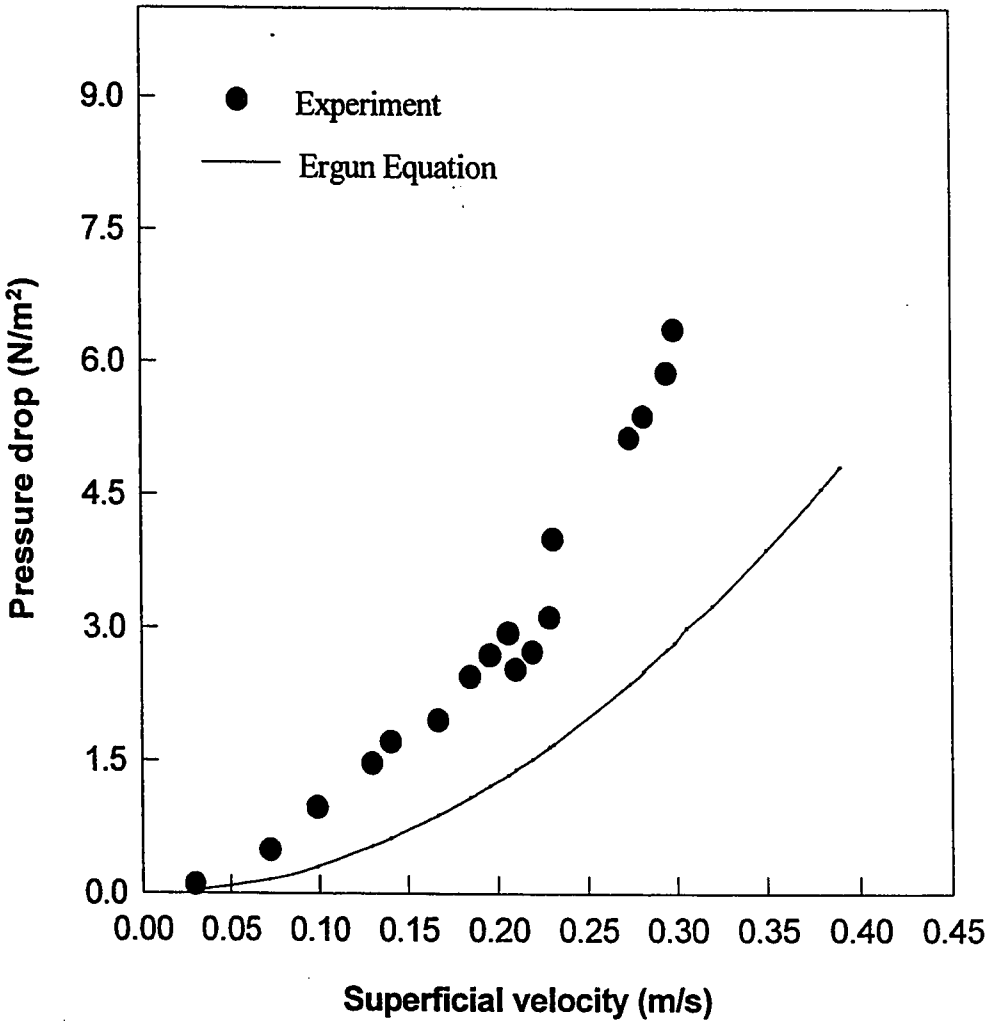

FIG. 5.38 COMPARISON BETWEEN THE EXPERIMENTAL PACKED CHANNEL PRESSURE DROP AND ERGUN'S PREDICTIONS.

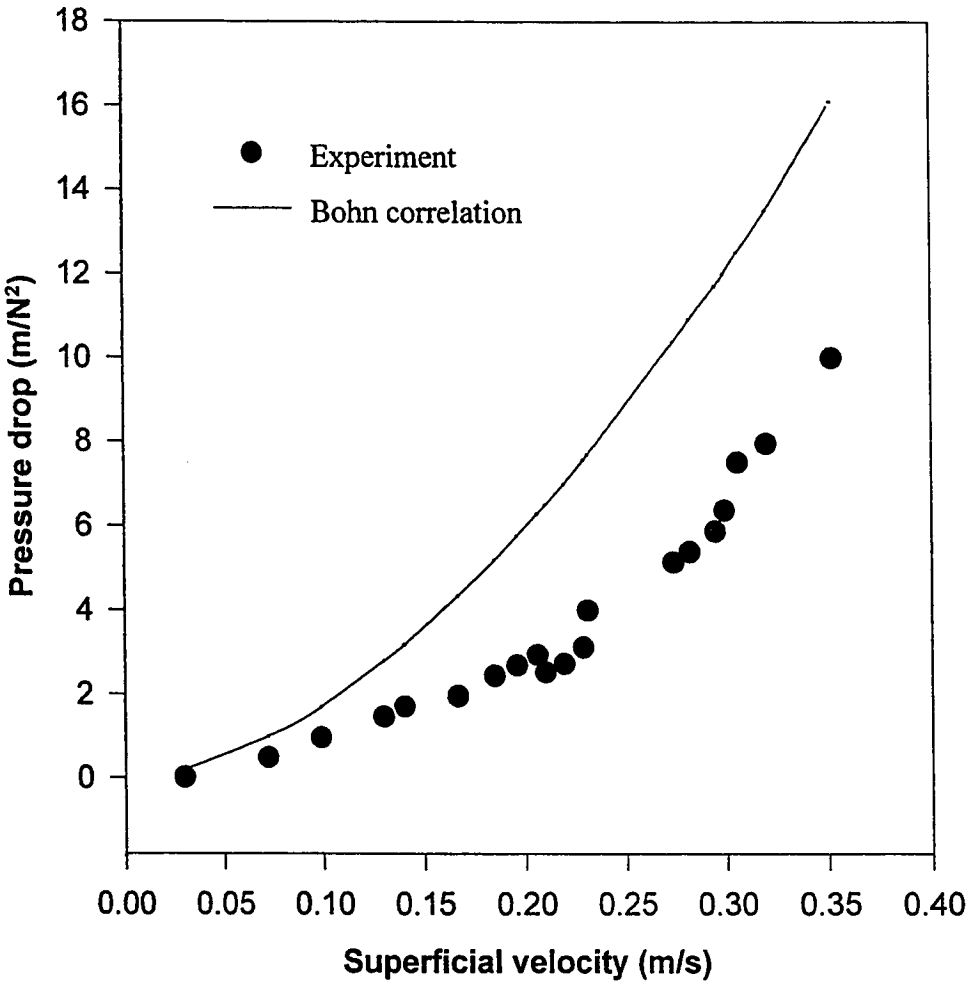

FIG. 5.39 COMPARISON BETWEEN EXPERIMENTAL AND PREDICTED PRESSURE DROP BY BOHN CORRELATION.

Table 5.3 Comparison between experimental and predicted pressure drop by Ergun equation.

Superficial velocity	Experimental ΔP ((N/m^2)	Predicted ΔP	% Erorr
0.071	0.49	0.16	68
0.099	0.97	0.31	67
0.130	1.47	0.54	63
0.140	1.72	0.63	63
0.167	1.96	0.89	54
0.185	2.45	1.09	55
0.196	2.69	1.23	54
0.206	2.94	1.36	53
0.210	5.53	1.42	74
0.219	2.73	1.54	43
0.228	3.12	1.71	45
0.231	4.00	1.71	57
0.274	5.14	2.41	53
0.282	5.39	2.55	52
0.295	5.88	2.79	52
0.299	6.37	2.88	54
0.305	7.50	3.00	60

Table 5.4 Viscous and inertia forces calculated by the original Ergun equation.

Reynolds number	Viscous forces	Inertia forces	% of viscous forces
805	0.009	0.102	8.0
1105	0.013	0.197	6.3
1452	0.174	0.338	4.9
1578	0.019	0.398	4.5
1873	0.022	0.562	3.8
2068	0.025	0.686	3.5
2194	0.026	0.770	3.3
2305	0.027	0.850	3.2
2352	0.028	0.880	3.1
2563	0.031	1.050	2.8
3068	0.037	1.507	2.3
3352	0.040	1.798	2.2

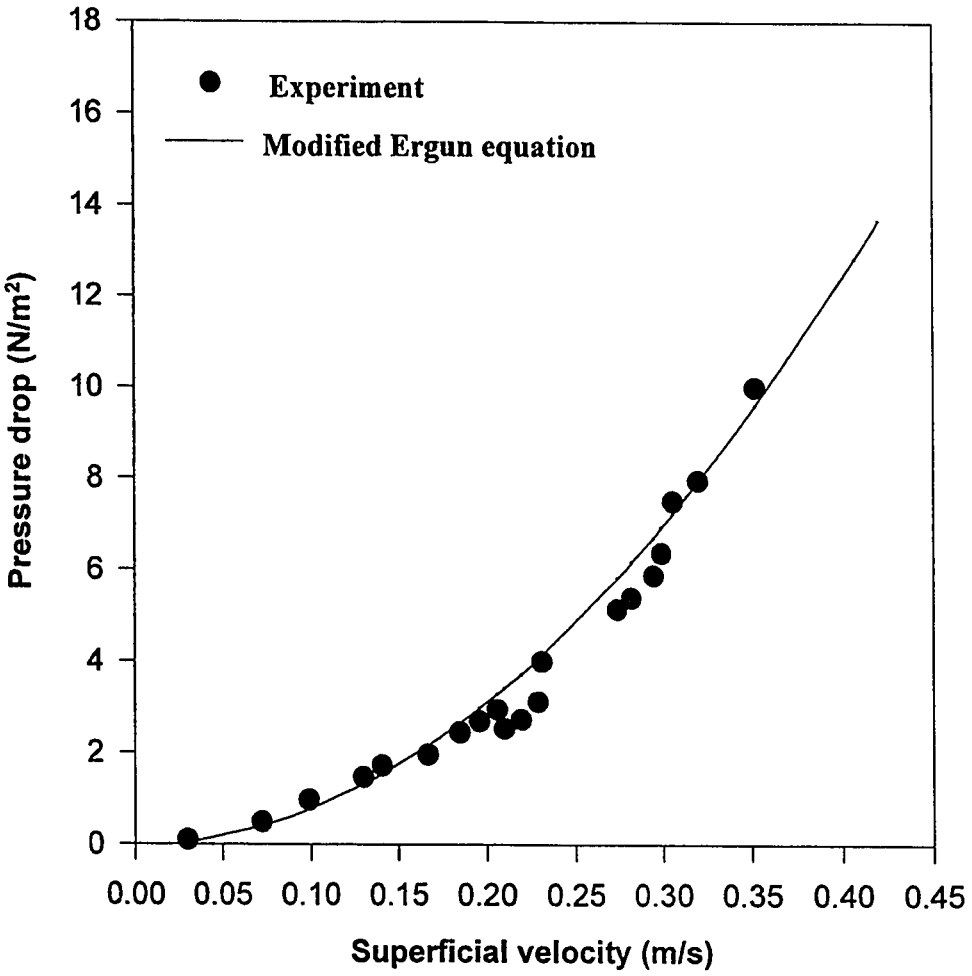

FIG. 5.40 BEST FIT VALUES OF THE PRESSURE DROP IN THE PACKED SECTION AS FUNCTION OF THE AIR SUPERFICIAL VELOCITY.

5.6 Correlative expression of Nusselt number

The convective heat transfer coefficient is given in a non-dimensional form by the nusselt number (*Nu)*, A dependence power law of *Nu* upon *Re* was searched for, assuming the mathematical form,

$$Nu = C\,\mathrm{Re}^{x} \tag{5.6}$$

On the basis of empirical equations reported in the literature for other cases of forced convection with constant heat flux (*6*).

Application of the method of least squares curve fit the algorithm of *Nu* and *Re* has yielded,

$$Nu = 0.8334\,\mathrm{Re}^{0.6836} \tag{5.7}$$

Equation (*5.7*) is graphically represented by the solid line in figure *5.41*. Experimental data are indicated with symbols. Reproduction of data is satisfactory: The maximum deviation is *7 %*; the standard error of the coefficient *C* is 0.1663 and *0.02436* for the coefficient *x*.

It is worth noting that the above correlative expression of *Nu* is valid only for a rectangular channel with asymmetric heating, aspect ratio $\frac{W}{H}$ =*8.0*

and for a particle to channel effective diameters ratio $\frac{D_p}{D_e} = 0.127$ for the range of operating conditions considered in this study.

5.7 Simulation results

5.7.1 Velocity distribution

The results for the fully developed velocity profiles were calculated numerically using the modified Brinkman-Ergun model. The viscous forces which has been found to represent less than *5%* were neglected in the momentum equation. Figure *5.42* shows the variation of the local air velocity as function of the transverse distance at *Re=1388* and *3860*. From these local velocity profiles, two important observations are shown, (i) the velocity profile almost has a plug flow model shape. (ii) the velocity attains its maximum at a distance of about *0.2* times the effective packing diameter from the surrounding walls.

Fig *5.43* shows a comparison between the calculated velocity profiles at a wide range of *Re*. As expected, the velocity increases considerably as the *Re* increases.

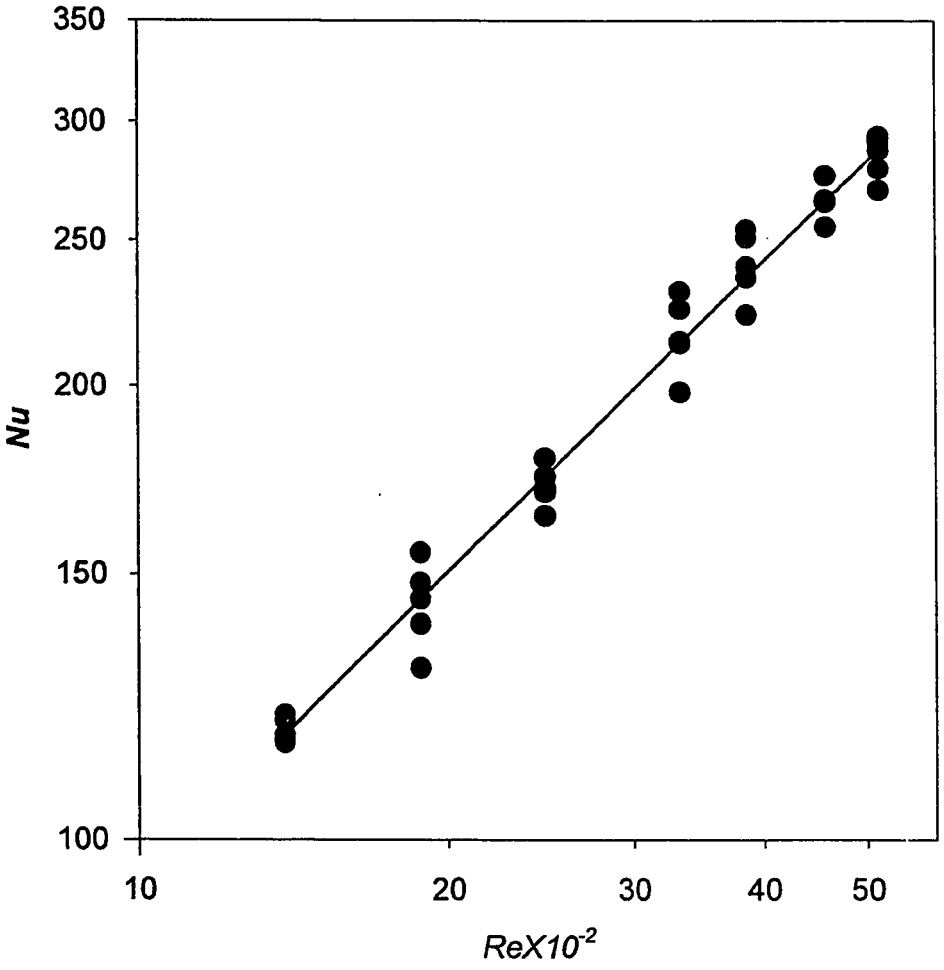

FIG. 5.41 BEST FIT VALUES FOR THE *Nu* AS FUNCTION OF *Re*.

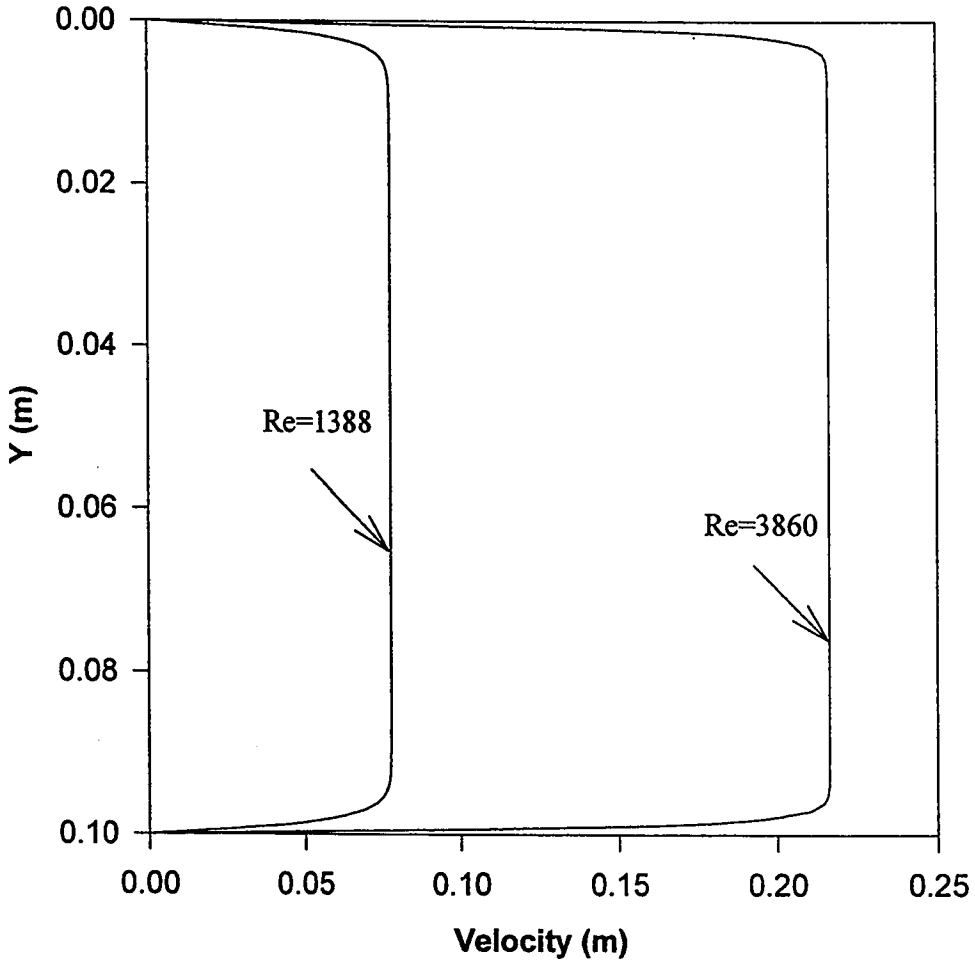

FIG. 5.42 FULLY DEVELOPED VELOCITY PROFILES IN THE PACKED CHANNEL AS FUNCTION OF THE TRANSVERSE DISTANCE

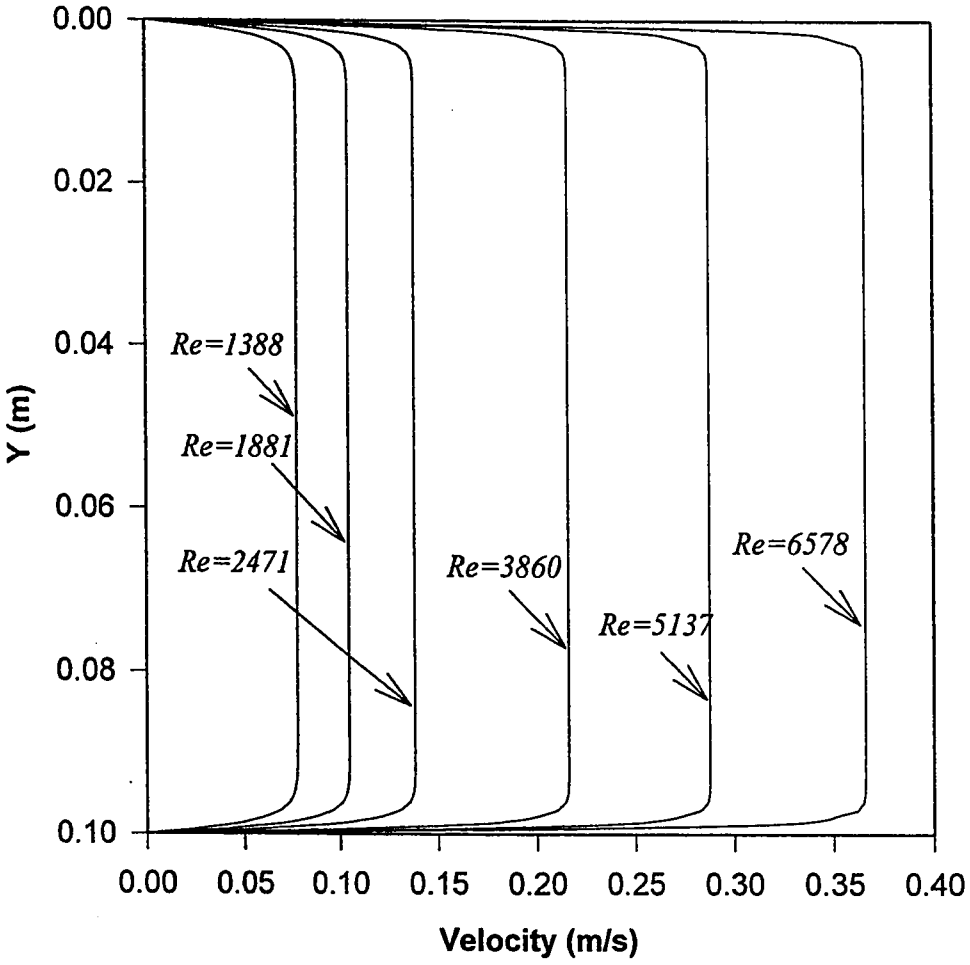

FIG. 5.43 FULLY DEVELOPED VELOCITY PROFILES IN THE PACKED CHANNEL AS FUNCTION OF THE TRANSVERSE DISTANCE AT DIFFERENT *Re*.

5.7.2 Temperature distribution

The predicted transverse and axial air temperature distribution inside the packed channel has shown good agreement with the experimental data. Figures *5.44* and *5.45* shows a comparison between the predicted And experimental air temperature inside the packed channel at two different *Re*. It is seen from these figures that the model results are perfectly predicting the air temperature distribution inside the packed channel. The transverse air temperature profiles are shown in figures *5.46* and *5.47* for different *Re* and at low heat flux. These plots also show the good agreement between the model and the experimental data. The predicted and experimental air bulk temperature profiles as function of the axial distance at different *Re* are shown in figure *5.48*.

5.7.3 Heat transfer coefficient

The numerical evaluation for the local heat transfer coefficient was based on the following equation

$$h_w = \frac{k_e \left(\frac{\partial T}{\partial y}\right)_{y=0}}{A_i \left(T_w - T_b\right)_i} \qquad (5.8)$$

The heat transfer coefficient in non-dimensional form is written in terms of *Nu* which is defined as follows,

$$Nu = \frac{h_w D_e}{k_f} \qquad (5.9)$$

Considering the air flow in a rectangular packed channel, the fully developed Nusselt number is considerably increased as *Re* increases, Comparison between the experimental and the predicted nusselt number are shown in figures *5.49* and *5.50* for a wide range of *Re*. It is shown that the model is slightly over predicting the experimental results as the Reynolds increases, but the overall prediction is satisfactory compared to previous predictive models. The difference between the model prediction and the experimental *Nu* is mainly attributed to the differences between the predicted and the experimental top heated plate temperature. It is worth noting that there is a little doubt on the effect of the radiation on the top plate thermocouples.

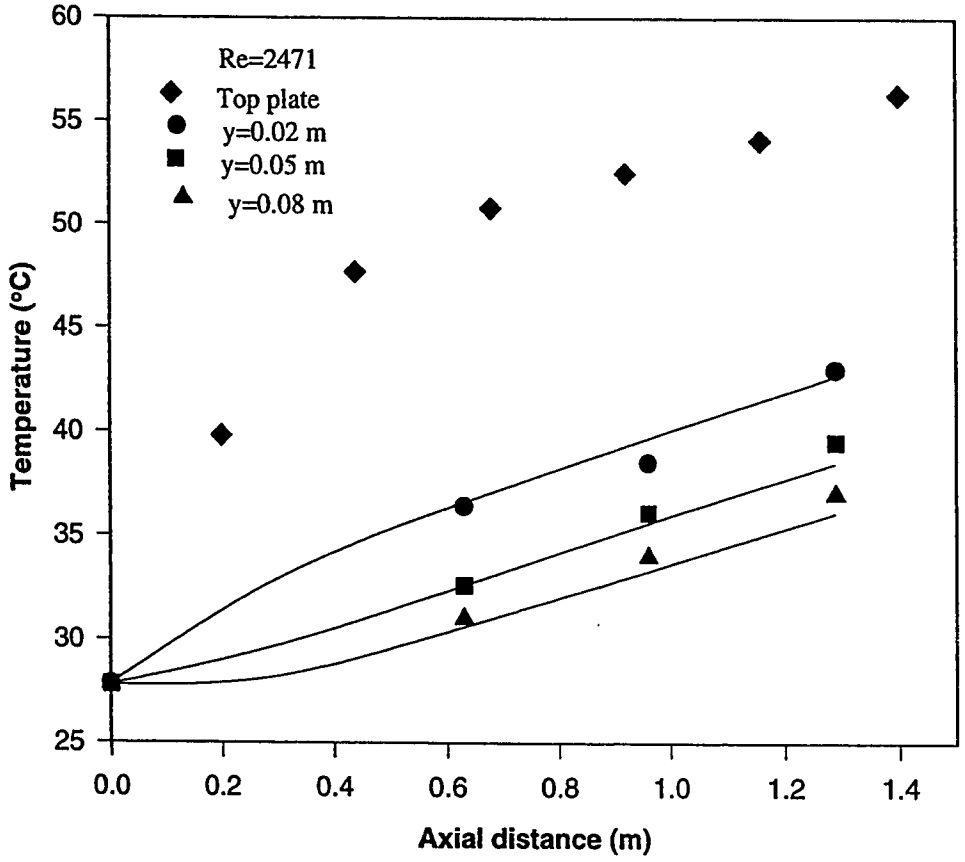

FIG. 5.44 EXPERIMENTAL AND PREDICTED AIR TEMPERATURE PROFILES IN THE PACKED CHANNEL AT Q=230 W/m^2

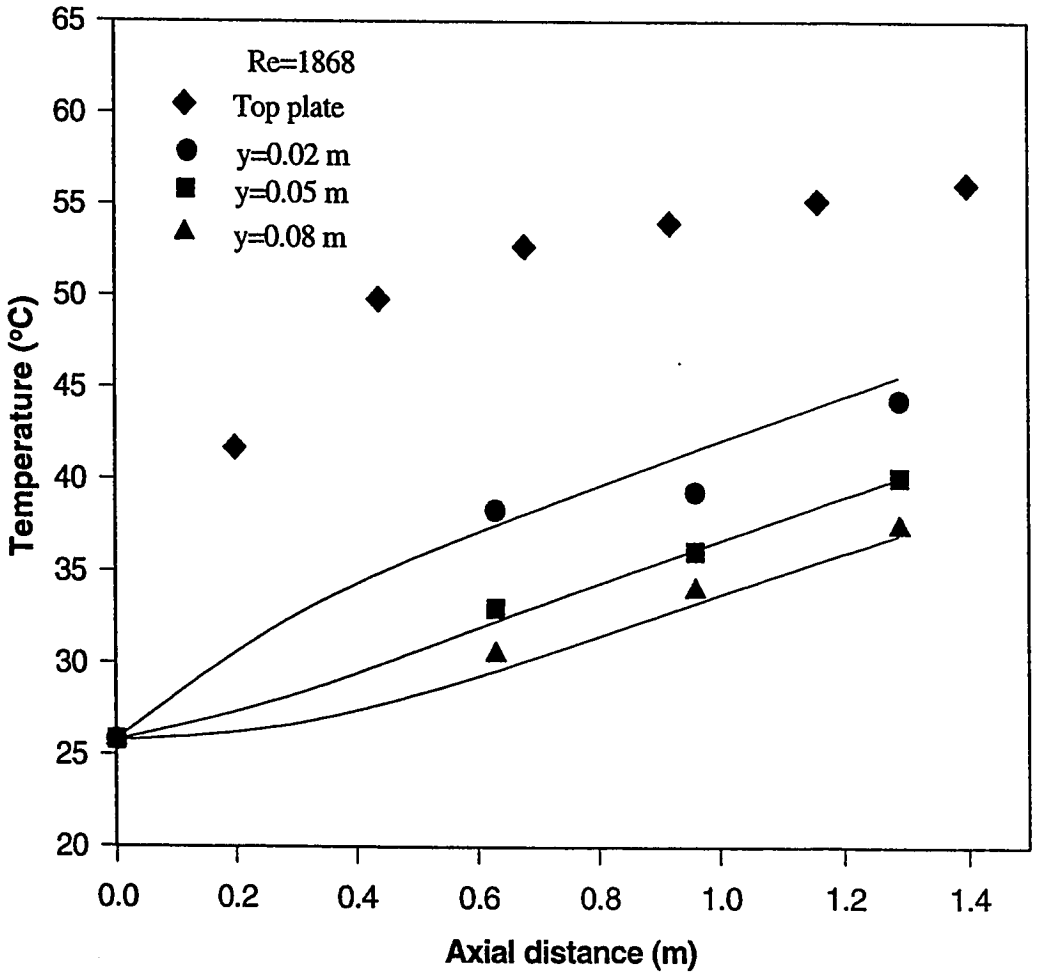

FIG. 5.45 EXPERIMENTAL AND PREDICTED AIR TEMPERATURE PROFILES IN THE PACKED CHANNEL AT Q=230 W/m^2

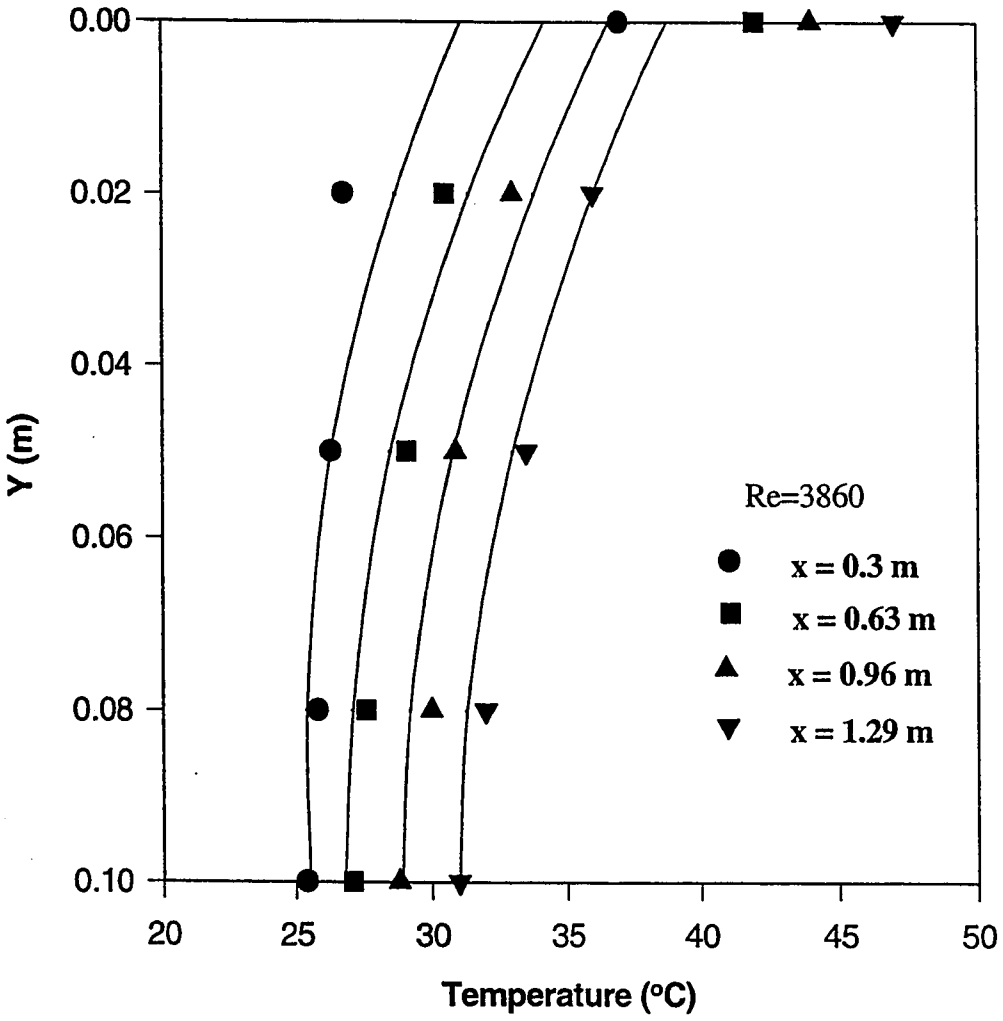

FIG. 5.46 EXPERIMENTAL AND PREDICTED TRANSVERSE AIR TEMPERATURE PROFILES IN THE PACKED CHANNEL AT Q=230 W/m^2

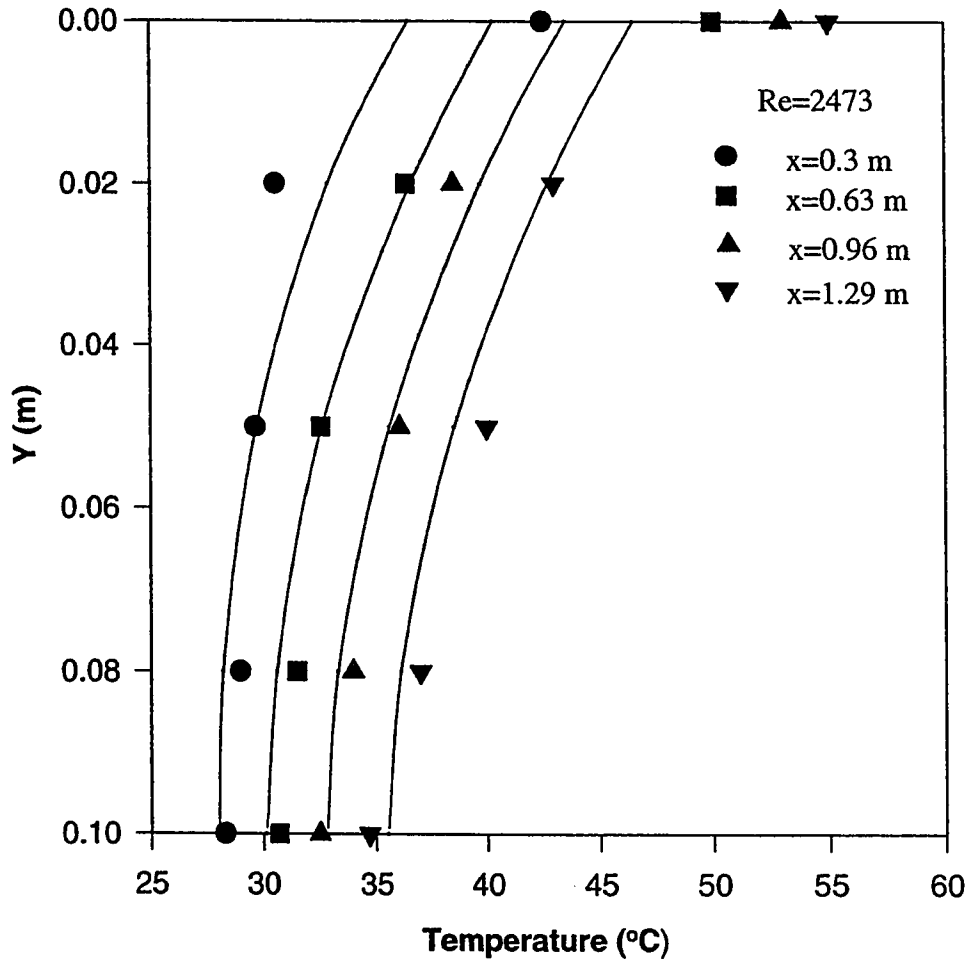

FIG. 5.47 EXPERIMENTAL AND PREDICTED TRANSVERSE AIR TEMPERATURE PROFILES IN THE PACKED CHANNEL AT Q=230 W/m^2

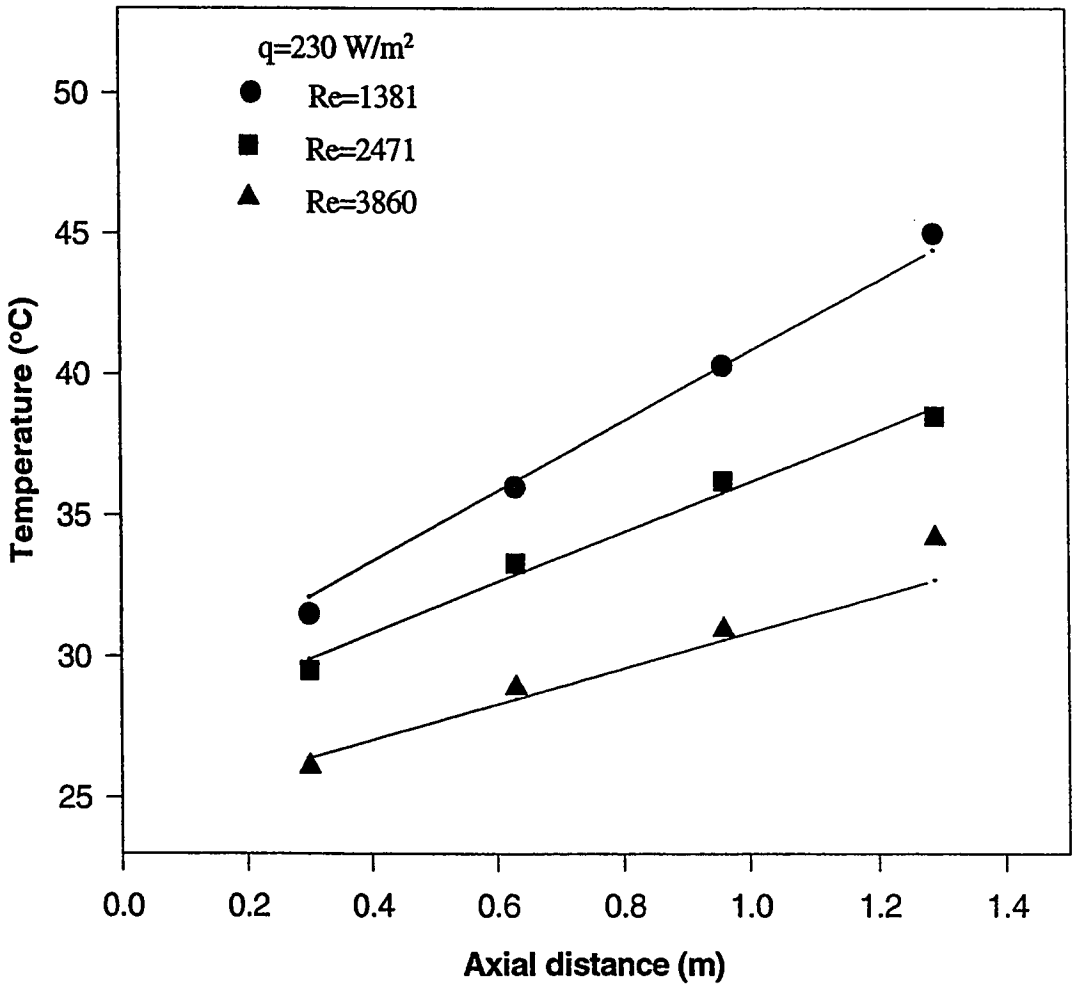

FIG. 5.48 EXPERIMENTAL AND PREDICTED AIR BULK TEMPERATURE AS FUNCTION OF THE AXIAL DISTANCE.

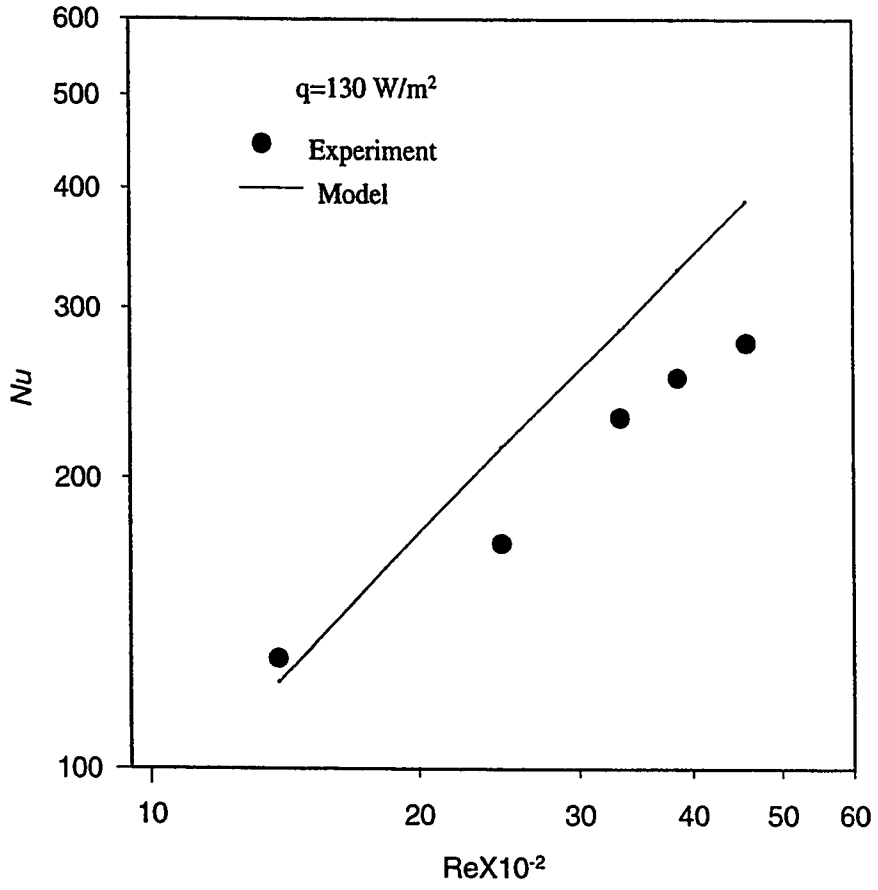

FIG. 5.49 EXPERIMENTAL AND PREDICTED FULLY DEVELOPED *Nu* AT X=1.29 m.

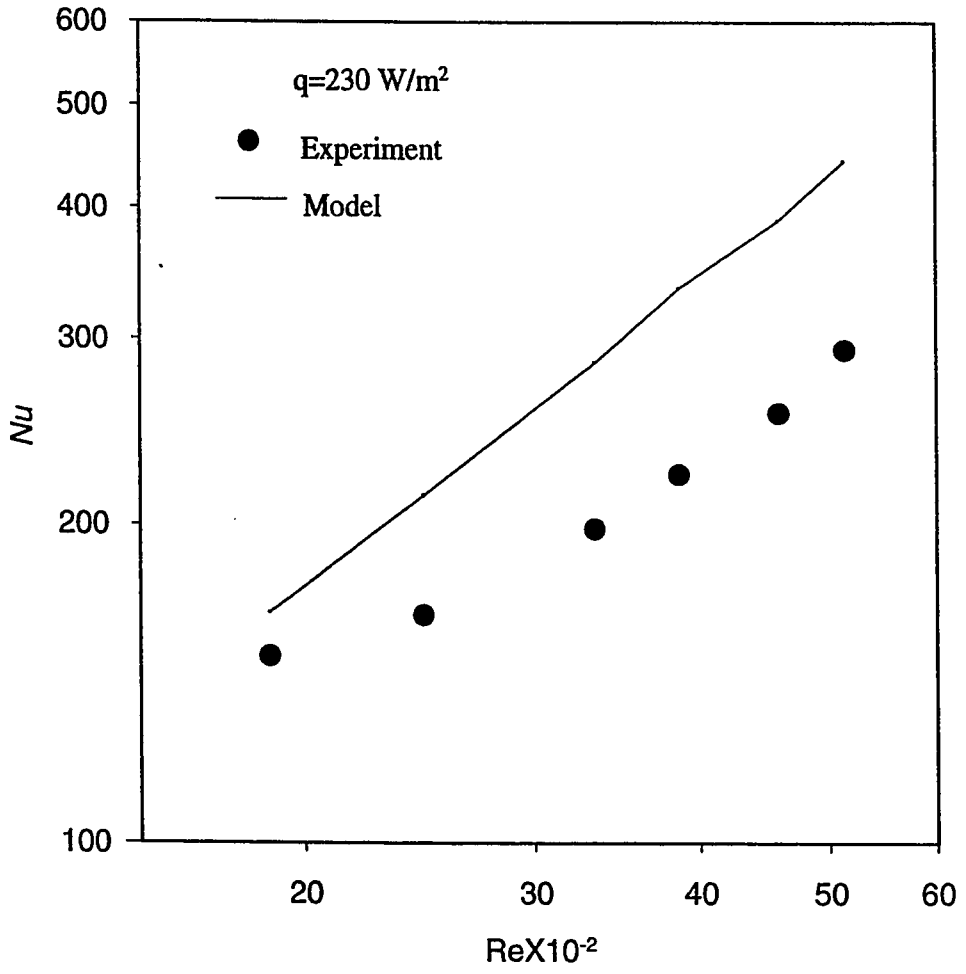

FIG. 5.50 EXPERIMENTAL AND PREDICTED FULLY DEVELOPED *Nu* AT X=1.29 m.

5.8 Comparison between empty and packed channel performance

5.8.1 Temperature distribution

A comparison between the temperature distribution as function of the axial distance (from the inlet) in the channel with and without packing at a mass flux=*0.227* kg/m^2s is presented in figure *5.51*. It is shown that the wall temperature in the empty channel is higher than that in the packed one and the air temperature profile has almost a horizontal shape after an axial distance of *0.3 m* from the inlet distributor plate, while in the packed channel the air temperature increases considerably as it moves towards the exit section, this is mainly attributed to the good mixing caused by the presence of packing in the air flow passage. It is also observed that the difference between the air temperature in the packed and empty channel decreases as the air moves towards the exit section of the channel.

Figure *5.52* shows a comparison between the transverse temperature profiles obtained with the empty and packed channel at a mass flux=*0.357* kg/m^2s. It is shown that the temperature gradient at the wall is higher in the empty channel, which is contradicting the experimental results obtained by Hwng et al (*6*) in an empty and packed channel with smaller size of packing, in their results it was shown that the temperature gradient at the wall decreases

when packing is used. The increase in the wall temperature gradient obtained in our results can be justified from the fact that; with a packed channel the air mixing process is higher which results in an increase it the bulk air temperature. A comparison between the air bulk temperature obtained with and without packing is shown in figure *5.53*.

5.8.2 Pressure drop

The comparison between the empty and packed channel pressure drop has shown a considerable decrease in the pressure drop obtained with the empty channel. The empty channel pressure drop was almost about *5* times lower than that obtained with the packed channel. This is graphically represented in figure *5.54*, the pressure drop in N/m^2 is plotted against the air superficial velocity.

5.8.3 Heat transfer coefficient

A comparison between the heat transfer coefficient obtained with and without packing in the asymmetrically heated channel as function of the mass flow rate is shown graphically in figure *5.55*. It is shown that as the flow rate increases the *Nu* obtained in the packed channel increases as shown in the previous sections, while for the empty channel the *Nu* is shown to be independent of the air flow rate as expected. Table *5.5* shows the *Nu* as

function of the mass flux for the empty and packed channel along with the percentage increase of *Nu* for the packed channel. It was found that the *Nu* in the packed channel is approximately *6* times higher than that in empty channel for *Re* ranging from *1000* to *5500*.

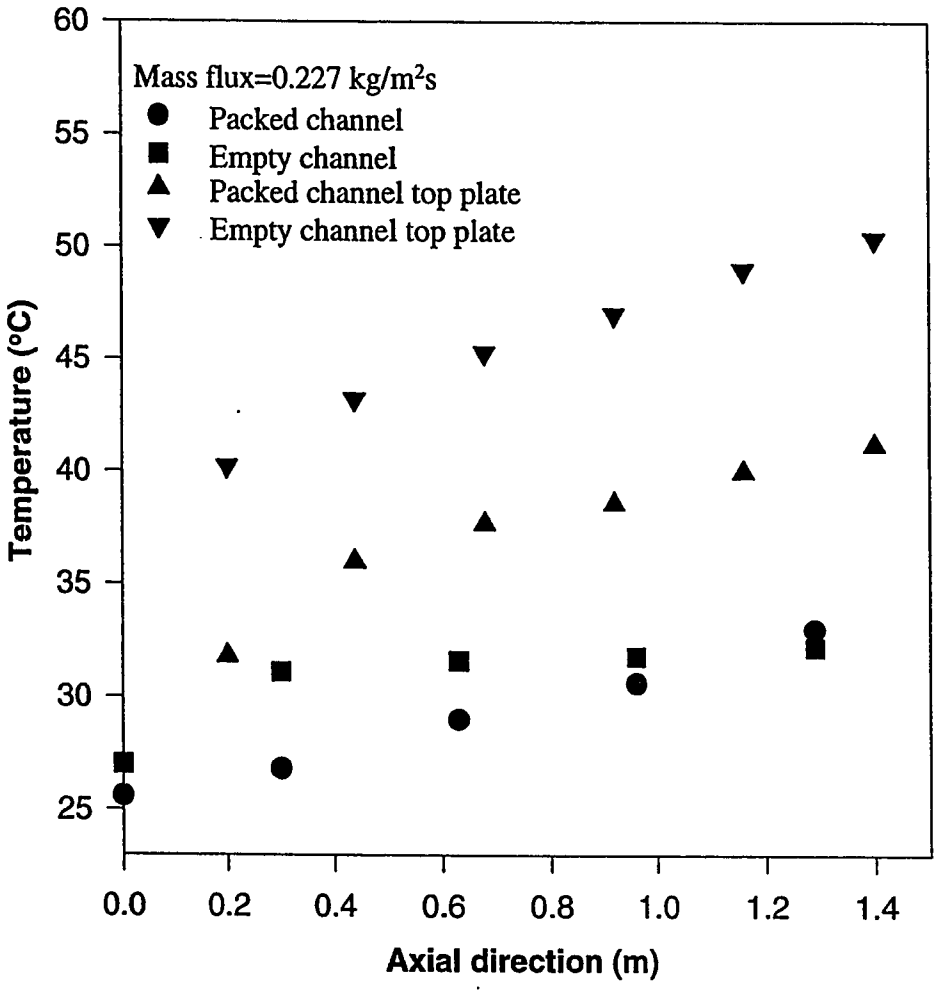

FIG. 5.51 COMPARISON BETWEEN THE EXPERIMENTAL AXIAL AIR EMPERATURE PROFILES IN THE EMPTY AND PACKED CHANNEL AT Y=0.05, Q=130 W/m^2

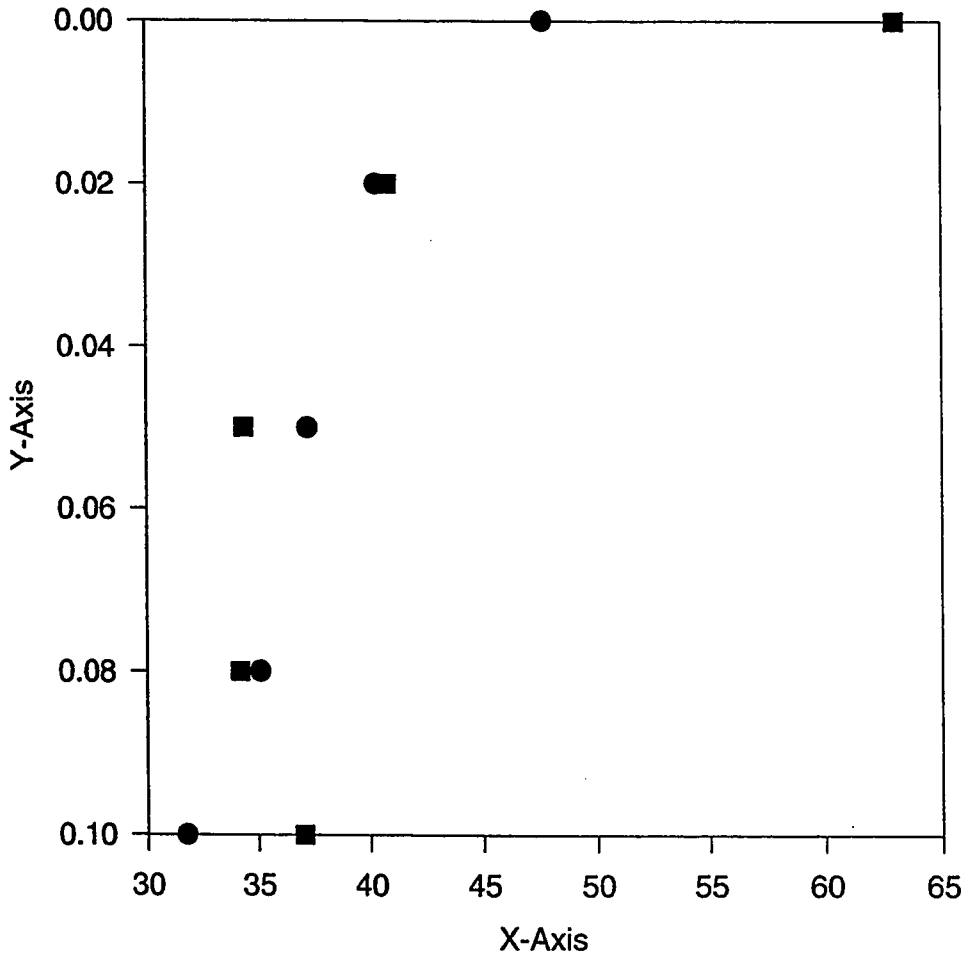

FIG. 5.52 EXPERIMENTAL TRANSVERSE AIR TEMPERATURE PROFILES IN THE EMPY AND PACKED CHANNEL AT X=1.29 m, Q=230 W/m^2

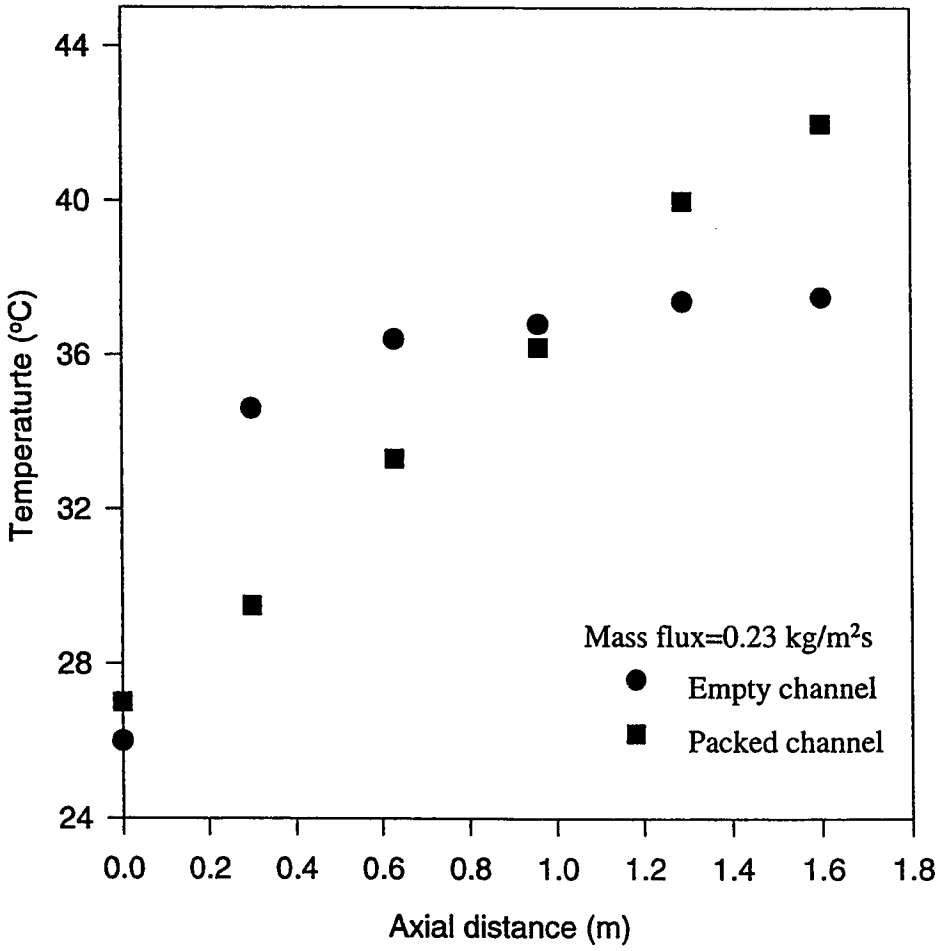

FIG 5.53 COMPARISON BETWEEN EMPTY AND PACKED CHANNEL AIR BULK TEMPERATURE AT *Re*=2471.

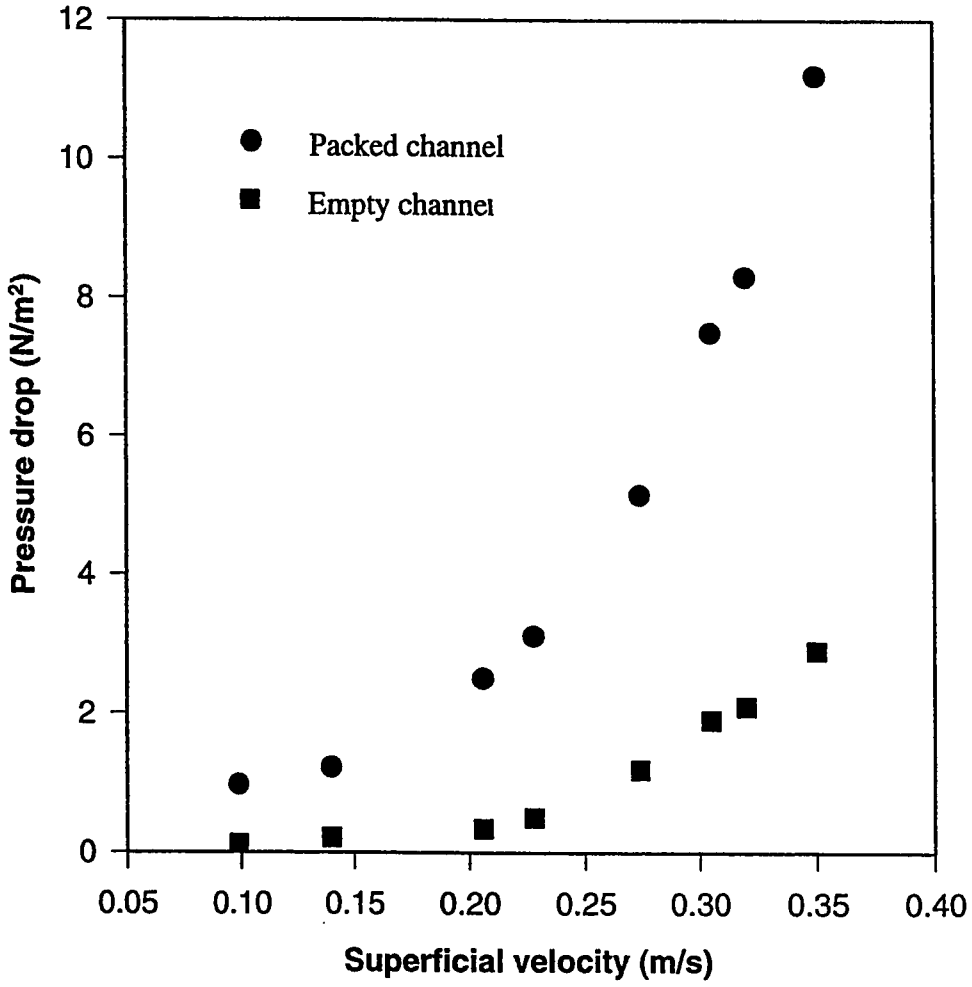

FIG. 5.54 COMPARISON BETWEEN EMPTY AND PACKED CHANNEL PRESSURE DROP.

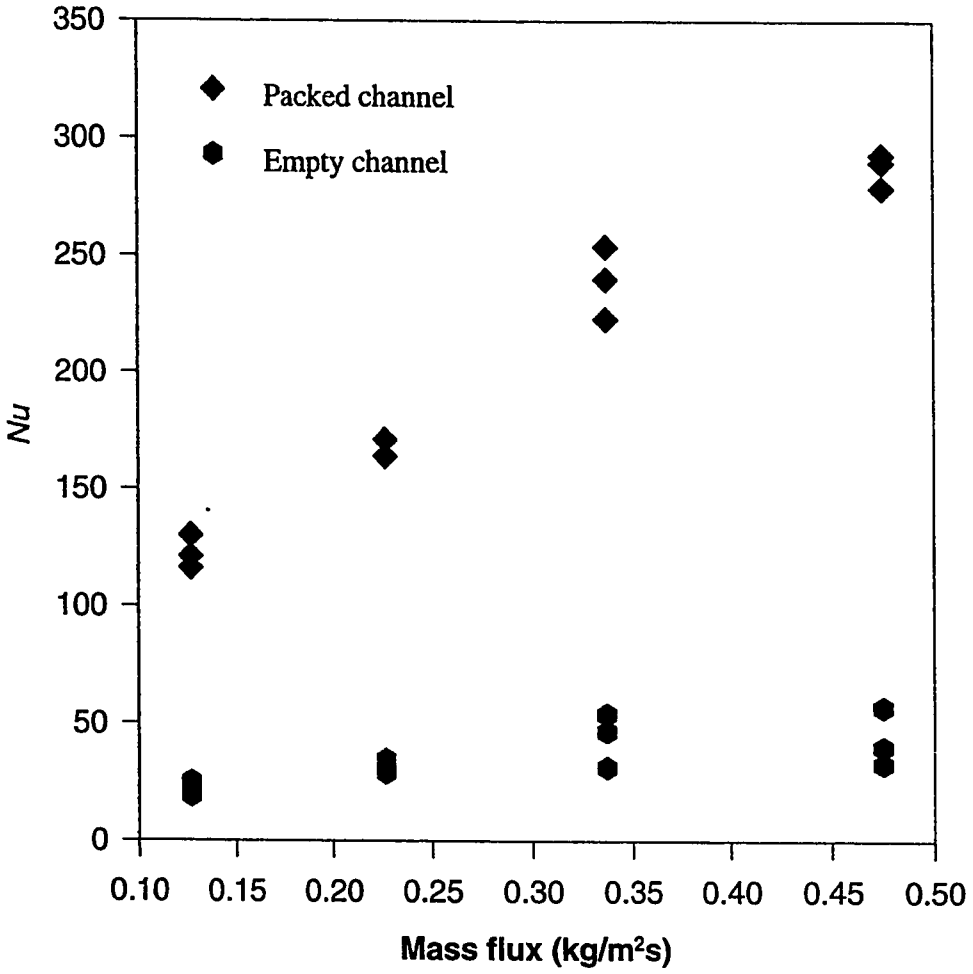

FIG. 5.55 COMPARISON BETWEEN *Nu* OBTAINED IN THE EMPTY AND PACKED CHANNEL AT Y=1.29 m.

Table 5.5 Comparison between empty and packed channel *Nu*.

Heat supplied (W/m^2)	Mass flux (kg/m^2s)	Nu_{empty}	Nu_{packed}	% Increase in *Nu*
130	0.127	21.6	121	460
	0.227	29.0	171	490
	0.337	31.3	254	711
	0.475	32.9	290	781
230	0.127	19.0	116	510
	0.227	33.6	164	388
	0.337	46.7	223	377
	0.475	40.0	293	632
350	0.127	25.6	130	408
	0.227	34.5	164	375
	0.337	54.0	240	344
	0.475	57.0	279	389

CHAPTER 6

CONCLUSION AND RECOMMENDATIONS

1. An experimental investigation of heat transfer in a rectangular packed channel with constant heat flux and asymmetrical wall temperatures has been conducted. The unique features of this experimental study are that it has been conducted in a large scale experimental equipment with a large void fraction and heated from top wall only.

2. A comprehensive numerical model For the simulation of air velocity and temperature profiles in a rectangular packed channel with constant heat flux has been developed. The new features of this model that it is the first to be developed for such a large void fraction packed rectangular channel with asymmetric heating.

3. Based on the experimentally determined air and wall temperature distribution a new correlative expression for *Nu* number ($=\frac{h_w D_e}{k_f}$) in terms of

Re number ($=\frac{Gd_p}{\mu(1-\varepsilon)}$) has been obtained. Least square fit procedure was used to evaluate the parameters.

4. For comparison between the empty and packed channel thermal performance a set of experiments has been conducted in the same channel and without packing. Under the same operating conditions the comparison in terms of *Nu* has shown that an increase of about *6* times in the value of *Nu* has been found compared to the empty channel in the range of *Re* considered in this study.

5. Experimental investigation in the packed channel on the effect of the flow regime on *Nu* has shown a considerable increase in the value of *Nu* as the flow rate increases in the range of $1000<Re<5500$.

6. A modified Equation for the pressure drop prediction in the packed channel has been obtained based on the original Ergun equation. The experimental packed channel pressure drop data and a least square curve fit procedure was used to evaluate the fitting parameters.

7. The experimental study has been carried out by one size and type of packing which limits our results and conclusions with the operating conditions considered in the study. Therefore it is recommended to investigate the thermal performance of the system under different sizes, shape and type of packing.

8. The correlative expression obtained for *Nu* is limited within the range of *Re* considered in this study. It would be better for further experimental studies to operate under higher values of *Re*.

9. The numerical program was developed to simulate the flow and thermal behavior of air flow under low heat supplied ($q<550\ W/m^2$) and constant physical properties. I recommend for further theoretical studies to modify the present program so as to simulate the system behavior under moderate heating taking into consideration the temperature and pressure variation effects on the physical properties of the media.

NOMENCLATURE

A	charactristic area
B_i	wall Biot number ($=h_wR/k_e$)
Bo_h	radial Bodenstein number for heat ($=\rho v C_p D_p/k_e$)
C_p	specific heat at constant pressure
D_e	equivelent diameter of channel
D_p	equivelent diameter of packing
f_o	friction factor
f_1	viscous forces
f_2	inertia forces
G	mass flux
H	Channel hight
h_w	wall-to-air/fluid heat transfer coefficient
k_{dy}	dynamic thermal conductivity
k_e	effective thermal conductivity
k_f	fluid/air thermal conductivity
k_{st}	stagnent thermal conductivity
L	channel length
N	number of packing particles

Nu Nusselt number based on effective channel diameter ($=\frac{h_w D_e}{k_f}$)

Nu_h Nusselt number based on channel height ($=\frac{h_w H}{k_f}$)

Pe heat transfer Peclet number ($=\frac{GC_p D_p}{k_e}$)

ΔP total pressure drop

Q , q_w heat flux

R tube radius

Re modified Reynolds number ($=\frac{\rho \upsilon D_p}{\mu(1-\varepsilon)}$)

Re_h Reynolds number based on the channel hight ($=\frac{\rho \upsilon H}{\mu}$)

T temperature

υ velocity component in the axial direction

W Channel width

x axial direction

y transverse/radial direction

Greek symbols

α_e effective thermal conductivity

ε bed void fraction

μ	fluid/air viscosity
ν	fluid/air kinamatic viscosity
ρ	fluid/air density

Subscribes

b	bulk
e	effective
f	fluid
g	gas
i	local
p	particle
s	solid
t	tube
w	wall

References

[1] Y. Demirel, "Experimental Investigation of Heat Transfer in a Packed Duct With Unequal Wall Temperatures", Experimental Thermal and Fluid Science, Vol. 2, 425-430, 1989.

[2] Y. Demirel and S.Kunc, "Thermal Performance Study of a Solar Air Heater With Packed Flow Passage", Energy Convers. Mgmt, Vol. 27, 317-325, 1987.

[3] K. Renken and D. Poulikakos, "Experiment and analysis of forced convection heat trasport in a packed bed of spheres" Int. J. Heat Mass Transfer, Vol. 31, 1399-1408, 1988.

[4] G. M. Chrysler and R. E. Simons, "An Experimental Investigation of the Forced Convection Heat Transfer Characteristics of Fluorocarbon Microelectronics Heat Source", ASME J. of Heat Transfer,Vol. 131, 21-27, 1990.

[5] A.P Colburn, "Heat Transfer and Pressure Drop in Empty, Baffled, and Packed Tubes", Ind. Eng. Chem., Vol. 23, 910-923, 1931.

[6] T. H. Hwang, Y. Cai and P. Cheng, "An Experimental Study of Forced Convection in a Packed Channel With Asymmetric Heating", Int. J. Heat Mass Transfer, Vol. 35, 3029-3039, 1992.

[7] D. Poulikakakos and K. Renken, "Forced Convection in a Channel Filled With Porous Medium, Including the Effect of Flow Inertia, Variable Porosity, and Brinkman Friction", J. of Heat Transfer, Vol.109, 880-888. 1987.

[8] K. Vafi and C. L. Tien, "Boundary and Inertia Effects on Flow and Heat Transfer in Porous Media ". Int. J. Heat Mass Transfer, Vol. 24, 95-203, 1981.

[9] J. G. H. Borking and K. R. Westerterp, " Significance of The Rdial Prosity Profile for the Description of Heat Transport in Wall-Cooled Packed Beds ", Chem. Eng. Sci., Vol. 49, 863-876, 1994.

[10] E. J. Osinski, P. V. Barr, and J. K. Brimacombe, "Mathematical Model for Ggas Flow Through a Packed Bed in The Presence of Source and Sink", The Can. J. of Chem. Eng. , Vol. 67, 722-730, 1989.

[11] C. Choudhury and H. P. Garg, "Performance of Air-Heating Collectors With Packed Air Flow Passage", Solar Energy, Vol. 50, 205-221, 1993.

[12] J. M. Smith, "Chemical Engineering Kinetics", Second Edition. McGraw-Hill, New York, 1970

[13] A. G. Dixon, "Wall and Particle-Shape Effects on Heat Transfer in Packed Beds", Chem. Eng. Comm. , Vol. 71, 217-285, 1988.

[13] A. G. Dixon, "Wall and Particle-Shape Effects on Heat Transfer in Packed Beds", Chem. Eng. Comm. , Vol. 71, 217-285, 1988.

[14] F. C. Chou, W. Y. Lien and S. H. Lin, "Analysis and Experiment of Non-Darcyan Convection in Horizontal Square Packed-Sphere Channels-Forced convection", Int. J. Heat and Mass transfer, Vol. 35, 95-205, 1992.

[15] J. H. Borkink and K. R. Westerterp, "Influence of Tube and Particle Diameter on Heat Transport in Packed Beds ", Int. J. of Heat Mass Transfer, Vol. 38, 703-714, 1992.

[16] J. Beek , "Design of Packed Catalytic reactors" Adv. Chem. Engng., vol. 3, 323-339, 1962.

[17] V. HLavacek V., "Aspects in Design of Packed Catalytic reactors", Ind. Eng. Chem., Vol. 62, 9-14, 1970 .

[18] R. H. Perry and D. Green, "Perry's Chemical Engineers Handbook", 6th Edition, McGraw-Hill, 1984.

[19] R. B. Bird, W. E. stewart, E. Lightfoot, "Transport Phenomina", 1960

[20] E. A. Foumeny, F. Benyahia, J. Castro, H. Moallemt and S. Roshani, Int. J. Heat and Mass Transfer, Vol. 36, 536-540, 1993.

[21] P. Cheng, C. T. Hsu and A. Chowdhury, "Forced Convection in the Entrance Region of a Packed Channel With Asymmetric Heating", Transaction of the ASME, Vol. 110, 946-954, 1988.

[22] K. Vafi and C. L. Tien, "Boundary and Inertia Effects on Flow and Heat Transfer in Porous Media " . Int. J. Heat Mass Transfer, Vol. 24, 195-203, 1981.

[23] J. G. H. Borking and K. R. Westerterp, "Significance of Aial Heat Dispersion of Heat Transport in Wall-Cooled Packed Beds", Chem. Eng. Technol., Vol. 15, 371-384, 1992.

[24] L. C. Young and B. A. Finlayson, Ind. Eng. Chem. Fundam., Vol. 12, 412-422, 1973.

[25] Odendoal, W. , Gobie , W., Carberry, J. J., "Thermal Parameters Sensitivity in the Simulation of the Non-isothermal Non-adiapatic Fixed Bed Catalytic Reactor-the Two-dimensional Hetrogenous Model, Chem. Eng. Commun., Vol. 58, 37-62, 1987.

[26] J. E. Gatica, J. A. Romagnoli, A. F. Erazu ,J. A Porres, "Steady State and Non-steady State Modeling of Heat Transfer in Packed Beds", Chem. Eng. Commun., Vol. 78, 69-73, 1989.

[27] D. Handley and P. J. Hegs, Tran. Inst. Chem. Engrs.,Vol. 46, 251-265, 1968.

[28] M. S. Bohn and L. W. Swanson, " A Comparison of Models and Experimental Data for Pressure Drop and Heat Transfer in Irrigated Packed Beds", Int. J. Heat Mass Transfer, Vol. 34, 2509- 2519, 1991.

[29] Chi-hsiung and B. Finlayson, " Heat Transfer in Packed Beds-A Reevaluation", Chemical Engineering Science", Vol. 32, 1055-1066, 1977.

[30] M. E. Arevo and N. N. Umnik, J. Tech. Phys. , Vol. 21, 1351, 1951.

[31] A. G. Dixon and D. L. Cresswell, "Theretical Prediction of Effective Heat Transfer Parameters in Packed Beds", Am. Inst. Chem. Engr., Vol. 25, 663-675, 1979.

[32] R. N Lyon, Chem. Eng. Prog., Vol. 47, 75-79, 1951.

[33] B. D. Kulkarni and L. K. Doraiswamy, "Estimation of Effective Transort Properties in Packed Bed Reactors", Catal. Rav.-Sci. Eng., Vol. 22(3), 431-483, 1980.

[34] S. Ergun, "Fluid Flow Through Packed Columns", Chem. Eng. Prog., Vol. 48, 89-95, 1952.

[35] H. Y. Zhang, A. Campo, and M. Ebadian, Aalytical/Numerical Solution of Convective Heat Transfer in the Thermal ntrance Region of Irregular Ducts", National Heat Transfer Conference,Vol. 110, 1-8, 1989.

[36] Stephen Whitaker, "Forced Convection Heat Transfer Correlations for Flow in Pipes, Past Flat Plates, Single Cylinders, Single Spheres, and for Flow in Packed Beds and Tubes Bundels", AICHE Journal, Vol. 18, 361-371, 1972.

[37] W. Chney and D. Kincaid, "Numerical Mathematics and Computation", Second edition, 1985.

[38] K. S. Schnoebelen and S. I. Abdel-khalik, "Local Nusselt Number for Flowing Packed Particle Beds in Circular Tubes With Constant Wall Heat Flux", Trabsaction of the ASME, Vol. 108, 466-469,1986.

APPENDIX A

MAIN PROGRAM AND SUBROUTINES USED

```
C  ************************************************************************
C  ** COMPUTER PROGRAM NAME:-
C  **
C  ** "HEAT TRANSFER IN ARECTANGULAR PACKED CHANNEL WITH CONSTANT HEAT FLUX "
C  **
C  ** THIS PROGRAM IS WRITTEN TO PERFORM A NUMERICAL SIMULATION OF A STEADY STATE
C  ** THERMAL BEHAVIOR OF AN AIR FLOW IN A RECTANGULAR CHANNEL HEATED FROM THE
C  ** TOP PLATE.
C  **
C  ** DESCRIBTION OF PARAMETERS:-
C  **
C  **   X , Y          : AXIAL AND TRANSVERSE DIRECTIONS.
C  **   DELY           : INCREMENT IN DISTANT FROM THE WALL .
C  **   DELX           : INCREMENT IN DISTANCE FROM THE ENTERANCE.
C  **   N              : NUMBER OF GRID POINTS.
C  **   UOLD           : VELOCITY DISTRIBUTION.
C  **   VEL            : SUPERFECIAL VELOCITY BASED ON EMPTY CHANNEL.
C  **   TNEW,TOLD      : TEMPERATURE DISTRIBUTION.
C  **   To             : INLET TEMPERATURE.
C  **   Po             : INLET PRESSURE.
C  **   Tamb           : AMBIENT TEMPERATURE.
C  **   Tb             : BULK AIR TEMPERATURE.
C  **   Ro             : AIR DENSITY TAKEN AT THE INLET CONDITIONS
C  **   VIS            : VISCODITY OF THE AIR AT THE INLET CONDITIONS
C  **   PHY            : BED VOID FRACTION.
C  **   Cp             : SPECIFIC HEAT OF THE AIR AT INLET CONDITIONS
C  **   G              : MASS FLOW RATE.
C  **   DELP           : PRESSURE DROPIN THE PACKED SECTION.
C  **   W, L, H        : WIDTH,LENGTH AND HIGHT OF THE CHANNEL RESPECTIVELY
C  **   dp,De          :EFFECTIVE DIAMETERS OF THE PACKING AND CHANNEL
C  **                    RESPECTIVELY
C  **   q              : ACTUAL HEAT SUPPLIED TO THE SYSTEM.
C  **   kf,ks          : THERMAL CONDUCTIVITY OF AIR & PACKING RESPECTIVELY.
C  **   ke             : EFFECTIVE THERMAL CONDUCTIVITY.
C  **   kins,kglas     : THERMAL CONDUCTIVITY OF INSULATION & GLASS PLATE.
C  **   CONS           : CONSTANT USED IN ERGUN EQUATION.
C  **   Re             : REYNOLD NUMBER BASED ON SUBERFECIAL VELOCITY
C  **   HCOF           : WALL TO AIR HEAT TRANSFER COEFFICIENT.
C  **   NUS            : NUSSELT NUMBER BASED ON PARICLE DIAMETER.
C  **   A,B,C,D        : MATRIX COEFFICIENTS IN THOMAS ALGORITHM.
C  **   BETA,GAMMA: THE DEPENDENT VARIABLES USED IN THOMAS ALGORITHM-
C  **   J              : SMALL POSITIVE NUMBER USED IN ACCURACY CHECK FOR THE
C  **                    MOMENTUM EQUATION SOLUTION.
C  **
```

```
C   ** SUBROUTINES USED:-
C   **
C   ** SUBROUTINE DATA: FOR READING THE REQUIRED DATA.
C   ** SUBROUTINE GRID: FOR FIXING THE GRID POINTS IN THE TRANSVERSE DIRECTION.
C   ** SUBROUTINE INIT1 & INIT2: FOR INITIALIZING THE VARIABLES.
C   ** SUBROUTINE ERGUN: FOR CALCULATE THE PRESSURE DROP.
C   ** SUROUTINE LOAD1 & LOAD2: FOR CALCULATING THE COEFFICIENTS  A, B, C, D
C   ** SUBROUTINE REYNOLD: FOR CALCULATING THE REYNOLD NUMBER.
C   ** SUBROUTINE BULK: FOR CALCULATING THE AIR BULK TEMPERATURE.
C   ** SUBROUTINE HEATCOEF: FOR CALCULATING THE HEAT TRANSFER COEFFICIENT &
C   **                              NUSSELT NUMBER.
C   ** SUBROUTINE THOMAS1 & THOMAS2: TO SOLVING A SET OF LINEAR ALGEBRIC
C   **                                      EQUATIONS
C   ** SUBROUTINE RESET: TO RESET THE NEW VALUES OF TEMPERATURE AS OLD ONES.
C   ** SUBROUTINE PRINT: TO PRINT THE SOLUTION RESULT AT SPECIFIC AXIAL
C   **                          POSITIONS.
C   **
C   ** WRITTEN BY   : YASSIR T. MAKKAWI
C   ** DATE         : MAR. 1,1995
C   **
C   ********************************************************************************

C   ********************************************************************************
C   **              MAIN PROGRAM
C   ********************************************************************************
      IMPLICIT REAL*8(A-H,O-Z)
      PARAMETER(N=50)
      REAL*8 ke,ks,kf,kins,kglas,kwood,L,NUS
      DIMENSION UOLD(0:N),DUOLD(0:N)
      DIMENSION A1(0:N),B1(0:N),C1(0:N),D1(0:N),F1(0:N),F2(0:N)
      DIMENSION A2(0:N),B2(0:N),C2(0:N),D2(0:N)
      DIMENSION BETA(0:N),GAMMA(0:N),DELY(0:N),Y(0:N)
      DIMENSION DTOLD(0:N),TOLD(0:N),TNEW(0:N),F(0:N)
      OPEN(UNIT=1,FILE='THESIS.OUT',STATUS='OLD')
      REWIND(1)
        ICOUNT=0
        DELX=0.00005
        X=DELX
      CALL DATA(To,Tamb,Ro,Po,VIS,PHY,W,H,L,dp,De,q,kf,ks
     & ,kins,kglas,kwood,Cp,G,VEL)
      CALL REYNOLD(Re,Ro,dp,VIS,VEL)
      CALL GRID(N,DELY,Y)
      CALL INIT1(N,UOLD)
      CALL INIT2(N,TOLD,To)
      CALL ERGUN(DELP,PDROP,G,PHY,dp,L,Ro,CONS)
   10 CONTINUE
      CALL LOAD1(N,UOLD,PDROP,DELY,F1,F2,A1,B1,C1,D1,CC2,PHY,Ro,VIS,dp
     & ,De,CONS)
      CALL THOMAS1(N,DUOLD,BETA,GAMMA,A1,B1,C1,D1)
      CALL SOLVE1(N,J,DUOLD,UOLD)
      IF (J .LT. N/2+1) GO TO 10
      CALL THERMCON(Re,PHY,kf,ks,ke,dp,De)
   30 CONTINUE
      CALL LOAD2(N,UOLD,TOLD,DELY,DELX,A2,B2,C2,D2,F,q,ke,kins,kglas,
     & kwood,Tamb,Ro,Cp)
```

```
      CALL THOMAS2(N,DTOLD,BETA,GAMMA,A2,B2,C2,D2)
      CALL SOLVE2(N,TNEW,DTOLD)
      CALL BULKTEMP(N,TNEW,UOLD,Tb)
      CALL HEATCOEF(N,DELY,NUS,HCOF,TNEW,Tb,De,kf,ke)
      CALL PRINT(N,X,ICOUNT,Y,UOLD,VEL,TNEW,To,Po,Tb,q,G,PDROP,HCOF,NUS,Re)
      CALL RESET1(N,TNEW,TOLD)
      ICOUNT=ICOUNT+1
      X=DELX+X
      IF (X .LT. 1.6) GO TO 30
      PRINT*,'    END OF CALCULATION'
      WRITE(1,*) '  END OF CALCULATION'
      END

C     ********************************************************************************
C     **              SUBROUTINE DATA
C     **               DATA SECTION
C     ********************************************************************************

      SUBROUTINE DATA(To,Tamb,Ro,Po,VIS,PHY,W,H,L,dp,De,q,kf,ks,kins,
     &kglas,kwood,Cp,G,VEL)
      IMPLICIT REAL*8(A-H,O-Z)
      REAL*8 kf,ks,kins,kglas,kwood,L
       W=0.8
       H=0.1
       L=1.6
       dp=0.0369
       De=0.29
       R=287.0
       Cp=1006.2
       VIS=0.000018
       PHY=0.81
       kwood=0.04
       kglas=0.04
       kins=0.1408
       kf=0.0258
       ks=0.14
       VEL=25.0*0.011
       q=130
       Tamb=22.5
       To=26.0
       Po=101344.2
       Ro=Po/(R*(To+273.0))
       G=VEL*Ro
      RETURN
      END

C     ********************************************************************************
C     **              SUBROUTINE ERGUN
C     ** CALCULATING THE PRESSURE DROP USING ERGUN EQUATION
C     ********************************************************************************
      SUBROUTINE ERGUN(DELP,PDROP,G,PHY,dp,L,Ro,CONS)
      IMPLICIT REAL*8(A-H,O-Z)
      REAL*8 L
      CONS=5.0
      F2=CONS*(1.0-PHY)/(PHY**3*Dp)
```

```
      DELP=F2*G**2/Ro
      PDROP=DELP*L
      RETURN
      END

C     ************************************************************************
C     **            SUBROUTINES GRID
C     **    FIXING THE GRID POINTS IN THE TRANSVERSE DIRECTION
C     ************************************************************************
      SUBROUTINE GRID(N,DELY,Y)
      IMPLICIT REAL*8(A-H,O-Z)
      DIMENSION  DELY(0:N),Y(0:N)
      Y(0)=0.0
      DO 10 I=0,N
      DELY(I)=0.002
   10 Y(I+1)=Y(I)+DELY(I)
      RETURN
      END

C     ************************************************************************
C     **            SUBROUTINES INIT1
C     **    FOR INITILIZING THE VELOCITY DISTRIBUTION
C     ************************************************************************
      SUBROUTINE INIT1(N,UOLD)
      IMPLICIT REAL*8(A-H,O-Z)
      DIMENSION  UOLD(0:N)
      UOLD(0)=0.0
      DO 10 I=1,N/2
        UOLD(I)=0.05
   10 CONTINUE
      UOLD(N)=0.0
      RETURN
      END

C     ************************************************************************
C     **            SUBROUTINE INIT2
C     **    FOR INITILIZING THE TEMPERATURE DISTRIBUTION
C     ************************************************************************
      SUBROUTINE INIT2(N,TOLD,To)
      IMPLICIT REAL*8(A-H,O-Z)
      DIMENSION TOLD(0:N)
      DO 10 I=0,N
        TOLD(I)=To
   10 CONTINUE
      RETURN
      END

C     ************************************************************************
C     **            SUBROUTINE LOAD1
C     ** CALCULATING THE MATRIX COEIFFICENTS OF THE MOMENTUM EQUATION
C     ************************************************************************
      SUBROUTINE LOAD1(N,UOLD,PDROP,DELY,F1,F2,A1,B1,C1,D1,CC2,PHY,Ro,
     &VIS,dp,De,CONS)
      IMPLICIT REAL*8(A-H,O-Z)
      DIMENSION UOLD(0:N),A1(0:N),B1(0:N),D1(0:N)
```

```
      DIMENSION DELY(0:N),C1(0:N)
      DIMENSION F1(0:N),F2(0:N)
       CCo=PDROP*(PHY/VIS)
       CC2=CONS*Ro*(1.0-PHY)/(PHY**2*dp*VIS)
      DO 10 I=1,N/2
      F1(I)=2.0+2.0*CC2*DELY(I)**2*UOLD(I)
      F2(I)=CCo*DELY(I)**2
   10 CONTINUE
C     **NODE 0**
      A1(0)=0.0
      B1(0)=1.0
      C1(0)=0.0
      D1(0)=0.0

C     **INTERIOR NODES**
      DO 20 I=1,N/2-1
       A1(I)=1.0
       B1(I)=-F1(I)
       C1(I)=1.0
       D1(I)=-UOLD(I-1)+UOLD(I)*F1(I)-UOLD(I+1)-F2(I)
   20 CONTINUE

C     **NODE N/2**
      A1(N/2)=2.0
      B1(N/2)=-F1(N/2)
      C1(N/2)=0.0
      D1(N/2)=-2.0*UOLD(N/2-1)+UOLD(N/2)*F1(N/2)-F2(I)
      RETURN
      END

C     ********************************************************************************
C     **              SUBROUTINE REYNOLD
C     ** CALCULATING REYNOLD NUMBER BASED ON PARTICLE DIAMETER
C     ********************************************************************************
      SUBROUTINE REYNOLD(Re,Ro,dp,VIS,VEL)
      IMPLICIT REAL*8(A-H,O-Z)
      DIMENSION UOLD(0:N)
      Re=Ro*dp*VEL/VIS
      RETURN
      END

C     ********************************************************************************
C     **              SUBROUTINE THERMALCON
C     ** CALCULATING THE THERMAL CONDUCTIVITY USING A CORRELATIVE
C     ** EXPRESSION
C     ********************************************************************************
      SUBROUTINE THERMCON(Re,PHY,kf,ks,ke,dp,De)
      IMPLICIT REAL*8(A-H,O-Z)
      REAL*8 ke,ks,kf
      ke=kf*(PHY+(1.0-PHY)*(1.0/(0.18+(2.0/3.0)*kf/ks)))+0.0025*
     &Re/(1.0+46.0*(dp/De)**2)
      RETURN
      END
```

```
C   ********************************************************************************
C   **              SUBROUTINE LOAD2
C   ** CALCULATING THE MATRIX COEIFFICENTS OF THE ENERGY EQUATION
C   ********************************************************************************
    SUBROUTINE LOAD2(N,UOLD,TOLD,DELY,DELX,A2,B2,C2,D2,F,q,ke,kins,
   &kglas,kwood,Tamb,Ro,Cp)
    IMPLICIT REAL*8(A-H,O-Z)
    REAL*8 ke,kins,kwood,kglas
    DIMENSION DELY(0:N),A2(0:N),B2(0:N),C2(0:N),D2(0:N)
    DIMENSION TOLD(0:N),UOLD(0:N),F(0:N)
    DO 10 I=1,N-1
     F(I)=(DELX*ke)/(2*Ro*UOLD(I)*Cp*DELY(I)**2)
  10 CONTINUE
    F(0)=0.0
    F(N)=0.0
C   **NODE 0**
     A2(0)=0.0
     B2(0)=1.0
     C2(0)=0.0
     D2(0)=DELY(0)*q/ke+TOLD(1)
C   **INTERIOR NODES**
    DO 20 I=1,N-1
      A2(I)=F(I)
      B2(I)=-(1.0+2.0*F(I))
      C2(I)=F(I)
      D2(I)=-TOLD(I-1)*F(I)+TOLD(I)*(2.0*F(I)-1.0)-TOLD(I+1)*F(I)
  20 CONTINUE
C   **NODE N**
    R1=0.05/kins
    R2=0.015/kglas
    R3=0.03/kwood
    R=R1+R2+R3
    A2(N)=0.0
    B2(N)=1.0
    C2(N)=0.0
    D2(N)=(TOLD(N-1)+Tamb*DELY(N)/(ke*R))/(1.0+DELY(N)/(ke*R))
     RETURN
     END

C   ********************************************************************************
C   **              SUBROUTINE THOMAS1
C   **SOLVING THE LINEAR ALGEBRIC EQUATIONS OF THE MOMENTUM EQUATION
C   ********************************************************************************

    SUBROUTINE THOMAS1(N,DUOLD,BETA,GAMMA,A1,B1,C1,D1)
    IMPLICIT REAL*8(A-H,O-Z)
    DIMENSION BETA(0:N),GAMMA(0:N),DUOLD(0:N),A1(0:N),B1(0:N),C1(0:N)
   &,D1(0:N)
     BETA(0)=B1(0)
     GAMMA(0)=D1(0)/B1(0)
     DO 10 I=1,N/2
       BETA(I)=B1(I)-(A1(I)*C1(I-1)/BETA(I-1))
       GAMMA(I)=(D1(I)-A1(I)*GAMMA(I-1))/BETA(I)
  10  CONTINUE
     DUOLD(N/2)=GAMMA(N/2)
```

```
      DO 20 I=N/2,0,-1
       DUOLD(I)=GAMMA(I)-C1(I)*DUOLD(I+1)/BETA(I)
   20 CONTINUE
      RETURN
      END

C     ***************************************************************************
C     **              SUBROUTINE THOMAS2
C     ** SOLVING THE LINEAR ALGEBRIC EQUATIONS OF THE ENERGY EQUATION
C     ***************************************************************************
      SUBROUTINE THOMAS2(N,DTOLD,BETA,GAMMA,A2,B2,C2,D2)
      IMPLICIT REAL*8(A-H,O-Z)
      DIMENSION BETA(0:N),GAMMA(0:N),DTOLD(0:N),A2(0:N),B2(0:N),C2(0:N)
     &,D2(0:N)
      BETA(0)=B2(0)
      GAMMA(0)=D2(0)/B2(0)
      DO 10 I=1,N
        BETA(I)=B2(I)-(A2(I)*C2(I-1)/BETA(I-1))
        GAMMA(I)=(D2(I)-A2(I)*GAMMA(I-1))/BETA(I)
   10 CONTINUE
      DTOLD(N)=GAMMA(N)
      DO 20 I=N-1,0,-1
       DTOLD(I)=GAMMA(I)-C2(I)*DTOLD(I+1)/BETA(I)
   20 CONTINUE
      RETURN
      END

C     ***************************************************************************
C     **              SUBROUTINE SOLVE1
C     **      SOLVING FOR THE VELOCITY DISTRIBUTION
C     ***************************************************************************
      SUBROUTINE SOLVE1(N,J,DUOLD,UOLD)
      IMPLICIT REAL*8(A-H,O-Z)
      DIMENSION DUOLD(0:N),UOLD(0:N)
       J=0
      DO 10 I=0,N/2
       UOLD(I)=DUOLD(I)+UOLD(I)
       UOLD(N-I)=UOLD(I)
   10 CONTINUE
      UOLD(0)=0.0
      DO 20 I=0,N/2
       IF (ABS(DUOLD(I)) .LT. 1D-12)  J=J+1
   20 CONTINUE
      RETURN
      END

C     ***************************************************************************
C     **              SUBROUTINE SOLVE2
C     **      SOLVING FOR THE TEMPERATURE DISTRIBUTION
C     ***************************************************************************
      SUBROUTINE SOLVE2(N,TNEW,DTOLD)
      IMPLICIT REAL*8(A-H,O-Z)
      DIMENSION DTOLD(0:N),TNEW(0:N)
      DO 10 I=0,N
        TNEW(I)=DTOLD(I)
```

```
 10 CONTINUE
    RETURN
    END

C   ***************************************************************************
C   **              SUBROUTINE BULKTEMP
C   **    CALCULATING THE BULK TEMPERATURE OF THE FLUID
C   ***************************************************************************
    SUBROUTINE BULKTEMP(N,TNEW,UOLD,Tb)
    IMPLICIT REAL*8(A-H,O-Z)
    DIMENSION TNEW(0:N),UOLD(0:N)
    SUM1=0.0
    SUM2=0.0
    SUM3=0.0
    SUM4=0.0
    SUM5=0.0
    SUM6=0.0
    SUM7=0.0
    SUM8=0.0
    SUM1=TNEW(20)*UOLD(20)+4.0*TNEW(21)*UOLD(21)
    DO 10 I=22,N-22
      SUM2=SUM2+2.0*TNEW(I)*UOLD(I)
  10 CONTINUE
    SUM3=TNEW(80)*UOLD(80)+4.0*TNEW(79)*UOLD(79)
    SUM4=SUM1+SUM2+SUM3
    SUM5=UOLD(20)+4.0*UOLD(21)
    DO 20 I=22,N-22
      SUM6=SUM6+2.0*UOLD(I)
  20 CONTINUE
    SUM7=UOLD(80)+4.0*UOLD(79)
    SUM8=SUM5+SUM6+SUM7
     Tb=SUM4/SUM8
    RETURN
    END

C   ***************************************************************************
C   **              SUBROUTINE HEATCOEF
C   **    CALCULATING THE WALL-AIR HEAT TRANSFER COEFFICIENT
C   ***************************************************************************

    SUBROUTINE HEATCOEF(N,DELY,NUS,HCOF,TNEW,Tb,De,kf,ke)
    IMPLICIT REAL*8(A-H,O-Z)
    DIMENSION DELY(0:N),TNEW(0:N)
    REAL*8 kf,ke,NUS
    HCOF=ke*(TNEW(0)-TNEW(1))/((TNEW(0)-Tb)*DELY(0))
    NUS=De*HCOF/kf
    RETURN
    END

C   ***************************************************************************
C   **              SUBROUTINE PRINT
C   **          PRINTING THE CALCULATION RESULTS
C   ***************************************************************************
     SUBROUTINE PRINT(N,X,ICOUNT,Y,UOLD,VEL,TNEW,To,Po,Tb,q,G,PDROP,
    &HCOF,NUS,Re)
```

```
      IMPLICIT REAL*8(A-H,O-Z)
      REAL*8 NUS
      DIMENSION TNEW(0:N),UOLD(0:N),Y(0:N)
      IF (ICOUNT .EQ. 0) THEN
       PRINT*,'OPERATING CONDITIONS:-'
       PRINT*,'To =',To,' C'
       PRINT*,'Po =',Po,' N/m^2'
       PRINT*,'G  =',G,' kg/sm^2'
       PRINT*,'q  =',q,' W/m^2'
       PRINT*,'Re =',Re
       PRINT*,'DELP=',PDROP,' N/m^2'
      PRINT*,' '
       WRITE(1,10)
       WRITE(1,20) To
       WRITE(1,30) Po
       WRITE(1,40) VEL
       WRITE(1,50) G
       WRITE(1,60) q
       WRITE(1,70) PDROP
       WRITE(1,80)
      DO 5 I=0,N
    5   WRITE(1,90) Y(I),UOLD(I)
      END IF
      IF(ABS(X-0.3).LE.1E-5 .OR. ABS(X-0.63).LE.1E-5 .OR. ABS(X-0.95)
     &.LE.1E-5 .OR. ABS(X-1.29).LE.1E-5 .OR. ABS(X-1.6).LE.1E-5) THEN
       PRINT*,'X=',X
       PRINT*,'BULK TEMP =',Tb
       PRINT*,'HEAT COEFF=',HCOF
       PRINT*,'NUS=',NUS
       PRINT*,' '
       WRITE(1,100)  X
       WRITE(1,110) Tb
       WRITE(1,120) HCOF
       WRITE(1,130) NUS
       WRITE(1,140)
       DO 15 M=0,N
    15   WRITE(1,150)  Y(M),TNEW(M)
      END IF
     10 FORMAT(/,' OPERATING CONDITIONS:-',/)
     20 FORMAT('INLET TEMPERATURE   =',10X,F10.3,' (C)')
     30 FORMAT('INLET PRESSURE      =',10X,F10.3,' (N/m^2)')
     40 FORMAT('SUPERFECIAL VELOCITY =',10X,F10.3,' (m/s)')
     50 FORMAT('MASS FLOW RATE      =',10X,F10.3,' (kg/sm^2)')
     60 FORMAT('HEAT SUPPLIED       =',10X,F10.3,' (W/m^2)')
     70 FORMAT('PRESSURE DROP       =',10X,F10.3,'  (N/m^2)',//)
     80 FORMAT(15X,'Y','(m)',16X,'VELOCITY','(m/s)')
     90 FORMAT(10X,F10.4,15X,F10.4)
    100 FORMAT(//,'AXIAL DISTANCE      =',F10.6,' (m)')
    110 FORMAT('BULK AIR TEMPERATURE =',F10.3,' (C)')
    120 FORMAT('LOCAL h              =',F10.3,' (W/Cm^2)')
    130 FORMAT('LOCAL Nu             =',F10.3,//)
    140 FORMAT(15X,'Y','(m)',16X,'TEMPERATURE','(C)')
    150 FORMAT(10X,F10.4,15X,F10.4)
      RETURN
      END
```

```
C  ***************************************************************************
C  **              SUBROUTINE RESET1
C  ** TO RESET THE OLD VALUES OF THE TEMERATURE TO THE NEW ONES
C  ***************************************************************************
C  **SUBROUTINE RESET1**
   SUBROUTINE RESET1(N,TNEW,TOLD)
   IMPLICIT REAL*8(A-H,O-Z)
   DIMENSION TNEW(0:N),TOLD(0:N)
   DO 10 I=0,N
 10  TOLD(I)=TNEW(I)
   RETURN
   END
```

APPENDIX B

PACKED CHANNEL EXPERIMENTAL DATA ANALYSIS

SET NO. 1

Measured variables	Unit						
Electric heating power per unit area, Q	W/m^2	**55**	**130**				
Air inlet temperature, T_o	^oC	25.6	26.9	25.6	25.9	26.0	27.0
Air outlet temperature, T_{exit}	^oC	29.7	36.5	34.2	33.9	33.6	33.5
Ambient temperature, T_{amb}	^oC	22.5	22.0	22.0	22.0	22.5	22.5
Mean top plate temperature, T_w	^oC	31.3	43.5	37.5	37.1	35.8	35.0
Superficial velocity	m/s	0.19	0.11	0.19	0.23	0.29	0.36
Calculated variables							
Mass flux	kg/m^2s	0.22	0.13	0.22	0.28	0.34	0.42
Overall Wall-to-air heat transfer coefficient, h_w	W/m^2C	11.6	10.4	14.8	20.0	22.6	26.5
Non-dimensional variables							
Modefied Reynolds number, $Re=\rho \upsilon D_p/\mu(1-\varepsilon)$		2471	1388	2471	3332	3860	4544
Nusselt number, $Nu=h_w D_e/k_f$		130	121	172	231	254	276

SET NO. 2

Measured variables	Unit							
Electric heating power per unit area, Q	W/m^2	**230**						
Air inlet temperature, T_o	^oC	27.6	25.8	27.8	27.5	24.9	27.0	25.0
Air outlet temperature, T_{exit}	^oC	44.4	39.1	40.0	38.8	36.4	37.2	32.1
Ambient temperature, T_{amb}	^oC	22.0	22.0	22.5	22.5	22.5	22.5	23.0
Mean top plate temperature, T_w	^oC	55.2	51.4	50.0	45.0	42.4	40.6	37.5
Superficial velocity	m/s	0.11	0.15	0.19	0.23	0.29	0.36	0.40
Calculated variables								
Mass flux	kg/m^2s	0.12	0.17	0.22	0.27	0.34	0.42	0.47
Overall Wall-to-air heat transfer coefficient, h_w	W/m^2C	10.3	12.3	14.6	17.6	19.9	22.8	26.0
Non-dimensional variables								
Modified Reynolds number, $Re = \rho \upsilon D_p / \mu(1-\varepsilon)$		1388	1860	2471	3332	3860	4544	5137
Nusselt number, $Nu = h_w D_e / k_f$		116	138	164	198	223	255	293

SET NO. 3

Measured variables	Unit							
Electric heating power per unit area, Q	W/m^2	**350**						
Air inlet temperature, T_o	^oC	27.6	25.8	27.8	27.5	24.9	27.0	25.0
Air outlet temperature, T_{exit}	^oC	44.4	39.1	40.0	38.8	36.4	37.2	32.1
Ambient temperature, T_{amb}	^oC	22.0	22.0	22.5	22.5	22.5	22.5	23.0
Mean top plate temperature, T_w	^oC	55.2	51.4	50.0	45.0	42.4	40.6	37.5
Superficial velocity	m/s	0.11	0.15	0.19	0.23	0.29	0.36	0.40
Calculated variables								
Mass flux	kg/m^2s	0.12	0.17	0.22	0.27	0.34	0.42	0.47
Overall Wall-to-air heat transfer coefficient, h_w	W/m^2C	10.3	12.3	14.6	17.6	19.9	22.8	26.0
Non-dimensional variables								
Modified Reynolds number, $Re = \rho \upsilon D_p / \mu(1-\varepsilon)$		1388	1860	2471	3332	3860	4544	5137
Nusselt number, $Nu = h_w D_e / k_f$		116	139	164	198	223	255	293

SET NO. 4

Measured variables	Unit			
Electric heating power per unit area, Q	W/m^2	**500**		
Air inlet temperature, T_o	^oC	28.5	28.2	26.0
Air outlet temperature, T_{exit}	^oC	64.0	51.5	42.0
Ambient temperature, T_{amb}	^oC	22.0	22.0	24.0
Mean top plate temperature, T_w	^oC	83.0	68.0	58.0
Superficial velocity	m/s	0.19	0.29	0.40
Calculated variables				
Mass flux	kg/m^2s	0.22	0.34	0.47
Overall Wall-to-air heat transfer coefficient, h_w	W/m^2C	15.9	22.5	24.0
Non-dimensional variables				
Modified Reynolds number, $Re = \rho \upsilon D_p / \mu(1-\varepsilon)$		2471	3860	5137
Nusselt number, $Nu = h_w D_e / k_f$		179	252	270

APPENDIX C

EMPTY CHANNEL EXPERIMENTAL DATA ANALYSIS

SET NO. 1

Measured variables	Unit				
Electric heating power per unit area, Q	W/m^2	**55**		**130**	
Air inlet temperature, T_o	^oC	27.7	29.6	29.5	28.7
Air outlet temperature, T_{exit}	^oC	29.2	37.4	32.1	30.5
Ambient temperature, T_{amb}	^oC	22.5	23.0	23.0	22.0
Mean top plate temperature, T_w	^oC	35.7	48.1	46.3	42.3
Superficial velocity	m/s	0.19	0.11	0.19	0.23
Calculated variables					
Mass flux	kg/m^2s	0.22	0.13	0.22	0.28
Overall Wall-to-air heat transfer coefficient, h_w	W/m^2C	2.59	2.60	3.52	2.8
Non-dimensional variables					
Reynolds number, $Re = \rho \upsilon D_p / \mu$		470	264	470	733
Nusselt number, $Nu = h_w D_e / k_f$		29	22	40	31

SET NO. 2

Measured variables	Unit			
Electric heating power per unit area, Q	W/m^2	**230**		
Air inlet temperature, T_o	^oC	29.7	29.5	28.9
Air outlet temperature, T_{exit}	^oC	35.7	34.5	33.9
Ambient temperature, T_{amb}	^oC	23.0	22.0	23.0
Mean top plate temperature, T_w	^oC	61.8	59.1	56.5
Superficial velocity	m/s	0.11	0.19	0.29
Calculated variables				
Mass flux	kg/m^2s	0.13	0.22	0.34
Overall Wall-to-air heat transfer coefficient, h_w	W/m^2C	2.1	3.0	4.1
Non-dimensional variables				
Reynolds number, $Re=\rho \upsilon D_p/\mu$		264	470	733
Nusselt number, $Nu=h_w D_e/k_f$		23	33	47

SET NO. 3

Measured variables	Unit				
Electric heating power per unit area, Q	W/m^2	350			
Air inlet temperature, T_o	^oC	30.0	29.2	28.9	26.5
Air outlet temperature, T_{exit}	^oC	43.7	43.3	40.0	34.1
Ambient temperature, T_{amb}	^oC	22.5	23.0	22.5	22.0
Mean top plate temperature, T_w	^oC	81.4	78.3	73.3	56.6
Superficial velocity	m/s	0.11	0.19	0.29	0.4
Calculated variables					
Mass flux	kg/m^2s	0.13	0.22	0.34	0.46
Overall Wall-to-air heat transfer coefficient, h_w	W/m^2C	3.4	3.9	4.9	3.0
Non-dimensional variables					
Reynolds number, $Re=\rho \upsilon D_p/\mu$		264	470	733	976
Nusselt number, $Nu=h_w D_e/k_f$		38	44	54.8	33.6